thickest part is estimated to be approximately 300 m in thickness.

Stratigraphic Relations

The volcanic sediments cover the Lampa Volcanic Rocks conformably near Mt. Negro. Near the village of San Jose de Ushua the volcanic sediments cover the Yura Group, Murco Formation and Arcurquina Formation unconformably.

(5) Mollebamba Volcanic Rocks (Vm)

Distribution

The Mollebamba Volcanic Rocks comprise lava flows produced by local eruptions, and are distributed as small-scale bodies around Mt. Sara Sara, in the southwest of Mt. Apaiñuñu, in flatlands west and northeast of Mt. Solimana, around Mt. Acco in the northeast of the survey area, Mt. Auquihuato and in the area east of this mountain.

Rock Facies

The volcanic rocks consist of lavas of dark grey hornblende andesite with flow-structure or blackish grey to dark grey massive compact non-prophyritic andesite. Microseopically, the hornblende andesites contain phenocrysts of hornblende (0.5 to 1.2 mm) and plagioclase (0.5 to 1.0 mm) and the groundmass is composed predominantly of glass with fluidal structure, microcrystals of plagioclase and hornblende. The non-porphyritic andesites consist mainly of glass and minor amount of microcrystals of plagioclase and a very small amount of augite.

Stratigraphic Relations

The Mollebamba Volcanic Rocks cover the underlying formations in a form of disconformity.

(6) Alluvium (al)

Distribution

The alluvium is distributed along the major rivers of the survey area, forming belts of flatlands. It is also distributed, though on a smaller scale, on gentle mountain slopes, and along valleys and basins in the Altiplano plateau.

Rock Facies

The alluvium varies in color from place to place and consists essentially of gravels, sands and clay.

4-2-2 Intrusive Rocks

The intrusive rocks occurring in the survey area comprise Coast batholith, (CB), Accha stock (Di) and andesite stocks and dikes (An).

(1) Coast Batholith (CB)

Distribution

The Coast batholith is distributed around Mt. Quirhuay in the southwest of the survey area, along the Cotahuasi River in the south and on the south of Mt. Solimana. These batholiths are part of the Coast batholiths distributed along the western edge of the South American Continent and continue southward beyond the survey area.

Rock Facies

The Coast batholith consists of composite rock bodies which comprise gabbros, diorites, tonalites, adamellites and granites. Of these, intermediate rocks are reported to have the most widespread distribution (Cabbing and Pitcher, 1972).

In the survey area, quartz diorites and granodiorites are distributed in the southwest and in the south, respectively. The quartz diorites are greenish grey massive medium-grained holocrystalline rocks. Microscopically, they have a holocrystalline texture and, to some extent, a porphyritic texture and are composed of plagioclase (0.5 to 2.5 mm; An 40 to 48%), hornblendes (0.5 to 1.7 mm; partly chloritized), biotite (0.8 to 1.3 mm) and quartz (0.5 to 0.8 mm). The granodiorites are grey to light grey massive coarse-grained holocrystalline rocks. Microscopically, they manifest a holocrystalline equigranular to somewhat porphyritic texture and are classified to hornblende-biotite granodiorite composed of plagioclase (2 to 7 mm; An 28 to 33%), quartz (1 to 3 mm), potassium feldspar (4 to 6 mm, orthoclase), hornblende (0.8 to 1.7 mm), biotite (0.5 to 1.3 mm) and a small quantity of rutile.

Mode of Occurrence and Time of Intrusion

The quartz diorites occurring in the southwest of the survey area have penetrated the Basement complex and the Chocolate Volcanic Rocks, the lowermost part of the Jurassic System of the survey area. Around the contact planes the quartz diorites are accompanied by large quantities of xenoliths elongated in a lens-like form and epidotes in reticulated veinse or veinlets. The Chocolate Volcanic Rocks around the bodies of quartz diorite are decolored and pyritized. The K-Ar dating of a sample (Gb-110) of the quartz diorites shows 80.3 $\pm$ 4.0 Ma which corresponds to the Late Cretaceous.

The granodiorites occurring to the south of Solimana are unconformably covered by the Alpabamba Formation of Tertiary age. The K-Ar dating of a sample (Gd-32) of these granodiorites shows 57.1 $\pm$ 2.9 Ma which corresponds to Palaeocene age.

(2) Accha Stock (Di)

Distribution

There are 13 localities of Accha stock, small and large (separated into 23 exposures), in the survey area. In the zone extending from the central part to the northeast eight stocks with NE-SW arrangement (separated into 15 different exposures) are distributed along the right bank of the Cotahuasi River. Of these, the larger stocks are found at Pirca in the north of the detailed survey area B, on Mt. Yuca west of Cotahuasi and around Alca in the northeast. In the northwest of the survey area, five stocks with NW-SE arrangement (separated into eight different exposures) are found in the zone extending from Marcabamba to Bitama and vicinity. The rock bodies occurring in Marcabamba, Colta and Bitama are relatively on a large scale.

Rock Facies

The Accha stock consists mainly of medium to five-grained diorites and quartz diorites and include stocks of porphyritic quartz diorite containing porphyritic plagioclase and quartz.

In thin section the diorites and quartz diorites are composed of plagioclase (0.5 to 2 mm; An 36 to 48%), quartz (0.2 to 0.8 mm), hornblende (0.8 to 2 mm), an extremely small quantity of rutile, and opaque minerals. The bodies occurring in and around Alca contain augites (0.2 to 0.8 mm) and those found in and around Marcabamba contain biotites (0.4 to 0.8 mm).

The porphyritic quartz diorites are grey holocrystalline rocks in which plagioclase form a porphyritic texture. Microscopically the quartz diorites manifest a porphyritic texture and the phenocryst consists of plagioclase (2 to 4 mm), quartz (1 to 3 mm) and biotite (0.5 to 2 mm). The groundmass shows a mosaic texture of plagioclase and quartz, suggesting recrystallization, and quartz porphyry as original rock.

Mode of Occurrence and Time of Intrusion

The Accha stock penetrates the Yura Group, the Murco Formation and the Arcurquina Formation, all of Cretaceous age, the Huanca Formation of the Palaeogene and the Tacaza Group of the Neogene and are covered by the Alcabamba Formation. The strata surrounding the Accha stock are decolored and exhibit a white grey and are locally contaminated by ferrous oxides. Garnet skarns occur in part of the limestone layer of the Arcurquina Formation which contacts to the stocks. A part of the Accha stock occurring around the contact planes is partly contaminated by pyrites.

The K-Ar dating of a sample (Ca-4) of quartz diorites distributed in Alca

shows 53.7 ± 2.7 Ma which corresponds to the early Eocene. Judging from the fact that the Accha stocks have penetrated the Tacaza Group, it seems that the time of their intrusion ranged to the Miocene.

(3) Stocks and Dikes of Andesite (An)

Distribution

Two andesite stocks are found each in the north of Pirca, on Mt. Ararepata in the south, and around mountain top to the southwest. Smaller andesite stocks are found around Tauriswa north of the village of Cotahuasi and around Pampamarca to the northwest. All these andesite stocks penetrated the strata formed earlier than the Tacaza Group. Four NE-SW dikes are found near Marcabamba, dikes of N20°W in the Pararapa mine to the northeast, and smaller dikes in the mountains west of Alca.

Rock Facies

The stocks are composed of greenish grey to grey porphyritic hypocrystalline massive hornblende andesites. In thin section, they are shown to consist of phenocrysts composed of plagioclase (1 to 3 mm), augite (1 mm), and hornblende (1 mm), and groundmass composed of plagioclase and a small quantity of glass. The andesite stocks found in Taurisma contain phenocrysts of hornblende (about 0.6 mm), but not those of augite. These andesite stocks have undergone alteration, resulting in the formation of various minerals, chlorite from mafis minerals, and albite, chlorite and sericite from plagioclases.

The andesite dikes consist of greenish grey hornblende andesites and have generally been chloritized. The dikes which penetrated the Tacaza Group at Mina Pararapa consist of green to greenish grey altered porphyritic hornblende andesites and contain the phenocrysts of plagioclase (3 to 5 mm) and chloritized hornblende (1 to 3 mm). The groundmass has been heavily altered and contaminated by pyrites. Gold-silver bearing quartz veins are contained in the greenish grey hornblende andesites.

Mode of Occurrence and Time of Intrusion

The andesite stocks are hypocrystalline and exhibit the same pattern of intrusion as the Accha stock. They are presumed to have been intruded at substantially the same time as the Accha stock. The andesite dikes have penetrated the Accha stocks and, in the mountains west of Alca, they have penetrated the Alpabamba Formation. Judging from this, the dikes are presumed to have been intruded during the middle of later Miocene.

4-2-3 Chemical Composition of Rocks

Whole rock chemical analysis (covering 13 constituents) was made for 20 rock samples collected during the present fied survey and normative calculations were also performed under CIPW classification. The results of the analysis and normative calculations are presented in Appendix 3.

Described below are the results of analysis of volcanic rocks found in the Survey area according to a simple method of classification of the type of volcanic rocks on the basis of the SiO_2 and $Na_2O + K_2O$ contents (classification method of Middlemost, E.A.K. (1972)) (refer to the classification diagram of Fig. 4-3, after [Petrology II], 1975, Miyashiro and Kushiro).

Chemical analysis of a sample(Ad-1) collected from the Tacaza Group (Tc) distributed in the southwest of Marcabamba shows SiO_2 content of 61.97% and $Na_2O + K_2O$ content of 6.32%. These constituents are plotted around the boundary between non-alkalic andesite and dacite. In this section, the specimen (Ad-1) is seen to be hornblende andesite.

Four rock samples of the Alpabamba Formation (Al) collected in the mountains east and south of Alca (Gc-47 and Ca-13), mountains east of Marcabamba (Gb-93) and from the northeast of the survey area (Gi-83). They show SiO_2 content of 70.01 to 75.43% and $Na_2O + K_2O$ content of 7.97 to 10.17% and can be classified as rhyolite. The Alpabamba Formation manifests conspicuous facies changes and in the field many of the rocks were described as dacite. The sample Ca-13 corresponds to welded tuff, Gc-47 to perlite and the other two samples to dacite to rhyolite in the field observations.

Of the two samples included in the Senca Formation (Vse), the one (Gb-56) obtained northeast of Arma in the east of the survey area show SiO_2 content of 72.31% and $Na_2O + K_2O$ content of 9.22% and can be classified as rhyolite. The other sample (Gd-46), which was obtained near Pampa Huilauro shows SiO_2 content of 58.45% and $Na_2O + K_2O$ content of 6.60% and can be classified as a non-alkalic andesite. The Senca Formation consists mainly of rhyolitic to dacitic volcanic rocks which have a composition similar to that of the sample (Gb-56). The composition of the sample (Gd-46) corresponds to andesite lavas intercalated between the rhyolitic to dacitic volcanic rocks.

Samples derived from the Lower Formation of the Barroso Group (Vbl) show SiO_2 content of 59.48 to 67.35% and $Na_2O + K_2O$ content of 6.26 to 8.19% and can be classified as non-alkalic andesites on dacites. Of these samples, those collected in the southeast of the survey area (Gb-58, Gb-72 and Gb-75) show SiO_2 content of 59.48 to 63.97% and Na2 + K_2O content of 6.26 to 8.19%. On

the other hand, those samples obtained on the southwest of Mt. Firura (Gf-36) contain $Na_2O + K_2O$ of 8.72% and can be plotted around the boundary between dacite and trachyte. That sample obtained west of Mt. Solimana (Gf-52) has SiO_2 of as high as 67.35%. These differences in composition of the samples from the Lower Formation of the Barroso Group may be attributable to the chemical composition of magma which may have varied with the places of eruption. A sample from the Upper Formation of the Barroso Group (Vbu) southeast of Mt. Sara Sara (Gc-304) shows SiO_2 content of 70.96% and $Na_2O + K_2O$ content of 9.55% and can be classified as a rhyolite.

A sample (Ad-6) from the Lampa Volcanic Rocks (Vla) distributed in Marcabamba in the west of the survey area shows SiO_2 content of 61.97% and $Na_2O + K_2O$ content of 7.81% and can be classified as a non-alkali andesite.

A sample (Gb-108) of the lava erupted from Mt. Apainunu in the southeast of the survey area where Mollebamba Volcanic Rocks (Von) are distributed shows SiO_2 content of 60.73% and $Na_2O + K_2O$ content of 7.83% and can be classified as a non-alkalic andesite.

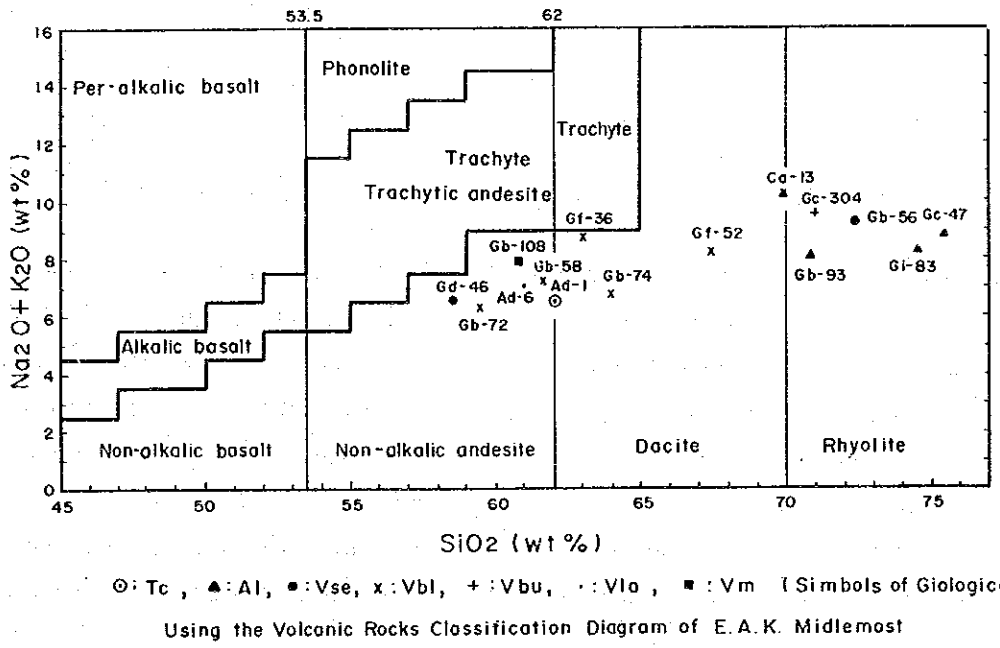

Fig. 4-3 SiO_2 - ($Na_2O + K_2O$) Variation Diagram of Volcanic Rocks

Fig. 4-4 illustrates the relationship between K_2O and MgO based on the results of the chemical analysis of rocks (13 constituents). The diagram of Fig. 4-4 shows that the MgO content tends to decrease with an increase of K_2O, but the rhyolitic rocks of the Alpabamba Formation (Al) have a lower MgO content

than other rocks and a correlation between the MgO content and the K_2O content cannot be established. A sample (Gb-56) from the Senca Formation (Vse) is a rhyolitic rock and exhibits a facies similar to that of the rhyolitic rocks of the Alpabamba Formation, but it shows a higher MgO content than the rhyolitic rocks of the Alpabamba Formation.

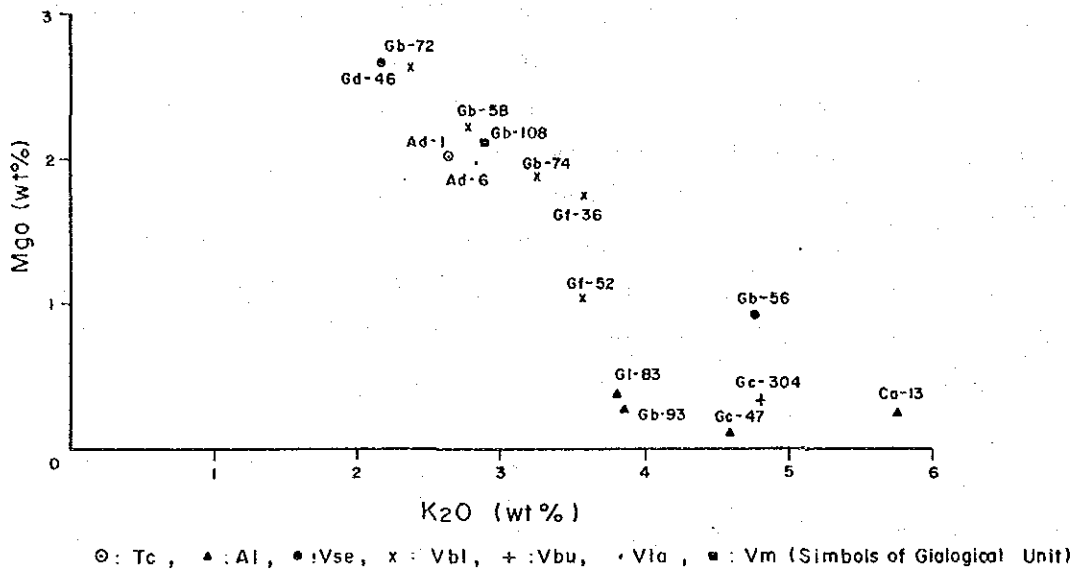

Fig. 4-4 K_2O-MgO Variation Diagram of Volcanic Rocks

With respect to intrusive rocks, whole rock chemical analysis was made for two samples (Gb-110 and Gb-32) of the Coast batholith (CB) and two samples (Af-2 and Ca-4) of the Accha stock. All these samples are granitic in composition and a triangular diagram of quartz - (albite + anorthite) -orthoclase was prepared on the basis of the classification of Bateman etal., (1963) selected from among the various classifications of felsic igneous rocks (Fig. 4-5).

The four samples can be classified as granodiorites. The Coast batholith in the south of the survey area tends to contain a slightly larger quantity of orthoclase.

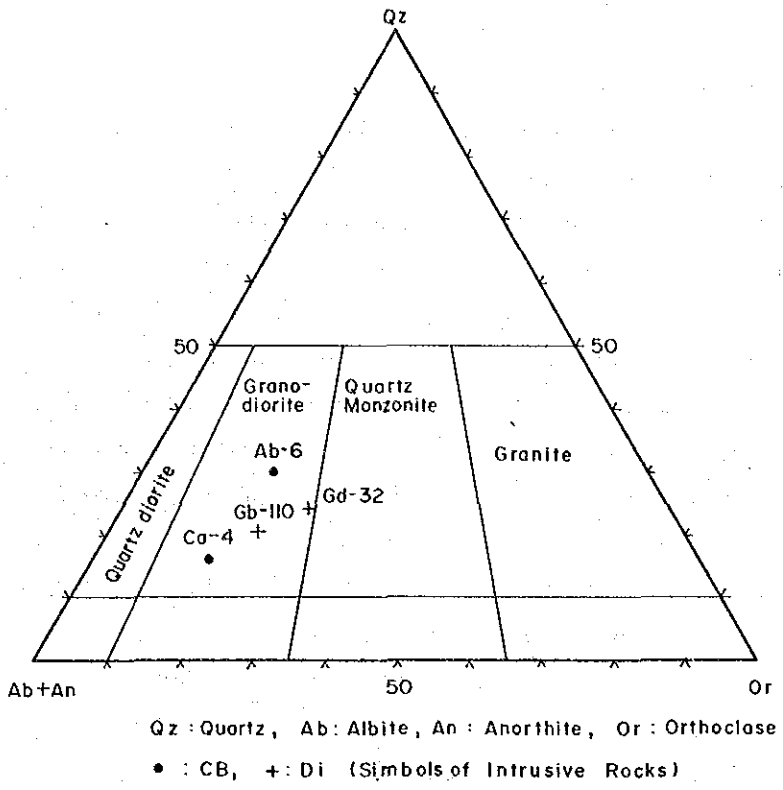

Fig. 4-5 Normative Quartz - Orthoclase - (Albite + Anorthite) Triangular Diagram of Some Igneous Rocks

4-2-4 Geological Structure and History

(1) Geological Structure

The geological structure of the Survey Area is highly characterized by the remarkable folds and faults formed in the Jurassic and Cretaceous rocks by the orogeny of the Andes. In the Tertiary formations strata show a gentle dip locally and small faults are observable. Judging from their scale, the strata in the Tertiary System do not seem to have undergone the effects of a vehement tectonic movement (PL.2, Fig. 4-1).

The folds found in the Jurassic and Cretaceous rocks include a large-scale syncline having a N70°W axis in the Socosani Formation occurring in the south of Mt. Taniseca, an E-W syncline found in the Yura Group west of the village of Velinga on the Cotahuasi River, NW-SE anticline and syncline, N-S anticlines and NE-SW anticlines in that part of the Arcurquina Formation extending from Lancacolla west of the village of Cotahuasi to Taurisma to the northeast.

The folds observed in the Tertiary rocks include small-scale anticlines and synclines with a NNW-SSE axis found in the Tacaza Group west of the village of Carcana in the north of detailed survey area B. No other folds are found in the

strata formed after Cretaceous age.

Faults are developed in the strata formed previous to the middle Miocene. The major faults have NW-SE direction and include a NW-SE fault passing by the village of Saima in the south of the detailed survey area A, an E-W fault in the valley of Palmadeas to the southeast, an NW-SE fault extending from a point east of Lamapa via the south of San Jose de Ushua to the vicinity of Mt. Tanisca and an NW-SE fault running along a valley south of Mina Picha. These faults have throws estimated to be over 1,000 m. Substantially parallel to these large-scale faults are other faults, such as those running across the northeast of Bitama, Mina Luicho and Puca Puca, all found in the west of the survey area, and those passing the valley of Ccolapa and the Chuquibamba River.

NNW-SSE faults are found to the west of Colta, to the east of Pomacocha and in the valley of Anirca northeast of Mina de Huayllura. NE-SW faults are located in a valley east of Quechualla on the Cotahuasi River, east of the village of Cotahuasi, near Puica in the northeast of the survey area and around Sumana east of Puica. All these NNW-SSE and NE-SW faults are on a relatively small scale and some of these have cut the Alpabamba Formation. The NW-SE and NE-SW orientations of fold axes and faults are regionally in substantially consistent with the NW-SE and NE-SW lineaments and the directions of arrangement of circular structures extracted from LANDSAT images. This presumably reflects the basement structure of the survey area.

(2) Geological History

Topographically, the survey area belongs to the Western Cordillera and geologically it is included in the central Andes.

Complex bodies of Precambrian gneissosed granites and diorites form the basement of the survey area.

Strata ranging from Cambrian to Triassic age are not formed in this area. During the upper Jurassic, the thick strata of the Chocolate Volcanic Rocks (Cho) formed by brisk volcanic activities were deposited directly covering the basement complex.

In the late Jurassic crustal movements comparable to the Nevadian orogeny in western North America took place in South America, resulting in noticeable folds and uplifts in Chile and Argentina. In the survey area and vicinity, however, such major crustal movement did not occur, but the Yura Group consisting mainly of thick-bedded sandstones was deposited in thick strata during the period from the late Jurassic to the early Cretaceous. Subsequently, there has taken place

no major crustal movement. During the period from the early to middle Cretaceous, the Murco Formation (Mu) consisting of alternating beds of brown sandstone and shale and the Arcurquira Formation (Ar) composed of thick-bedded limestones were deposited conformably.

During the Cretaceous and the early Cenozoic Coast batholith was intruded all along the western edges of South America, causing the orogenic movement of the Andes accompanied by uplift and folding. The effects of the intrusion of Coastal batholith and the orogeny of the Andes remain conspicuously in the survey area.

The Coast batholith (BC) found in the survey area was intruded during the period from the late Cretaceous to the Palaeocene and this caused the survey area to be uplifted largely to become a landmass. The uplifting resulted in major folding of the Jurassic System and Cretaceous System and they were turned into blocks by faulting.

During the period between the Palaeocene and the Oligocene there was no brisk volcanic activity, and in locally formed sedimentary basins sandstones and conglomerates were deposited. The Huanca Formation (Hc) found northeast of Cotahuasi has been thus formed.

In the Miocene volcanic activity became brisk and in its early stage large quantities of andesitic rocks were erupted at the eroded surface underlain by the Jurassic and Cretaceous rocks to form the Tacaza Group. These andesitic volcanic rocks have been intruded by the Accha stock (Di) and andesite stocks (An) and are accompanied by gentle folds and small-scale faults. Uplift of the area by the Andean orogeny continued during the early Miocene. During the period from the middle to late Miocene brisk volcanic activity brought about eruption of dacitic to rhyoritic rocks to form the Alpabamba Formation (Al) in a wide area and the Huaylillas Formation (Hy) and Senca (Vse) Formation locally. The Altiplano plateau ranging in height from 4,000 to 5,000 m localed in the survey area was substantially formed by the volcanic activities during the Miocene.

With the advent of the Pleistocene volcanic rocks consisting mainly of andesite lavas were poured out at the surfaces by eruptions and these lavas formed Mt. Solimana (6,093 m) rising above the Altiplano plateau and other mountains ranging in height from 5,500 to 6,000 m and flowed out over a wide range burying the neighboring lowlands. The Barroso Group (Vbl) was formed by these lava flows. In the late Pleistocene glaciers were formed on the high mountains, producing moraines in neighboring areas.

Large-scale volcanic activity did not take place during the Holocene, but the flow of basalt lava (Vbl, Vm) and the formation of volcanic sediments took place

locally. Alluvium was deposited along rivers and lowlands in the Altiplano plateau almost simultaneously with these minor extrusions.

4-2-5 Alteration and Mineralization

The occurrence of more than 17 large or small alteration zones and mineralized zones were confirmed by the present survey. Of the samples collected during the field survey, 25 were put to X-ray diffraction for identification of minerals, 22 others served for determination of ore minerals by microscope and still 24 others put to ore analysis (5 constituents). The results of these analyses are presented in Apx. 5, 6 and 8.

The alteration zones and mineralized zones in the survey area are described below.

(1) Distribution

The alteration zones and mineralized zones in the survey area are shown in Fig. 4-6 and PL.10. These zones are distributed mainly in the Jurassic and Cretaceous rocks and in the Tacaza Group of the Tertiary. Major among them are a) Mina Pararapa, b) Minas de Huayllura (East of Tanisca), c) West of Tanisca, d) Mina Luicho, e) Mina Picha, f) South of Maran, g) Oyolo and h) Pirca.

(2) General Description of Alteration Zones and Mineralized Zones

The alteration zone can be grouped according to the type of alteration into 1) white alteration with silicification, 2) brown alteration with silicification and argillization and 3) brown alteration contaminated with ferrous oxide (Fig. 4-6 and PL.10).

White alteration zones with silicification consist primarily of a combination of quartz and alunite and is locally accompanied by kaolinite. The major alteration zones of this type include the northern part of the alteration zone of West of Tanisca, the alteration zone of Pirca and the northeastern part of the Oyolo alteration zone. The south of Sara Sara zone and the alteration zone of Algodon Pascana are also classified as the white alteration zone with silicification.

Brown alteration zones with silicification and argillization consist mainly of quartz, with subordinate sericite, halloysite, montmorillonite, and Kaolinite. The alteration zones of this type include a) the area adjacent to Mina Pararapa, b) the area adjoining Mina de Huayllura, c) southern part of the alteration zone of West of Tanisca and g) the southwestern part of the Oyolo alteration zone.

Brown alteration zones contaminated with ferrous oxide are characterized by contamination with brown ferrous oxide taking place along fractur zones, joints and cracks. The alteration zones of this type include many alteration zones including b) Minas de Huayllura and d) Mina Luicho.

A skarn zone consists of garnet skarns and is found in Mina Picha.

White alteration with silicification is observed mainly from the Tacaza Group up to the Lower Formation of the Barroso Group and brown alteration accompanied by silicification and argillization is observable from the Yura Group up to the Tacaza Group. Thus some strata-bound is considered to exist for alteration.

Mineralization includes vein type mineralization of quartz veins bearing gold and silver; mineralization of gold and silver found in the zones of contamination with ferrous oxide along fractur zones and joints; contact metasomatic mineralization of gold, silver, copper, lead, zinc and magnetite occurring in skarns found in the area of contact between intrusive rocks and limestones; and pyritization of desimination type observable in and around intrusive rock bodies.

The mineralized zones with confirmed outcrops of gold-silver bearing quartz veins include a) Mina Pararapa, Copacahuana Mine in the Minas de Huayllura (b) and f) the south of Maran. In Mina Luicho the mineralized zone is locally accompanied by quartz veinlets which lack continuity.

(3) Detailed Description of Alteration Zones and Mineralized Zones

Table 4-2 and 4-3 show the scale, host rock, and characteristics of alteration and mineralization of each zone. The eight major mineralized zones are described below in detail.

a) Mina Pararapa

This zone contains an alteration zone which is about 1 km wide and extends about 2.5 km north to south. Almost in the middle of this zone is found a N20°W, 80°NE quartz vein bearing gold and silver. The quartz vein has been prospected through tunnels until very recently. The total length of the tunnels is nearly 700 m (position of the tunnels is shown in Fig. 4-7 and their geological sketches in Figs. 4-9 and 4-10).

The geology of the mine and vicinity consists of andesitic volcanic breccias (Tacaza Formation) which have undergone brown alteration and accompanied by silicification and argillization and altered (pyritized and chloritized) porphyritic andesite dikes intruded into the breccias. The gold-silver bearing quartz veins comprise the main vein found in the altered andesite dikes, parallel veins found around these dikes and veinlets formed in the altered andesitic volcanic breccias.

Table 4-2 List of Alteration Zones and Mineralized Zones - (1) (Major)

Name	Location	Scale	Host rock	Alteration	Mineralization
Mina Pararapa	Approx. 20 km North-northeast of Cotahuasi	1 km × 2.5 km	Andesite dikes (An) and Andesitic volcanic rocks (Tacaza Group)	•Brown altered zone contaminated by ferrous oxide •Hydrothermal alteration consisting primarily of silicification (quartz + halloysite, cb-11 quartz + montmorillonite cb-13) •The andesite dikes are chloritized and contaminated by pyrites.	•Mineralization of gold and silver in N20°W and 80°NE gold-silver bearing quartz veins •Quartz vein being prospected by tunnels is 0.5 to 1.5 m wide and 1.3 km long. •According to the mine data, the grade of gold ore is Au, max. 40 g/ton and average 4.6 g/ton. •The average grades of gold and silver ores contained in quartz dikes of 80 cm in width are Au 4.6 g/ton and Ag 288 g/ton.
Minas de Huayllura (East of Tonisca)	Approx. 30 km west-southwest of Cotahuasi	1∿2 km × 10 km	Quartzite (Yura Group)	•Brown altered zone contaminated by ferrous oxide •Hydrothermal alteration accompanied by quartz veinlets (quartz + sericite Bb-10 quartz + diaspore + sericite + jarosite Bb-9)	•Mineralization exists in oxidized zones occurring along fracture zones and joints and in gold-silver bearing quartz veins •Abandoned small-scale adits are found at several locations •Analysis of the quartz veins of Mina Copacahuana shows the grades of Au and Ag are 4.6 g/ton and 288 g/ton, respectively.
West of Tanisca	Approx. 33 km west-southwest of Cotahuasi and approx. 23 km east-southeast of Pausa	1.5 km × 4 km	Andesitic volcanic rocks (Tacaza Group)	•Essentially hydrothermal alteration of quartz + alunite and quartz + sericite + montmorillonite •Relationship between both types of alteration is not clear.	•Conspicuous mineralization not observable. •Analysis of altered rocks containing clay minerals revealed the content of Au 0.06 g/ton and Ag 0.31 g/ton.
Mina Luicho	Approx 5 km northeast of Pausa	1 km × 2 km	Quartzite (Yura Group)	•Silicification around quartz veinlets and contamination with ferrous oxide. (quartz + scorodite (Ae-22)	•Gold-silver bearing quartz veinlets and contamination with ferrous oxide are observable. Orientation of the veinlets is not clear. •A dozen or so small-scale stopes are scattered. •Spot samples from the stopes showed Au 26.0 g/ton, Ag 114.1 g/ton and Au 9.7 g/ton, Ag 30.2 g/ton.
Pirca	Apprqx. 15 km south of Pirca	2 km × 5 km	Andesite and pyroclastic rocks (Tacaza Group and lower part of Barroso Group)	•Mostly hydrothermal alteration of quartz + alunite.	•Contaminated with goethite near Pirca. •Vein-type mineralization not observable. •Analysis of samples from the zone contaminated with goethite showed the grade of Ag 0.6 to 1.6 g/ton.

Table 4-2 (Continued)

Name	Location	Scale	Host rock	Alteration	Mineralization
South of Maran	Approx. 15 km south-southeast of Pausa	1.5 km × 3.5 km	Andesitic tuff to tuff breccia (Chocolate Formation)	•Silicification around quartz veinlets, veinlike silicification and contamination with ferrous oxide.	•Gold-silver bearing quartz veins about 10 cm wide and contamination with limonite around fracture zones are observable as several locations. •Analysis of samples from pyrite-quartz veins (5 to 10 cm wide) showed the grades of Au 1.1 g/ton and Ag 0.3 g/ton. •There are many abandoned old adits. In downstream areas river sediments are washed for gold.
Oyolo	Approx. 20 to 25 km northeast of Pausa	2 km × 8 km	Dacitic pyroclastic rocks (Tacaza Formation to Alpabamba Formation)	•Hydrothermal alteration (primarily argillization). In the northeast cristobalite + alunite and in the southwest quartz + sericite	•Locally accompanied by contamination with ferrous oxide (grade: Ag 0.3 g/ton) •Conspicuous mineralization not observable.
Mina Picha	Approx. 22 km west-southwest of Cotahuasi	Small ore bodies scattered in an area of approx. 1 km × 2 km	Limestone (Arcurquina Formation) and diorite (stock)	Skarn type metasomatism (garnet (andradite) - calcite-quartz)	•Skarn type •Mineralization of Cu, Pb, Zn, Ag and Au. •Ore bodies are small lens-shaped bodies. •Analysis of mineral ores consisting mainly of galena and sphalerite showed the following grades: Au 7.7 g/ton, Ag 770 g/ton, Cu 1.38%, Pb 23.4%, Zn 21.6%

Table 4-3 List of Alteration Zones and Mineralized Zones - (2)
(Minor Alteration Zones, Small Mineralized Zones)

Name	Location	Scale	Host rock	Alteration or metamorphism	Mineralization
East of Colta alteration zone	Approx. 13 km north-northeast of Pausa	0.5 km × 1 km	Andesite (Tacaza Formation)	·Hydrothermal alteration (silicification + argillization) (quartz + sericite)	·Mineralization not observable
Sequella alteration zone	Approx. 20 km north of Pausa	0.5 km × 2.5 km	Andesite (Tacaza Formation)	·Hydrothermal alteration (silicified veins + argillization) (quartz + orthoclase + sericite) ·Contamination with pyrite	·Silicified veins of 1 to 2 m in width (N 45°E, 70°N) ·Assay results Au 0.19 g/t, Ag 17.5 g/t ·Old adits of several meters in length are found
South of Sara Sara alteration zone	Approx. 17 km southwest of Pausa	2 km × 2 km	Andesite (Barroso Group)	·Silicification ·Grey and porous silicified rocks	·Mineralization not observable
Mina Puca Puca	Approx. 20 km southeast of Pausa	Unknown	Unknown	Unknown	·Mineralization of Cu (malachite) Grade unknown
Mina Jatunsana	Approx. 27 km southeast of Pausa (local information)	Unknown	Unknown	Unknown	·Gold mine (local information)
Huauhua mineralization zone	Approx. 5 km west-northwest of Cotahuasi	Approx. 10 m × 50 m Two unknown location	Limestone (Arcurquina Formation diorite (stock)	Skarn type (clinopyroxene-calcite)	·Magnetite mineralization
Lucha mineralization zone	Approx. 13 km northeast of Cotahuasi	5 m × 30 m ?	Andisitic tuff (?) (Huanca Formation)	Hornfels to Skarn	·Magnetite mineralization concentrated in layers
Puica alteration zone	Approx. 30 km northeast of Cotahuasi	1 km × 1.5 km	Rhyolite, rhyolitic tuff (Alpabamba Formation)	White argillization alteration and locally contaminated with ferrous oxide. Accompanied by mordenite (quartz - mordenite) locally.	·No mineralization
Algodon Pascana alteration zone	Approx. 35 km east of Coltahuasi	0.4 km × 2.5 km	Andesite ? (Tacaza Formation)	·Quartz + alunite alteration ·Locally contaminated with ferrous oxide.	·No mineralization

Judging from its outcrop, the main quartz vein seems to continue about 1.3 km with an estimated width of 0.5 to 1.5 m. According to unpublished data of the Mina Pararapa, the highest grade of ores found in tunnels (No. 3 Adit) are 40 g/ton for Au and 1,228 g/ton for Ag and the average grades for the adit about 200 m in length and 0.9 m in width are 4.6 g/ton for Au and 173 g/ton for Ag. The outcrop of the quartz vein and the geology of the No. 3 Adit are as shown in Fig. 4-9.

The chemical analyses of ore samples from the quartz veins are shown in Table 4-4.

Table 4-4 Chemical Analyses of Ore Samples in the Mina Pararapa

Sample No.	Location	Thick-ness	Metal contents					Remarks
			Au (g/t)	Ag (g/t)	Cu (%)	Pb (%)	Zn (%)	
Cb-11	No. 1 adit Fig. 4-5	0.8 m	4.6	288.0	0.01	0.03	0.01	Quartz vein
Cb-12	No. 2 out-crop	0.5 m	0.2	12.8	<0.01	<0.01	<0.01	Quartz vein
Cb-13	No. 3 adit Fig. 4-4	1.3 m	1.4	131.6	<0.01	0.01	<0.01	Quartz vein and network quartz vein
CB-19	No. 5 adit	-	<0.06	23.0	0.02	0.08	0.18	Quartz vein

The results of microscopic observations of ore samples under polished section are presented in Table 4-5.

Table 4-5 Mineral Assemblage of Ore Samples in the Mina Pararapa

Sample No.	Location	Ore Minerals	Gangue Minerals	Remarks
Cb-14	No. 4 adit	py o	qz ◎ , pl ◎ , ch ◎ , sr o , ab o	Altered porphyritic andesite dike
Cb-18	No. 5 adit	py ◎	qz ◎ , pl ◎ , ch ◎ , sr o , ab o	Altered porphyritic andesite dike
Cb-19	No. 5 adit	py o , cp • , sp •	qz ◎ pl ◎	Quartz vein (waste)
Cb-20	No. 5 adit	py o	qz ◎ , pl ◎	Banded quartz vein (waste)

◎: Abundant, o: Common, •: Rare, py: Pyrite, cp: Chalcopyrite, sp: Sphalerite, qz: Quartz, ch: Chlorite, sr: Sericite, ab: Albite

b) Minas de Huayllura (East of Tanisca)

Many traces of small-scale mining sites were found in the alteration zone 1 to 2 km in width and nearly 10 km in length (five such traces confirmed). All these traces are located on steep mountain slopes (Fig. 4-8). The geology of the mine and vicinity consists of sandstones of the Yura Group, red shales of the Murco Formation, limestones of the Arcurquina Formation and andesitic volcanic rocks of the Tacaza Group (PL.6).

Mineralization is observable in small-scale gold-silver bearing quartz veins found in brown alteration zones contaminated by ferrous oxide along joints developed in sandstone beds and fracture zones in the Yura Group and it is also observed in gold-silver bearing brown ferrous oxide veins formed along the above-mentioned joints and fracture zones. In the Copacahuana Mine (Fig. 4-11) a quartz vein about 1.2 m in width (locally in network veinlets) is found and it continues about 35 m from the mouth of the adit in N80°E direction dipping 80° to 90°S and is cut by an N20°W·50°NE fault accompanied by a fracture zone of about 3 m in width.

Other abandoned adits, all on a small scale, were used to prospect the belts contaminated with ferrous oxide found along fracture zones or cracks.

The results of chemical analysis of ore samples obtained in the Minas de Huayllura and Microscopic observations of polished sections of the samples are shown in Tables 4-6 and 4-7, respectively. The positions of the adits of the mine are given in Fig. 4-8.

Table 4-6 Chemical Analyses of Ore Samples in the Minas de Huayllura

Sample No.	Location	Thick-ness	Metal contents					Remarks
			Au (g/t)	Ag (g/t)	Cu (%)	Pb (%)	Zn (%)	
Bb-6	No. 1 adit (Mina Copa-cahuana)	1.20 m	1.9	7.2	<0.01	0.03	0.02	Quartz vein
Bb-9	No. 2 adit	0.40 m	0.4	5.0	<0.01	0.08	<0.01	Shared zone
Bb-12	Old crusher	-	0.06	2.5	<0.01	0.35	0.05	Crushed sample

Table 4-7 Mineral Assemblage of Ore Samples in the Minas de Huayllura

Sample No.	Location	Ore mineral	Gangue mineral	Remarks
Bb-4	No. 1 adit (Mina Copacahuana)	hm ◎	qz grain ◎	Ore stock
Bb-8	West of No. 1 adit	py ◎ , hm ◎	qz ◎	Waste of quartz vein

c) West of Tanisca

This zone is a white alteration zone accompanied by silicification and argillization. The zone is 1.5 km wide and 4 km long. As shown in from the results of chemical analyses of ore samples (Table 4-8) conspicuous mineralization is not observable in this alteration zone. As noted later, however, a geochemical anomaly of gold was detected in this zone.

Table 4-8 Chemical Analyses of Altered Rocks in the West of Tanisca

Sample No.	Mineral assemblage	Metal contents					Remarks
		Au (g/t)	Ag (g/t)	Cu (%)	Pb (%)	Zn (%)	
Bf-1	qz ◎ , al ◎	-	-	-	-	-	Porphyritic altered rock
Bf-2	qz ◎ , sr o , mon •	0.06	0.31	<0.01	<0.01	<0.01	white altered rock

◎: Abundant, o: Common, •: Rare, qz: Quartz, al: Alunite,

sr: Sericite, mon: Montmorinite

d) Mina Luicho

This zone is a brown alteration zone contaminated with ferrous oxide. The zone is about 1 km wide and about 2 km long. Ore deposits are located substantially in the middle of the zone and about a dozen traces of small-scale prospecting (adits are mostly 2 to 3 m long and very few are about 20 m long) are scattered in an area of 500 m by 500 m. Chemical analysis of local ore samples obtained from a belt contaminated with ferrous oxide and formed along cracks at one of the abandoned pits shows high grades of Au and Ag (Au 26.0 g/ton and Ag 114 g/ton). Quartz veinlets lacking continuity are slightly observed in this alteration zone. The zone generally consists of belts contaminated with ferrous oxides and veins are hardly found.

Table 4-9 Mineral Assemblage and Chemical Analyses of Ore Samples in the Mina Luicho

Sample No.	Mineral assemblage	Metal contents					Remarks
		Au (g/t)	Ag (g/t)	Cu (%)	Pb (%)	Zn (%)	
Ae-20	qz ◎	9.67	30.17	<0.01	0.03	<0.01	Porous silicons rock
Ae-22	qz ◎ , sco o	26.00	114.14	0.05	0.02	<0.01	Quartz veinlets and iron oxides

◎ : Abundant, o: Common, qz: Quartz, sco: Scorodite

e) Pirca

The alteration zone is about 2 km wide and about 5 km long and consists of a white alteration zone accompanied by silicification and argillization and a brown alteration zone contaminated with ferrous oxide. This zone contains irregular lens-shaped assemblages of ferrous oxides, but veins are not observable.

Alunite is characteristically contained in the white alteration zone and mineralization of a very small quantity of silver is observable in the ferrous oxide-contaminated zone.

Table 4-10 Mineral Assemblage and Chemical Analyses of Ferrous Oxides in the Pirca Alteration Zone

Sample No.	Mineral assemblage	Metal contents					Remarks
		Au (g/t)	Ag (g/t)	Cu (%)	Pb (%)	Zn (%)	
Gi-102	hm •	<0.06	<0.31	<0.01	<0.01	<0.01	Silicified rock
Gi-104	hm o , gt o	<0.06	0.62	<0.01	<0.01	<0.01	Silicified rock
Gi-113	hm o , gt o	<0.06	1.56	0.01	<0.01	<0.01	Iron oxides

o: Common, •: Rare, hm: Hematite, gt: Goethite

Table 4-11 Mineral Assemblage of Altered Rocks in the Pirca Alteration Zone

Sample No.	Mineral Assemblage	Remarks
Gi-104	qz ◎ , gt o	Iron oxides
Gi-106	qz ◎ , km ◎ , al ◎	White altered rock (silicified)
Gi-108	qz ◎ , al ◎	White altered tuff
Gi-113	qz ◎ , gt o	Iron oxides

◎ : Abundant
o: Common
qz: Quartz
gt: Goethite
km: Kaorinite
al: Alunite

f) South of Maran

A brown alteration zone contaminated by ferrous oxides is found in this area. The zone is about 1.5 km wide and about 3.5 km long. Gold and silver mineralization is observed in quartz veinlets about 10 cm in width and ferrous oxide contaminated belts along fracture zones and joints, but the mineralization is weak and individual ore deposits are small in scale. A number of small abandoned adits where manual digging was carried out are scattered in this area. Some of these adits are still used for prospecting and mining on a small scale. Ores are carried out manually and crushed, and after panning, gold is recovered using mercury. In the downstream of a stream running across this mineralization zone river sediments are washed for gold.

Table 4-12 Mineral Assemblage and Chemical Analysis of Ore Samples in the South of Maran

Sample No.	Mineral assemblage	Metal contents					Remarks
		Au (g/t)	Ag (g/t)	Cu (%)	Pb (%)	Zn (%)	
Ge-88	hm o , py ·	-	-	-	-	-	Quartz vein (lenticular)
Ge-104	py o	1.06	0.31	<0.01	<0.01	<0.01	Quartz vein (thickness 5∿10 cm)
Ge-104'	py o	-	-	-	-	-	Quartz vein (thickness 5 cm)

o: Common, ·: Rare, hm: Hematite, py: Pyrite, -: No assay

g) Oyolo

The alteration zone of this area consists of a white alteration zone accompanied by silicification and argillization and a brown alteration zone contaminated with ferrous oxides. The zone is about 2 km wide and nearly 8 km long. There are no traces of previous prospecting activities in the zone and with the exception of some mineralization of pyrites, no major mineralization is observed in this area. Part of the ferrous oxide contaminated belts contains a very small quantity of silver (0.3 g/ton).

Table 4-13 Mineral Assemblage and Chemical Analysis of Altered Rocks in the Oyolo Alteration Zone

Sample No.	Mineral assemblage	Metal contents					Remarks
		Au (g/t)	Ag (g/t)	Cu (%)	Pb (%)	Zn (%)	
Gb-99	Cr ◎ , al ◎ kn o , mon •	-	-	-	-	-	White altered rock
Gb-100B	————	<0.06	0.31	<0.01	<0.01	<0.01	Light brown altered rock
Gb-102	qz ◎ , sr o	-	-	-	-	-	White altered rock

◎: Abundant, o: Common, •: Rare, Cr: Cristobarite, al: Alunite, km: Kaolinite, mon: Montmorillonite, qz: Quartz, Sr: Sericite, -: No assay

h) Mina Picha

A skarn zone and ferrous oxide contaminated zone 1 km in width and nearly 2 km in length are formed in the contact zone between quartz diorite (Di) bodies and limestone beds of the Arcurquina Formation (Ar). The ore deposits consist of small-scale lens-shaped massive ore occurring in skarns and impregnated ores. Massive ores consist mainly of galena and sphelerite and also contain chalcopyrite, pyrite and native gold. The impregnated ores consist mainly of impregnated pyrites and contain a small quantity of tennantite, tetrahedrite and bornite. The skarn which forms the host rock is a garnet skarn composed of quartz, light green garnet, orthoclase and calcite.

In this zone silicified altered veins (BgM-1) in sandstones close to quartz diorite bodies and dark grey silicified veins (BgM-2 and BgM-3) in quartz diorite bodies are found and mineralization of silver is observed in these silicified veins.

Table 4-14 Chemical Analyses of Ore Samples in the Mina Picha

Sample No.	Metal contents					Remarks
	Au (g/t)	Ag (g/t)	Cu (%)	Pb (%)	Zn (%)	
BgM-1	0.06	87.05	<0.01	0.15	<0.01	Strong silicified altered vein
BgM-2	0.12	59.71	0.03	0.01	0.02	Darkgrey silicified vein
BgM-3	0.12	345.21	0.36	0.06	0.06	Darkgrey silicified vein (thickness 0.4 m)
BgM-7	0.06	3.11	<0.01	<0.01	0.03	Skarn
BgM-10	7.7	777	1.38	23.4	21.6	Massive ore

Besides the alteration and mineralization zones described in a) to h) above, a number of other alteration zones and mineralized zones are found in the survey area, but mineralization is generally weak in these other zones (Table 4-3 and Fig. 4-6).

(4) Orcopampa

The Orcopampa Mine and vicinity where a geochemical exploration was carried out by way of a model survey for a mineral deposit is located in the distribution area of the Tacaza Group (Tm-vor of Apx.11) composed of andesite lavas and pyroclastic rocks of same nature. Ore deposits in this mine are vein type deposits formed along faults in the pyroclastic rocks and include such known veins as Mant, Calera, Tudela and Santiago. These veins are arranged about 800 m apart and substantially parallel with one another. They strike NE to SW and dip to SE or NW at 55° to 80°.

The Mant vein is the largest ore body and bonanza zones of about 6 m in maximum width and of 20 to 150 m in length are arranged intermittently. In other veins bonanzas are locally formed in the bends of the veins or branch veins, but these bonanzas are generally on a small scale.

Ore minerals contained in the ores of the Orcopampa Mine include silver-bearing tetrahedrite, galena, sphalerite, chalcopyrite, bornite, polybasite and native gold. Gangue minerals include pyrite, rhodochrosite and barite. These minerals generally consist of fine-grained crystals and occur by dissemination in banded parts of quartz veinlets and in country rocks as dissiminated minerals. Quartz veinlets contain pink rhodochrosites and are regarded as a guide to exploration of ore bodies. Similar vein type deposits have not been known in the Cotahuasi area.

(5) Mineralization Zones Outside Survey Area

The gold mine of Curuz Vuelta and the silver mine of Huayllacha are located in the Chururopampa area bordering the survey area on the southwest. The Curuz Vuelta deposit consist of gold bearing quartz clay veins occurring in an altered diorite body and are about 0.5 m wide and nearly 300 m long. They are located in flat lands and the mineralization zones are covered by alluvial deposits. Small-scale prospecting and mining are still carried out in the same way as the drilling of a well. There is a possibility of mineralized zones similar to the known deposits existing under the alluvium in the flat lands of the Chururopampa area (Apx.27).

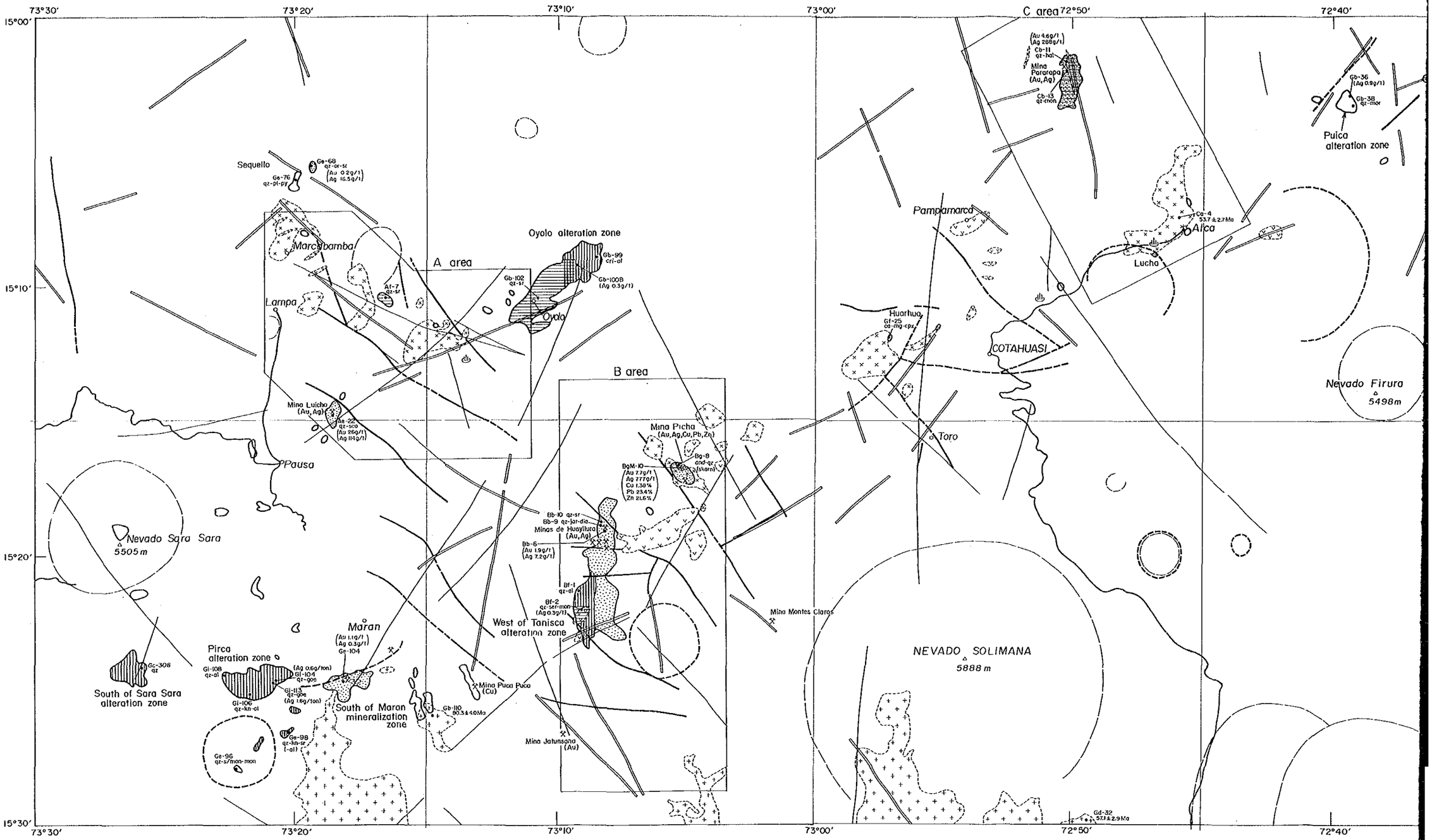
73°30′
73°20′
73°10′
73°00′
72°50′
72°40′
15°00′
15°10′
15°20′
15°30′
A area
B area
C area
Sequello
Ge-68
qz-or-sf
(Au 0.2g/t)
(Ag 16.5g/t)
Ge-76
qz-pl-py
Marcobamba
Lampa
Af-7
qz-sf
Oyolo alteration zone
Gb-99
cri-af
Gb-102
qz-sf
Gb-100B
(Ag 0.3g/t)
Oyolo
Mina Luicha
(Au, Ag)
Ae-22
qz-scp
(Au 26g/t)
(Ag 114g/t)
Pausa
Mina Picha
(Au, Ag, Cu, Pb, Zn)
Bg-8
qad-qz
(skarn)
BgM-10
(Au 7.7g/t
Ag 777g/t
Cu 1.38%
Pb 23.4%
Zn 21.6%
Bb-10 qz-sr
Bb-9 qz-jar-dia
Minas de Huayllura
(Au, Ag)
Bb-6
(Au 1.9g/t)
(Ag 7.2g/t)
Bf-1
qz-ol
Bf-2
qz-ser-mon
(Ag 0.3g/t)
West of Tanisca
alteration zone
Nevado Sara Sara
5505 m
Maran
(Au 1.1g/t)
(Ag 0.3g/t)
Ge-104
Pirca
alteration zone
Gi-108
qz-ol
(Ag 0.6g/ton)
Gi-104
qz-ser
Gi-113
qz-ser
(Ag 1.6g/ton)
Gi-106
qz-ka-ol
Gc-306
qz
South of Sara Sara
alteration zone
South of Maran
mineralization zone
Ge-98
qz-ka-ser
(-ol)
Ge-96
qz-sr/mca-mon
Mina Puca Puca
(Cu)
Gb-110
80.3±4.0Ma
Mina Jatunsaya
(Au)
Mina Montes Claros
NEVADO SOLIMANA
5888 m
Gd-32
57.1±2.9Ma
Pampamarca
Huarhua
Gf-25
ca-mg-cpx
COTAHUASI
Toro
Lucha
Alca
Cg-4
53.7±2.7Ma
(Au 4.6g/t)
(Ag 208g/t)
Cb-11
qz-hal
Mina
Pararopa
(Au, Ag)
Cb-13
qz-mon
Puica
alteration zone
Gb-36
(Ag 0.8g/t)
Gb-38
qz-mor
Nevado Firura
5498m

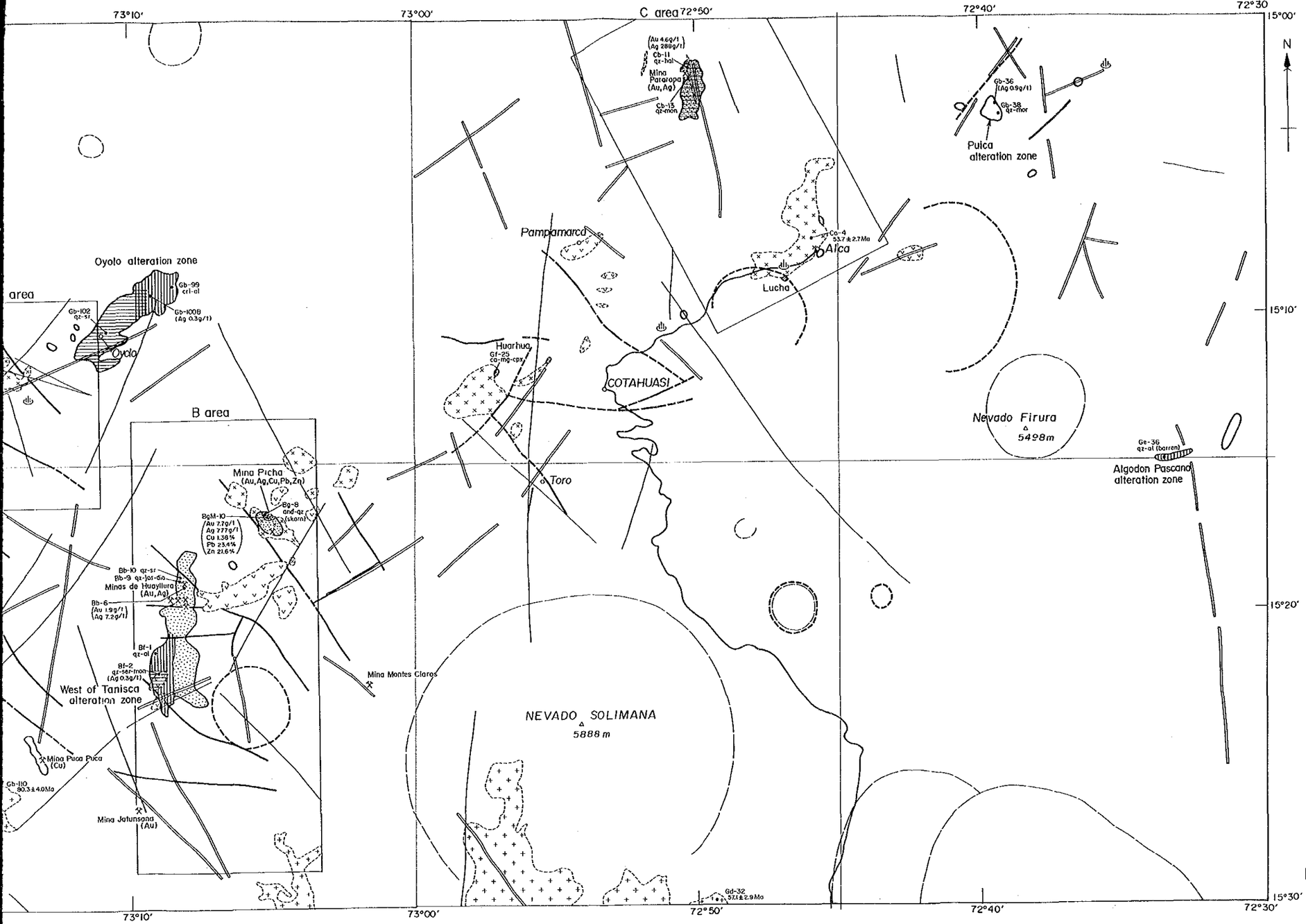

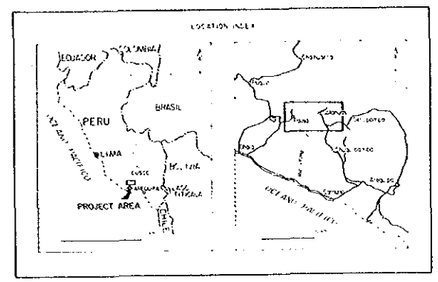

0 — 5 — 10km

LEGEND

Alteration zone

- mainly silicification (qz ± ol ± kn)
- silicification + argillization
- others (iron oxides stained zone)
- skarn
- Bf-2 samples
- mineralization zone
- mine
- hot spring

Intrusive rocks

- Batholith granitic rocks
- Stock dioritic rocks
- Stock and dyke andesitic rocks

- lineament (Landsat)
- fault
- lineament (aerial photograph)
- Curvicular structure (Landsat)
- Curvicular structure (aerial photograph)

minerals

qz	:	quartz
pl	:	plagioclase
or	:	orthoclase
ol	:	olunite
kn	:	kaolinite
hal	:	halloysite
sr	:	sericite
mon	:	montmorillonite
s/mon	:	sericite-montmorillonite mixed layer
dia	:	diaspore
mor	:	mordenite
and	:	andradite
cpx	:	clinopyroxene
co	:	calcite
py	:	pyrite
mg	:	magnetite
goe	:	goethite
sco	:	scorodite
jar	:	jarosite

Fig. 4-6 Location Map of Alteration and Mineralized Zones

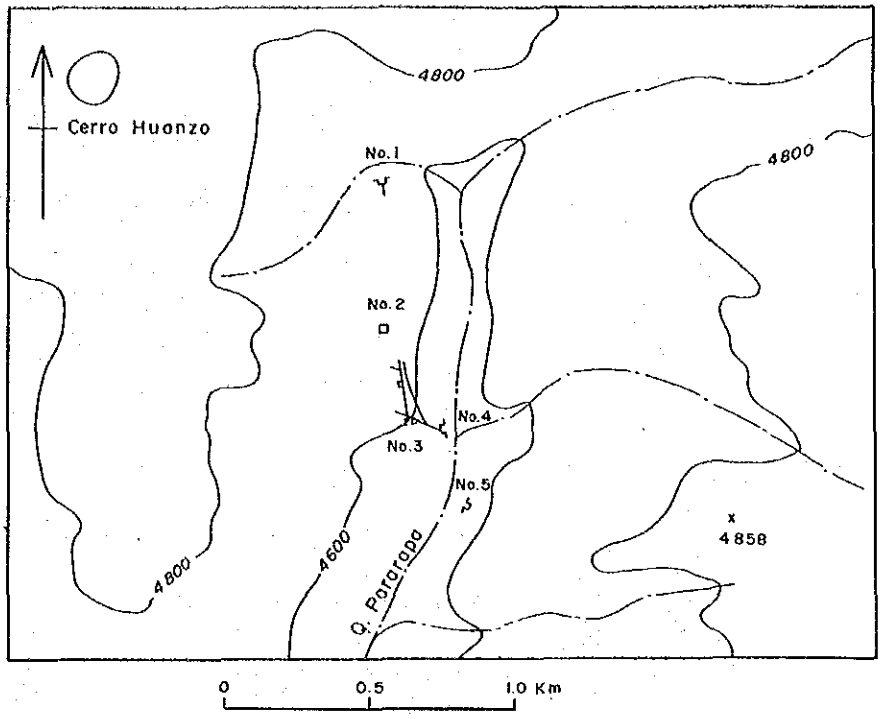

Fig.4-7 Location Map of Adits in the Mina Pararapa.

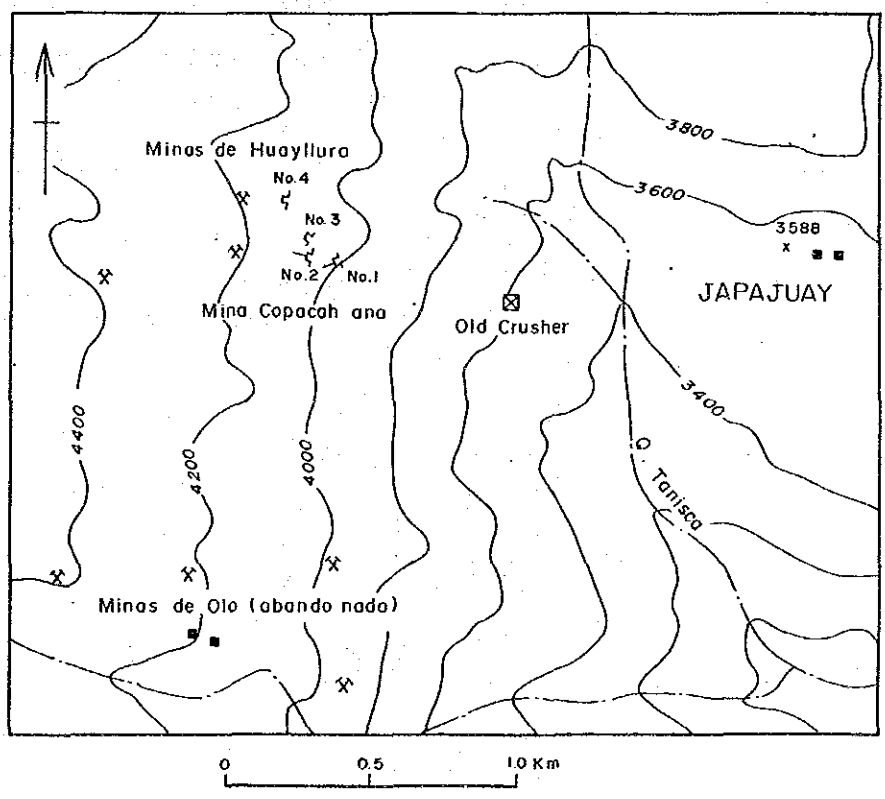

Fig.4-8 Location Map of Adits in the Minas de Huayllura.

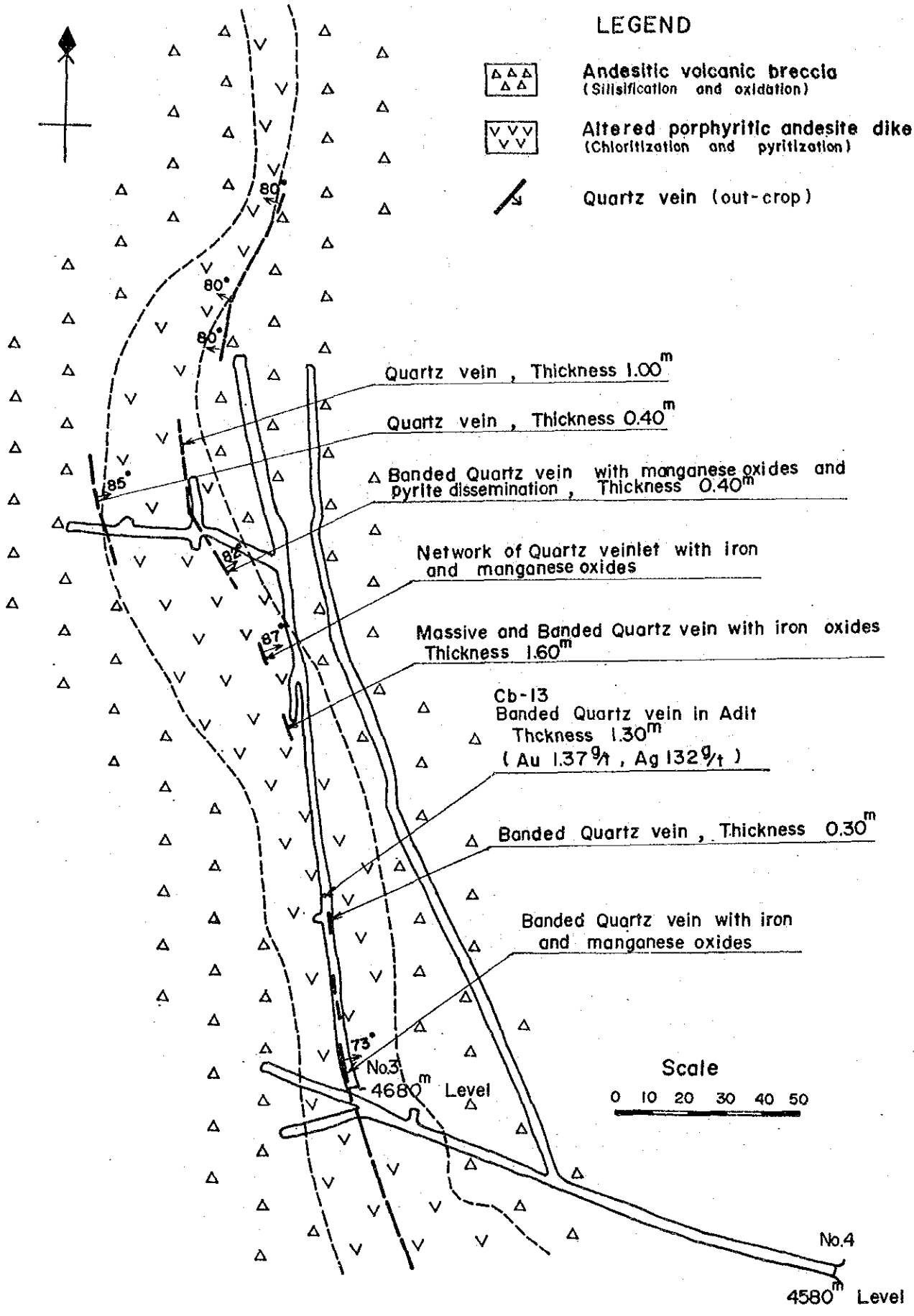

Fig.4-9 Location map of Quartz vein in the Mina Pararapa

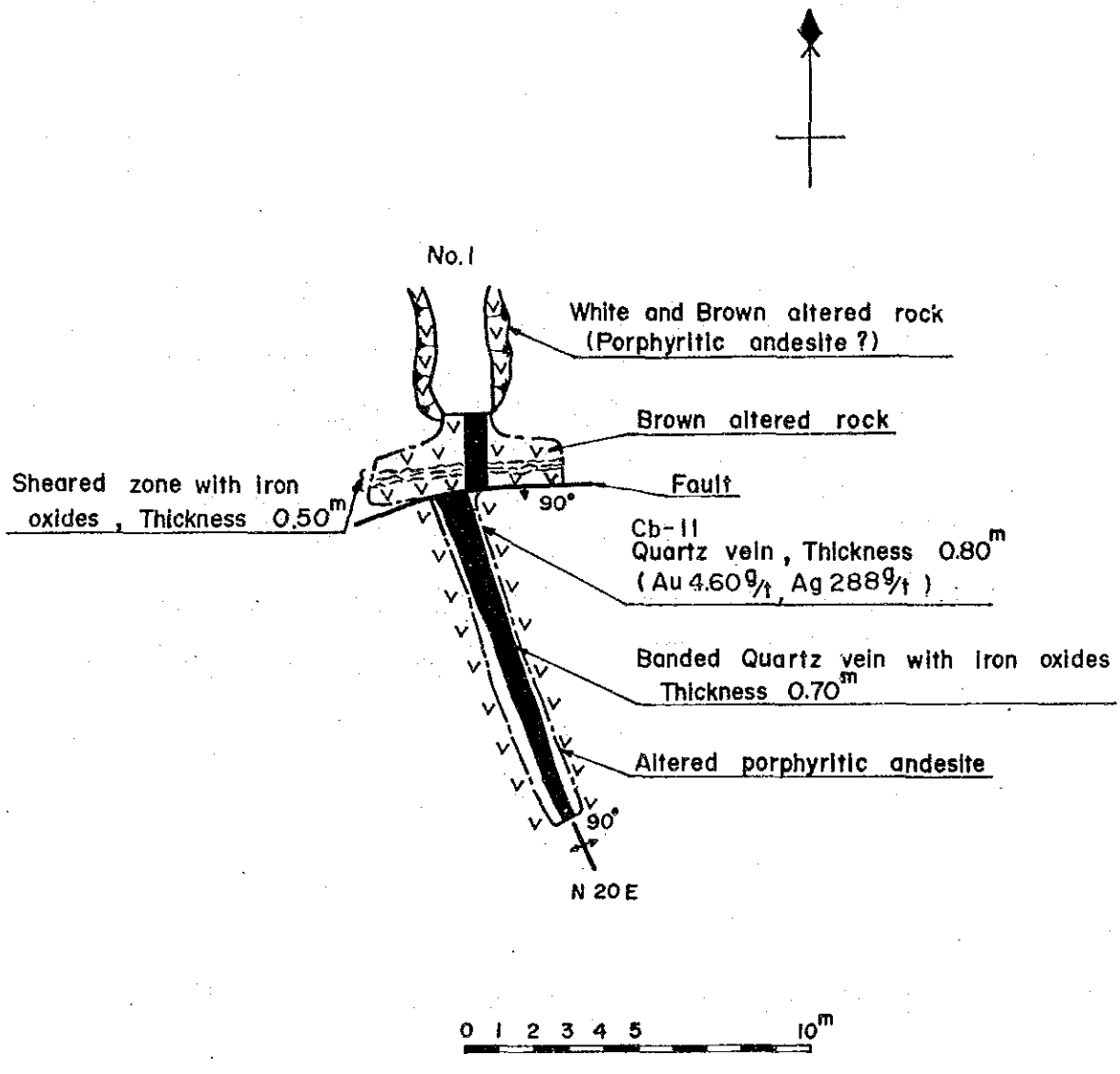

Fig.4-10 Geological Sketch of Adit in the Mina Pararapa

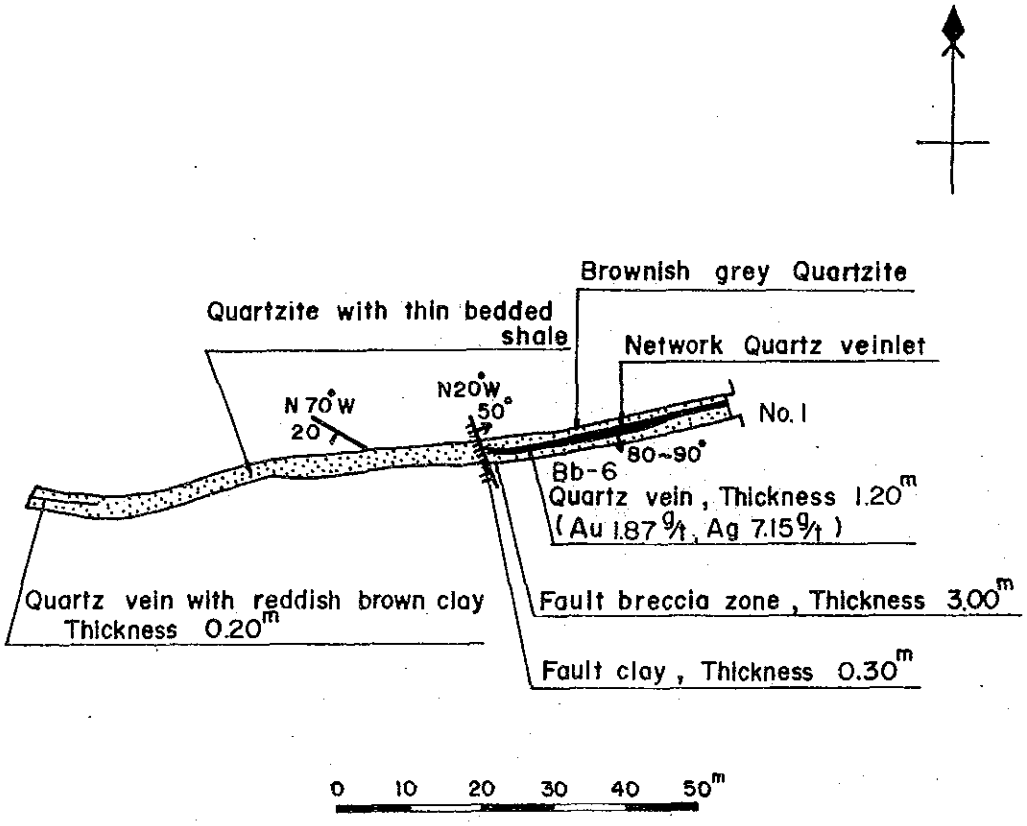

Fig.4-11 Geological Sketch of Adit in the Minas de Huayllura

CHAPTER 5 GEOCHEMICAL PROSPECTING

CHAPTER 5 GEOCHEMICAL PROSPECTING

Geochemical prospecting in the area was conducted with the purpose of detecting geochemical anomalies caused by mineralization and of obtaining basic data for mineral exploration in the next phase of the project.

In the prospecting, stream sediments were collected and six elements, gold (Au), silver (Ag), arsenic (As), copper (Cu), lead (Pb) and zinc (Zn) were analyzed as indicators of mineralization.

5-1 Method of Prospecting

5-1-1 Sampling and Number of Samples

Using 80-mesh sieves, about 50 g of stream sediment samples screened under 80-mesh were collected from river deposits on each sampling point of drainage systems on the prospecting routes. The collected samples were dried and divided into two for analysis and preservation at the base camp.

The number of collected samples amounted to 2,174, which can be broken down to 1,309 samples in the regional survey area, 815 samples in the detailed survey area and 50 samples in the surrounding area of Orcopampa mine. Accordingly, the sampling density is 2.52 samples per 10 km^2 in the regional survey area and 1.02 samples per km^2 in the detailed survey areas.

5-1-2 Preparation of Samples and Analytical Method

(1) Preparation of Samples

The samples that had been dried and separated for analysis were classified by the sample No., packed, sent to Chemex Labs. Ltd., Vancouver, Canada and served for analysis.

(2) Analytical Method

The analytical methods for the six indicator elements by Chemex Labs. Ltd. are shown in Table 5-1.

The detection limits are 1 ppb for Au, 0.1 ppm for Ag, and 1 ppm for As, Cu, Pb and Zn.

5-1-3 Data Processing

On each of As, Cu, Pb and Zn, univariate analysis was conducted based on

the statistical population putting together the values of all samples (2,174). On each of Au and Ag, univariate analysis was conducted on the two objectives of the population in which the values of samples from the regional survey area and detailed survey area are totaled and the other population consisting of the values of samples (50) from the surrounding area of Orcopampa mine only. The principal component analysis was conducted on a single population consisting of the values from all samples (2,174).

Univariate Analysis

It is experientially known that geochemical data belonging to a homogeneous population, especially the distribution of contents of trace elements, is similar to the logarithmic normal distribution. Therefore, the common practice in geochemical prospecting is that a deviation (especially that of the high-content side) from the logarithmic normal distribution shown by the majority of specimens (background) of a certain indicator element is treated as the geochemical anomaly of the particular indicator element. In other words, the objective of geochemical prospecting is the specimen population in which the "background population" which is outside of the influence of mineralization and a "geochemically anomalous population" that is expected to be different from the background population are compounded, and in an univariate analysis, the major purpose is to detect an anomalous value on the high-content side by obtaining the threshold value that separates both populations.

The methods of Lepeltier (1969) and Sinclair (1976) using the deviation from a line (normal distribution) shown by a cumulative frequency distribution of a complex population on a probability paper have conventionally been used to set such a threshold value. These methods are applied based on an assumption that individual populations that configurate the complex population would show normal distribution or logarithmic normal distribution. If the topographic, hydrogeological and meteorological conditions are comparatively even, the geochemical data is considered to correspond fairly with the underground chemical data, and the above methods of data processing are effective.

However, the objective survey district has large topographical difference in the height and this essentially causes much difference in the meteorological conditions. Furthermore, the hydrogeological conditions are greatly different between places of high elevation and lowland. The geochemical data obtained in such a district where the external conditions greatly vary is considered to indicate rather complicated values as a result of the principal underground geochemical data being affected by the various other conditions, and in the actual analysis, taking these

external conditions into consideration is extremely difficult.

Accordingly, in the prospecting such standard statistics as the mean value (M), standard deviation(σ), minimum value (Min.) and maximum value (Max.) were calculated and the classification of contents of each indicator element were determined based on these standard statistics (PL.12-1 through 6). Also, a geochemical interpretation map by univariate analysis was prepared (PL13) in which the geochemical anomalies of each indicator element were superimosed. On the two elements of gold and silver, the calculation was made individually for the Cotahuasi area and Orcopampa area.

Principal Component Analysis

Owing to the recent development of chemical analysis methods, a variety of elements can be easily analyzed at a lower cost these days. Therefore, the trend of current geochemical prospectings is that mineralization is distinguished by using a larger number of indicator elements. When conducting a univariate analysis using a number of indicator elements, the number of variables to handle increases and it is difficult to quantitatively express the relationship between each indicator element. Also, it is difficult to mathematically select a plurality of elements that relate with the mineralization. Therefore, the method of multivariate analysis has been introduced, and the method is now used more widely as the computer has propagated. In the geochemical prospecting this time, the principle component analysis, the most fundamental method among the multivariate analysis was conducted.

In the principle component analysis, the characteristics of data of each multiple variate related each other are summarized, and they are integrated according to the necessity. The mathematical theory of these methods is outlined in the following.

In these methods, the data possessed by characteristic values (a specific indicator element in this case) of p pieces "x_1, x_2 ....., xp" are summarized into integrated characteristic values "Z_1, Z_2, ..., Zm" (which are called the first, second ... and m-th principle component) of m pieces ($m < p$) that satisfy the following two conditions using equations (1) and (2) shown below:

Condition 1: The correlation between Z_r and Z_{r1}
($r \neq r^1$, $r = 1, 2, \ldots, m$) is always zero.

Condition 2: The dispersion of Z_1 is the largest in the dispersions of all primary expressions of (x_1, x_2, ..., xp).

The dispersion of Z_2 is the largest in the dispersions of all primary

Table 5-1 Method of chemical Analyses (by CHEMEX LABS LTD.)

GOLD

A 10 gram sample is fused in litharge, carbonate and silicious flux. The resulting lead button containing any gold in the sample is cupelled in a muffle furnace to produce a precious metals bead.

Sample beads, plus standard and blank beads are irradiated in a thermal neutron flux. The gamma emissions of the irradiated beads are counted utilizing a Ge (Li) detector and quantified for gold. The detection limit for a 10 gram sample is 1 ug/kg (ppb).

ARSENIC

A 1.0 gram sample is digested with a mixture of perchloric and nitric acid to strong fumes of perchloric acid. The digested solution is diluted to volume and mixed. An aloquot of the digested is acidified, reduced with KI and mixed. A portion of the reduced solution is converted to arsine with NaBH4 and the arsenic content determined using flameless atomic absorption. The detection limit is of 1 ppm.

SILVER

A 1.0 gram portion of sample is digested in conc. perchloric-nitric acid (HC104-HN03) for approx. 2 hours. The digested sample is cooled and made up to 25 mls. with distilled water. The solution is mixed and solids are allowed to settle. Silver is determined by atomic absorption technique using background correlation on analysis. The detection limit is of 0.1 ppm.

Copper, Lead, Zinc

A 1.0 gram portion of sample is weighed into a calibrated test chube. The sample is digested using hot 70% perchloric acid and concentrated nitric acid. Digestion time is two hours. Sample solutions are homogenized and allowed to settle before being analyzed by atomic absorption procedures.

Detection limits using Varian atomic absorption unit are as follows :

Copper - 1 ppm
Lead - 1 ppm
Zinc - 1 ppm

expressions that are not correlated with Z_1. The same applies to the subsequent characteristic values and the dispersion of Zm is the largest in the dispersions of all primary expressions that are not correlated with any and al of Z_1, Z_2, ..., Zm-1.

Z_2 Z_1 Zm $Z_1, Z_2, \ldots\ldots, Zm-1$

$$\left.\begin{aligned} Z_1 &= I_{11}x_1 + I_{12}x_2 + \cdots\cdots\cdots + I_{1p}xp \\ Z_2 &= I_{21}x_1 + I_{22}x_2 + \cdots\cdots\cdots + I_{2p}xp \\ &\cdots\cdots\cdots\cdots\cdots\cdots\cdots \\ Zr &= Ir_1x_1 + Ir_2x_2 + \cdots\cdots\cdots + Irp\,xp \\ &\cdots\cdots\cdots\cdots\cdots\cdots\cdots \\ Zm &= Im_1x_1 + Im_2x_2 + \cdots\cdots\cdots + Imp\,xp \end{aligned}\right\} \quad \ldots\ldots(1)$$

provided, $\sum_{i=1}^{P} Ir\,i^2 = 1 \quad (r = 1, 2, \ldots\ldots, m) \quad \ldots\ldots\ldots(2)$

The numerals used in this calculation are the standardized analytical value xi' of each indicator element, and the values obtained from the principle component analysis are eigenvalue λr (dispersion of main component), contribution (ratio of main component Zr to the whole dispersion), eigenvector (value of 1ri obtained from the above equations of (1) and (2) calculated under the above two conditions) and factor load (correlation between characteristic value xi and main component Zi).

This method is geometrically interpreted as follows.

That is, when a supposition is made to the effect that data of "n" pieces that are distributed in the p-dimension space are on a certain plane in the space almost completely, there will be no loss of data even if the state of scatter of "n" points on the plane only is observed since almost all points are projected onto the plane. Even if such an ideal plane does not exist, the next supposition that can be made is that these points are in the m-dimension space of $m < p$, and the variables to handle can be lowered to the m-dimension space. To determine this m-dimension space, make the dispersion of lengths of perpendiculars drawn from the p-dimension space to the m-dimension space the largest.

The principle component obtained by this principle component analysis has the following characteristics.

① The dispersion of principle component Zr is equal to eigenvalue λr.

② Since dispersion V [xi'] of standardized characteristic value xi' is equal to "1", the following is true.

$$\sum_{i=1}^{P} [xi'] = P$$

Accordingly, the contribution can be expressed as $\lambda r/p$ and the cumulative contribution can be calculated as $\sum_{r=1}^{m} \lambda r/p$.

③ Each principle component is not correleated.

④ Correlation (factor load) $\gamma(Zr, xi')$ between principle component Zr and characteristic value xi' can be expressed as $\sqrt{\lambda r} Iri$.

⑤ The sum of squares of factor loads is λr.

⑥ Contribution vi to original variable xi' of m pieces principle components $\{Z_1, Z_2 \ldots\ldots, Zm\}$ is defined by the following equation:

$$vi = \sum_{r=1}^{m} \gamma^2 (Zr, xi') = \sum_{r=1}^{m} \lambda r \; Iri^2$$

If "m" becomes equal to "p", "vi" becomes equal to "1".

By using characteristic value xαi of each sample and eigenvector 1ri of the principle component, out of the statistical values thus calculated, score Zr to the r principle component of each sample can be calculated as $Z\alpha r = \sum_{i=1}^{P} 1rix\alpha i$.

In the principle component analysis of the prospecting components up to the third were analyzed and its cumulative contribution is 77.0%, or the quantity of data that is lost from the initial data is 23.0%. The obtained score of each component are shown in PL.14 (1) - (3), separately provided, in the form of content of score and anomaly distribution map according to the statistic value of each score. Among them, the first and second principle components which relate with the mineralization are superimposed and thus the overall geochemical interpretation map of principle component analysis (PL15) is prepared.

5-2 Prospecting Results

5-2-1 Univariate Analysis

5-2-1-(1) Standard Statistical Values

The standard statistical values obtained by processing the related data are shown in Table 5-2, together with the average abundance of each element in the

Crust of the Earth and standard data of USGS G-1 and W-1 samples. On Au and Ag, since distribution of pretty high density values is recognized in the Orcopampa area compared with those values in the Cotahuasi area, the statistical processing was conducted separately for these two areas. In so doing, the data of excessively high analytical values (Au: 400 ppb or higher, Ag: 11 ppm or higher) in the Cotahuasi area were excluded.

Table 5-2 Statistical Values and Crustal Abundance of Indicator Element

Element	Number of samples	Maximum value	Minimum value	Mean (M)		Standard diviation		Classification of density			Abundance		
				Logarithmic base	Arithmetic	Logarithmic base	Arithmetic	M+σ	M+2σ	M+3σ	G-1 sample	Earth's crust	W-1 sample
Au (C)	2,108 (2,124)	376 (4,480)	0 (0)	1.6 (1.6)	6.1 (17.4)	3.00 (3.86)	30.2 (163.8)	4.7	14.1	42.4	2	4	4
Au (O)	50	863	0	8.2	64.6	8.65	145.8	70.5	609.3	5269.9			
Ag (C)	2,122 (2,124)	10.1 (21.0)	0.1 (0.1)	0.11 (0.11)	0.16 (0.17)	1.61 (1.68)	0.44 (0.69)	0.18	0.29	0.47	0.04	0.07	0.05
Ag (O)	50	33	0.1	0.45	2.56	6.41	5.42	2.98	19.13	122.63			
As	2,174	390	0	5.9	13.2	3.3	26.7	19.6	64.6	213.3	0.8	1.8	2.4
Cu	2,174	845	3	22.6	29.3	1.89	38.5	42.8	80.9	152.9	13	55	110
Pb	2,174	610	0	7.1	11.5	2.50	21.2	17.8	44.5	111.4	49	13	8
Zn	2,174	780	8	66.2	82.2	1.7	66.0	118.2	201.9	344.9	45	70	82

Note: Au is expressed in ppb and other elements in ppm.

Teh values shown in the Logarithmic base columns for the mean and standard deviation are the numerals of inverse logarithm converted from the logarithm.

(C) and (O) marked for Au and Ag in the element column represent Cotahuasi and Orcopampa respectively, and the values written in parentheses are the values which include the high content data.

The source of values for G-1, Earth's crust and W-1 for abundance is the Appendix table of Earth Science Vol. 4 (1979) published by Iwanami.

As the table shows, the arithmetic mean values of Au and Ag in the Orcopampa area are as high as 16.2 to 36.5 times of the crustal abundance, but these are 1.6 to 2.29 times in the Cotahuasi area, indicating less concentration of Au and Ag than that in the Orcopampa area. The arithmetic mean value of As is a total of the Cotahuasi and Orcopampa districts, and it is 7.33 times as much as the crustal abundance, indicating high concentration of As in the survey area. On the three indicator elements of Cu, Pb and Zn, the arithmetic mean values are close to the crustal abundance, not indicating any concentration.

5-2-1-(2) Correlation between Indicator Elements

Table 5-3 and Fig. 5-1-1 through 15 show the relationships between the content of each indicator element in the form of correlation coefficient table and scatter diagram on logarithmic base as observed on the 2,174 samples collected in the Cotahuasi and Orcopampa areas. As these table and figures show, all combinations excluding the combination of Au-Cu are in the positive correlation and they are on the 5% significant level. Correlation is especially high in the combinations of Pb-As and Au-Ag. The other combinations in the order of higher correlation coefficient after these two are Cu-As, Cu-Zn, Pb-Ag, Pb-Cu, Pb-Au, Ag-As, Au-Zn, Ag-Zn and Pb-Zn. Although the correlation coefficients of Au-As, Zn-As and Cu-Ag are on the 5% significant level, their correlation is not as high as others.

The trend of these correlations suggests ① Au and Ag are very closely related and the two belong to a group that is different from Pb-As and Cu-As, ② Zn has somewhat high correlation with Cu but low correlations with other elements, the mutual correlations between Cu, Pb, Zn, Au and Ag are about the same, except the low correlations of Cu with Au and Ag, indicating a different relation from that of ① , and variety of correlations by the areas.

Table 5-3 Correlation Coefficients in Logarithm Base (n = 2,174).

Element	Au	Ag	As	Cu	Pb	Zn
Au	1.00000					
Ag	0.51394	1,00000				
As	0.16477	0.26875	1,00000			
Cu	-0.02695	0.13564	0.40699	1.00000		
Pb	0.27839	0.33372	0.59914	0.31163	1.00000	
Zn	0.25816	0.22395	0.16374	0.35917	0.22326	1.00000

5-2-1-(3) Cumulative Frequency Distribution Curves

Fig. 5-2-1 through 6 and Apx.12 and 13 show the cumulative frequency distribution and frequency of indicator elements, Au, Ag, As, Cu, Pb and Zn, prepared on logarithmic probability papers. The distribution of each element group as shown in these figures have the characteristics described later. The condition of the distribution of each element are as follows:

Fig. 5-1 (1) Correlation of Au-Ag

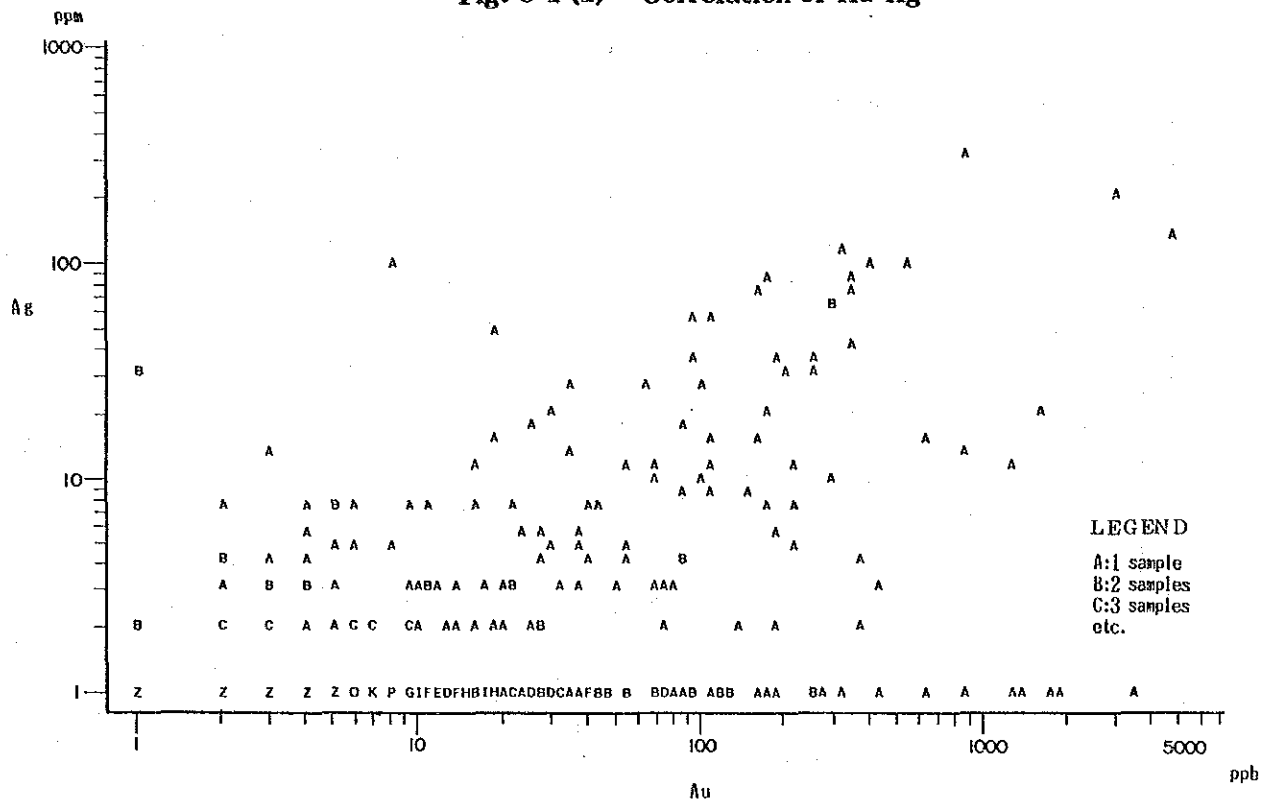

Fig. 5-1 (2) Correlation of Au-As

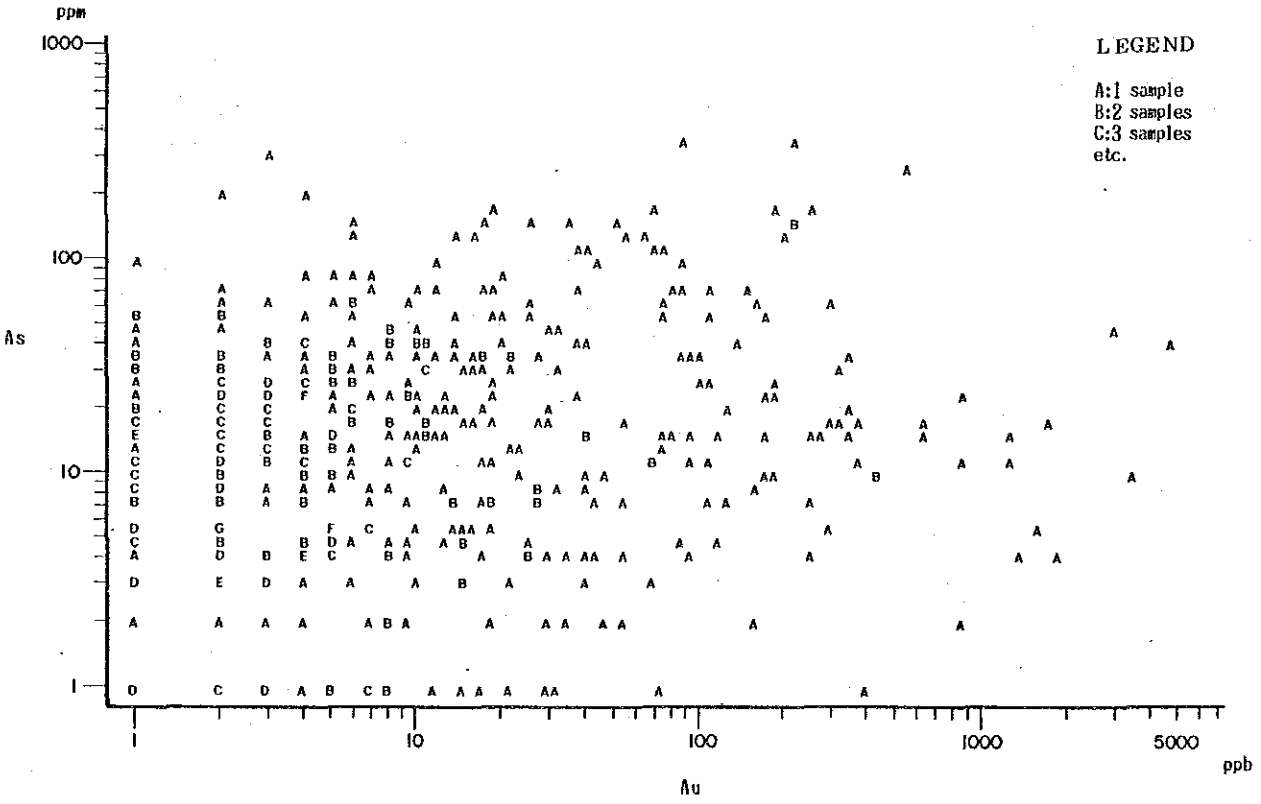

Fig. 5-1 (3) Correlation of Au-Cu

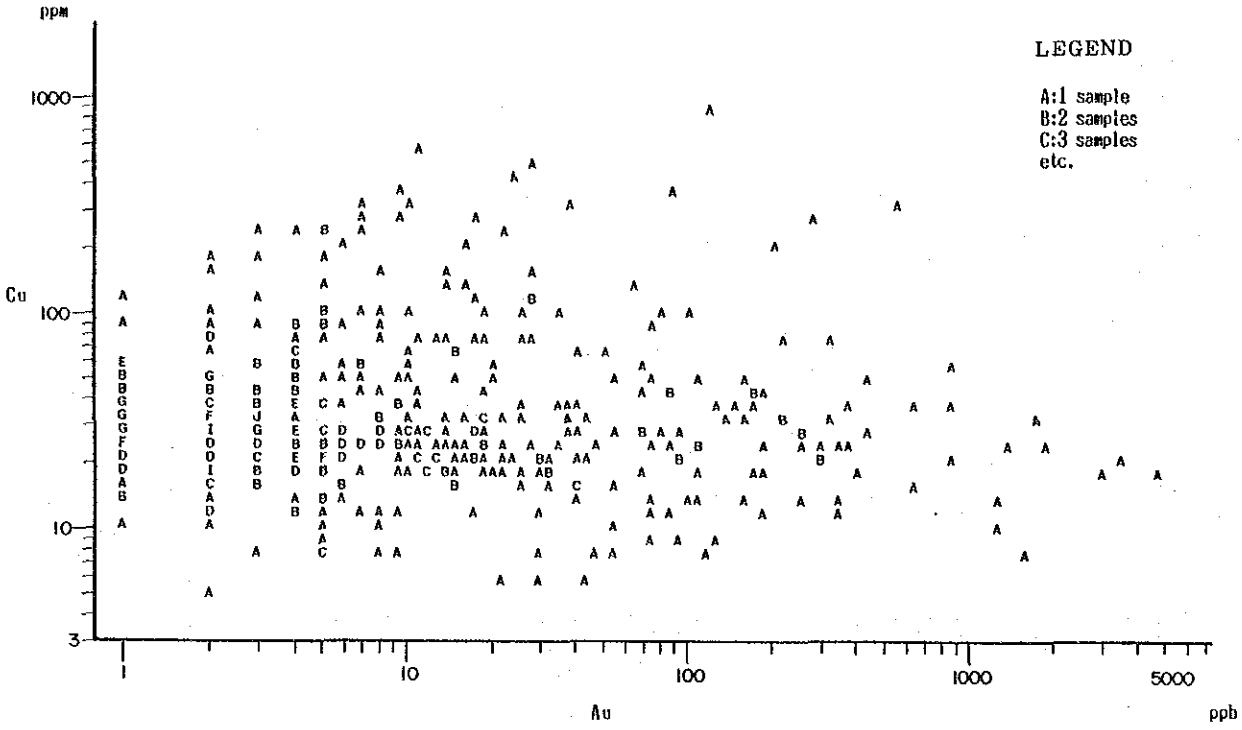

Fig. 5-1 (4) Correlation of Au-Pb

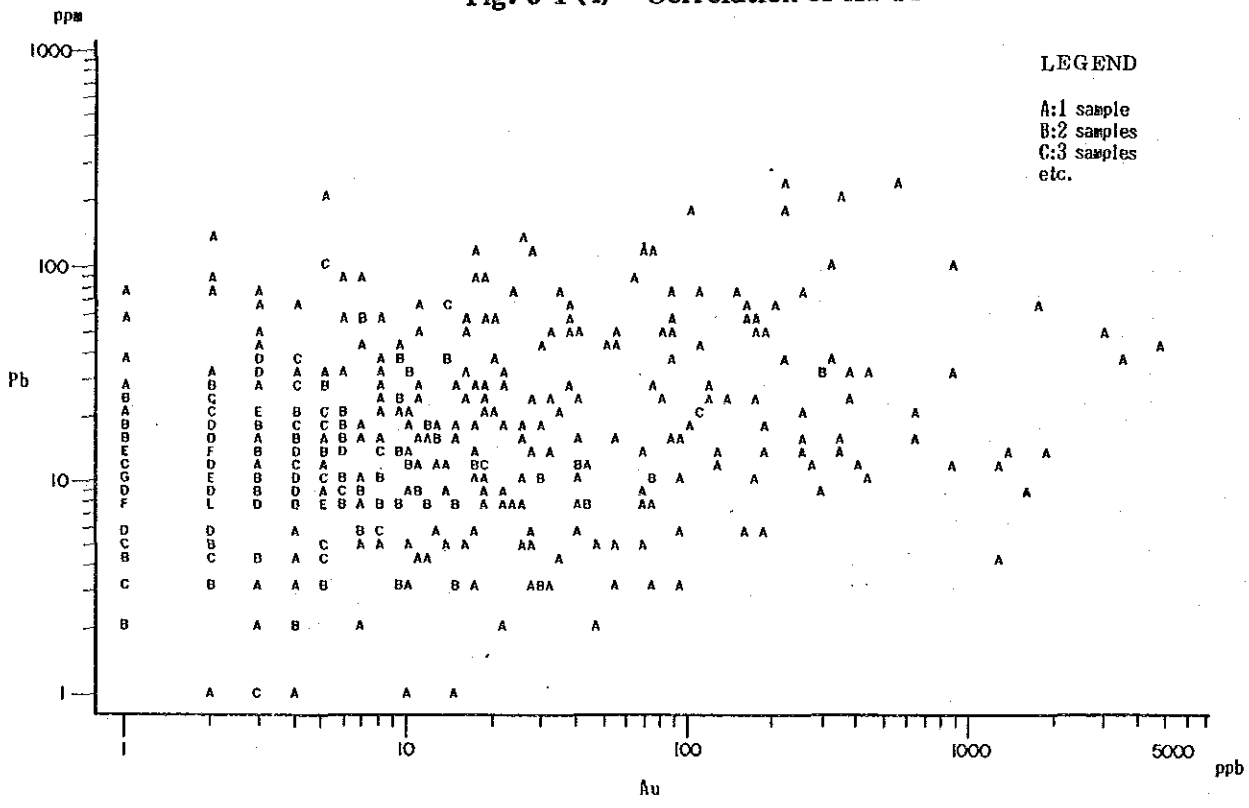

Fig. 5-1 (5) Correlation of Au-Zn

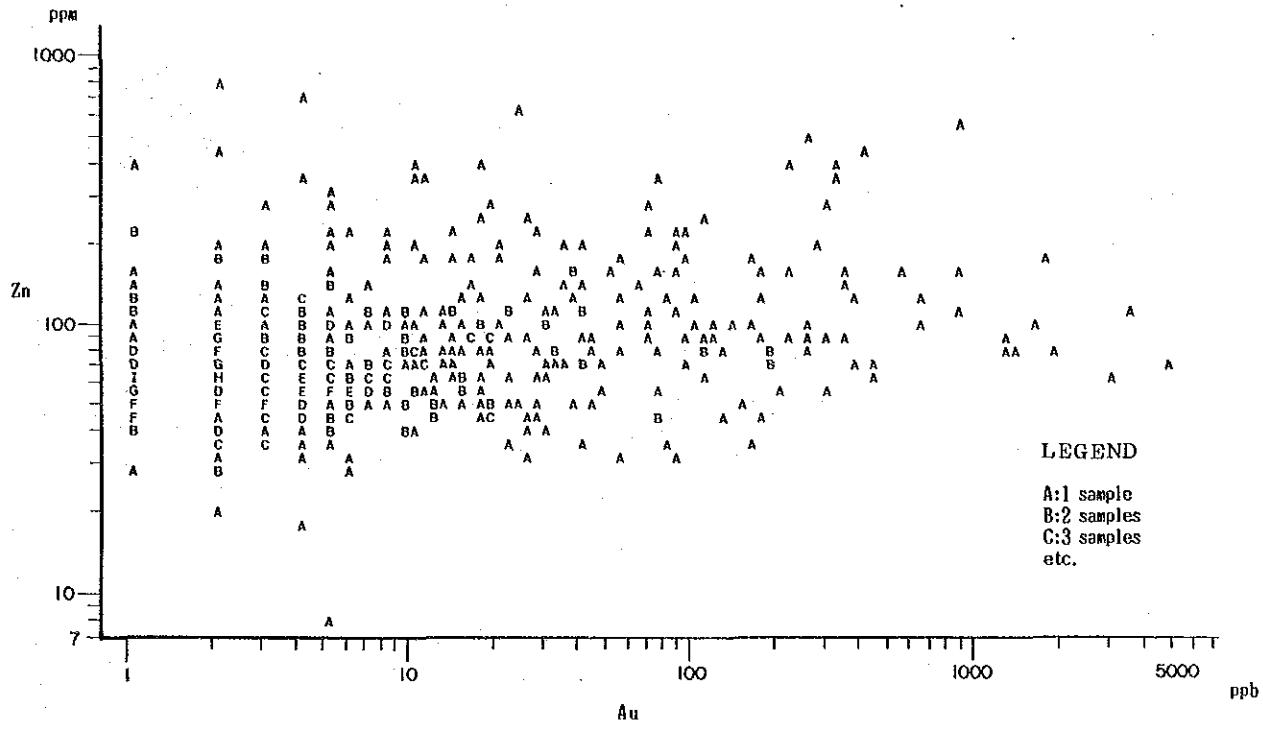

Fig. 5-1 (6) Correlation of Ag-As

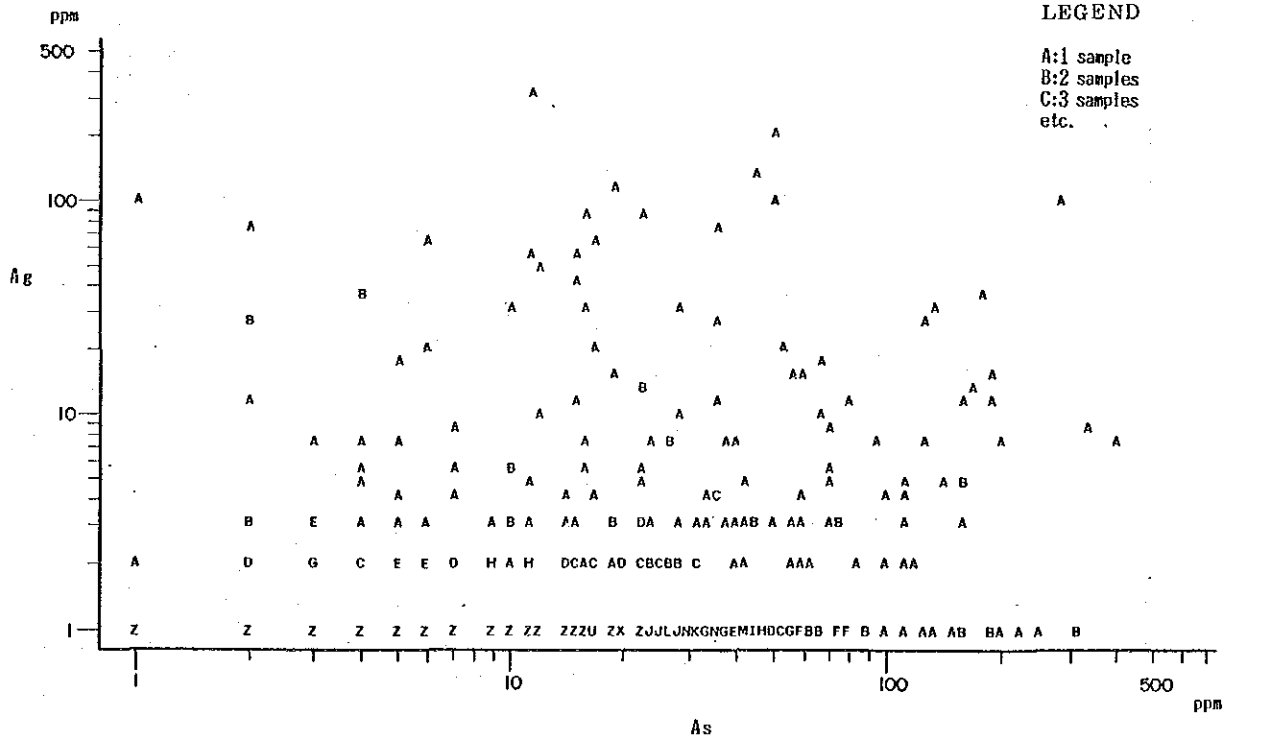

Fig. 5-1 (7) Correlation of Ag-Cu

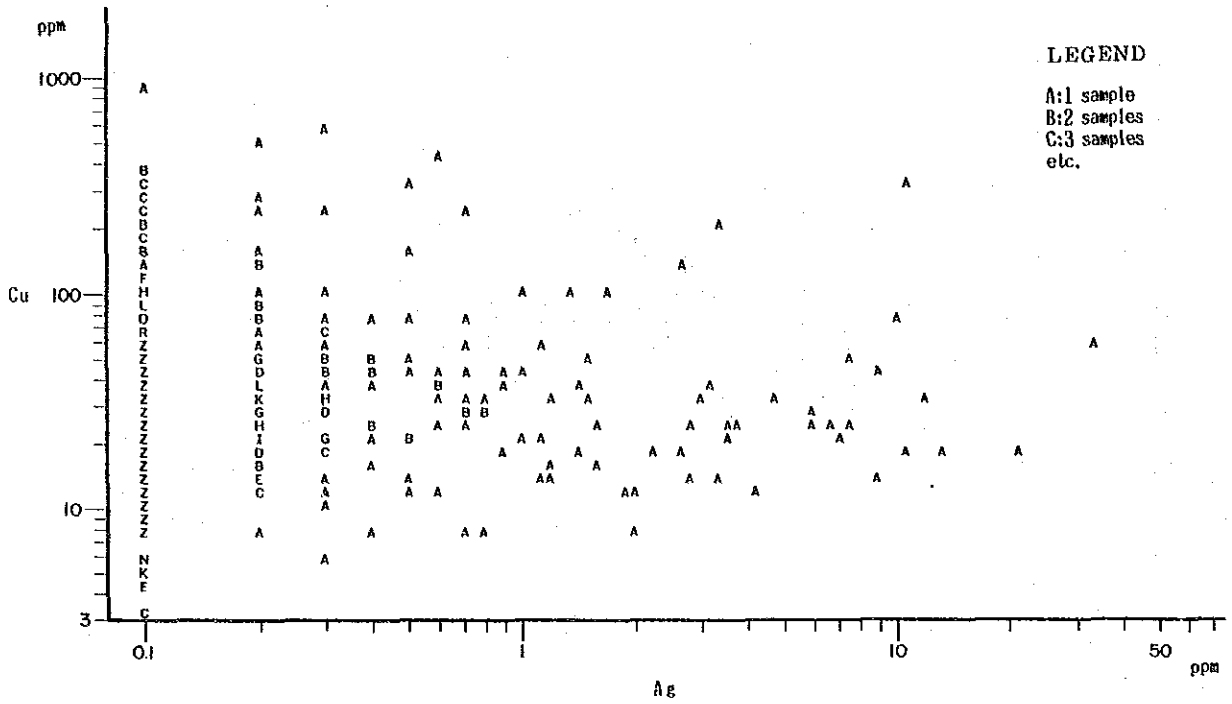

Fig. 5-1 (8) Correlation of Ag-Pb

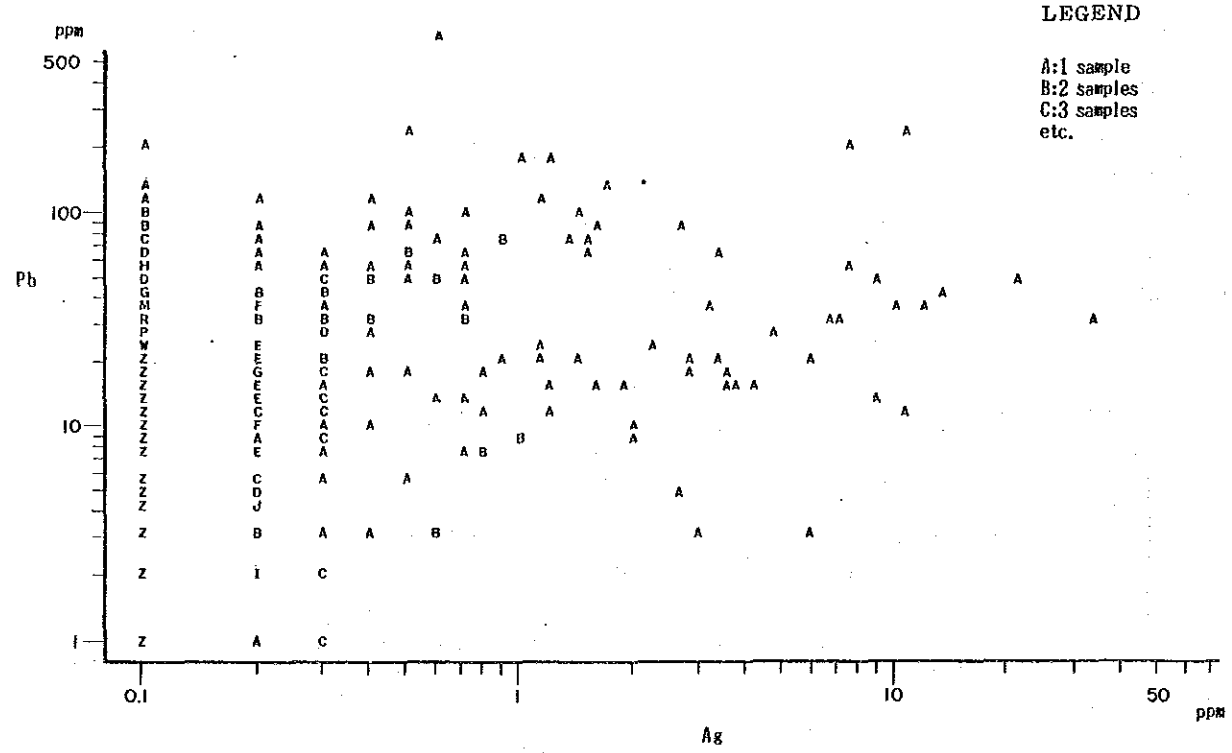

Fig. 5-1 (9) Correlation of Ag-Zn

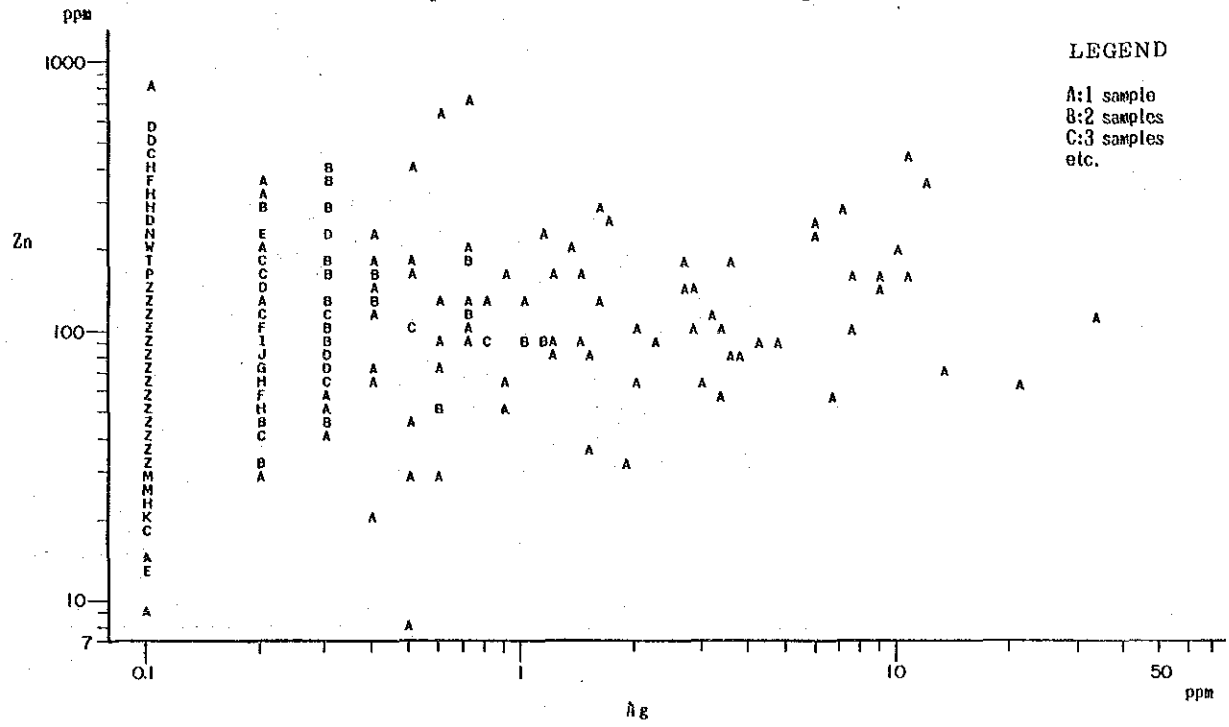

Fig. 5-1 (10) Correlation of As-Cu

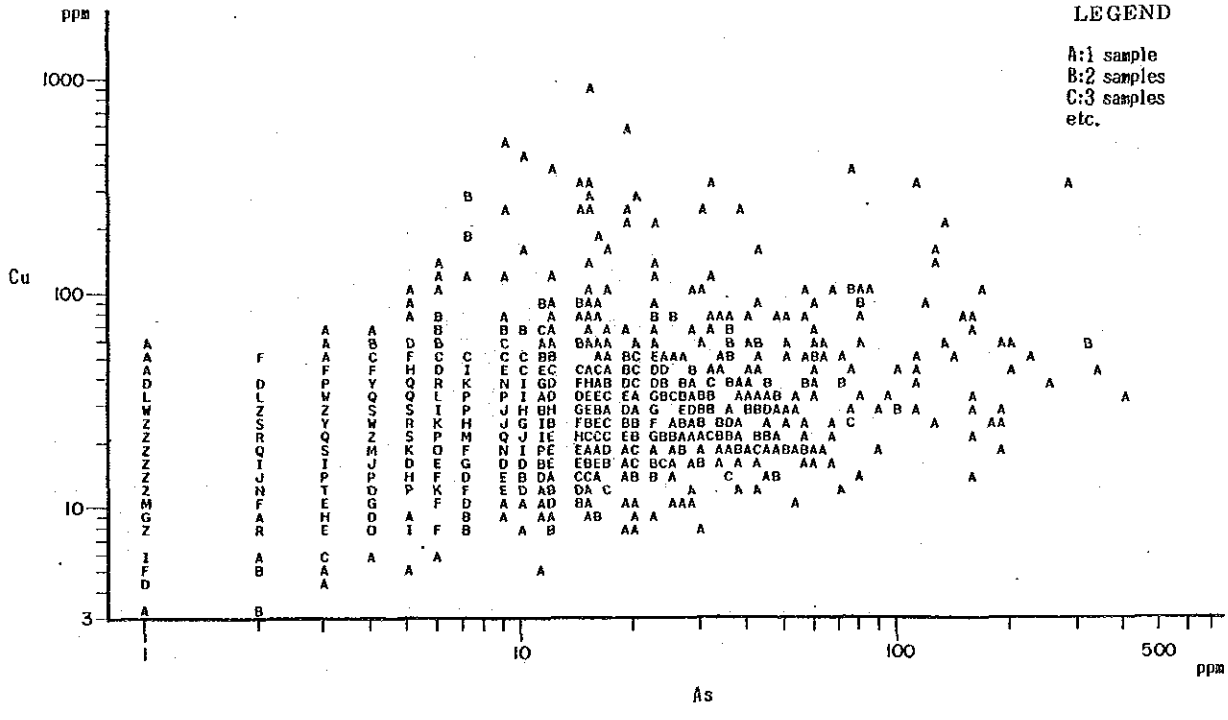

Fig. 5-1 (11) Correlation of As-Pb

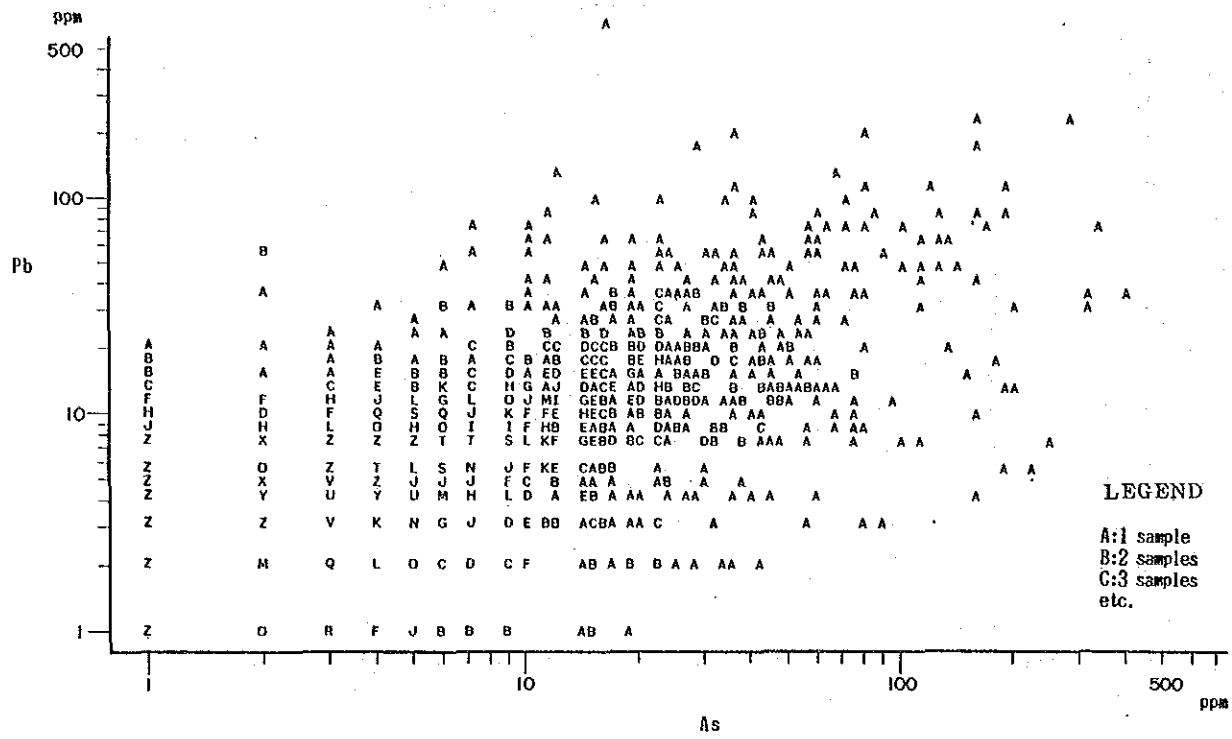

Fig. 5-1 (12) Correlation of As-Zn

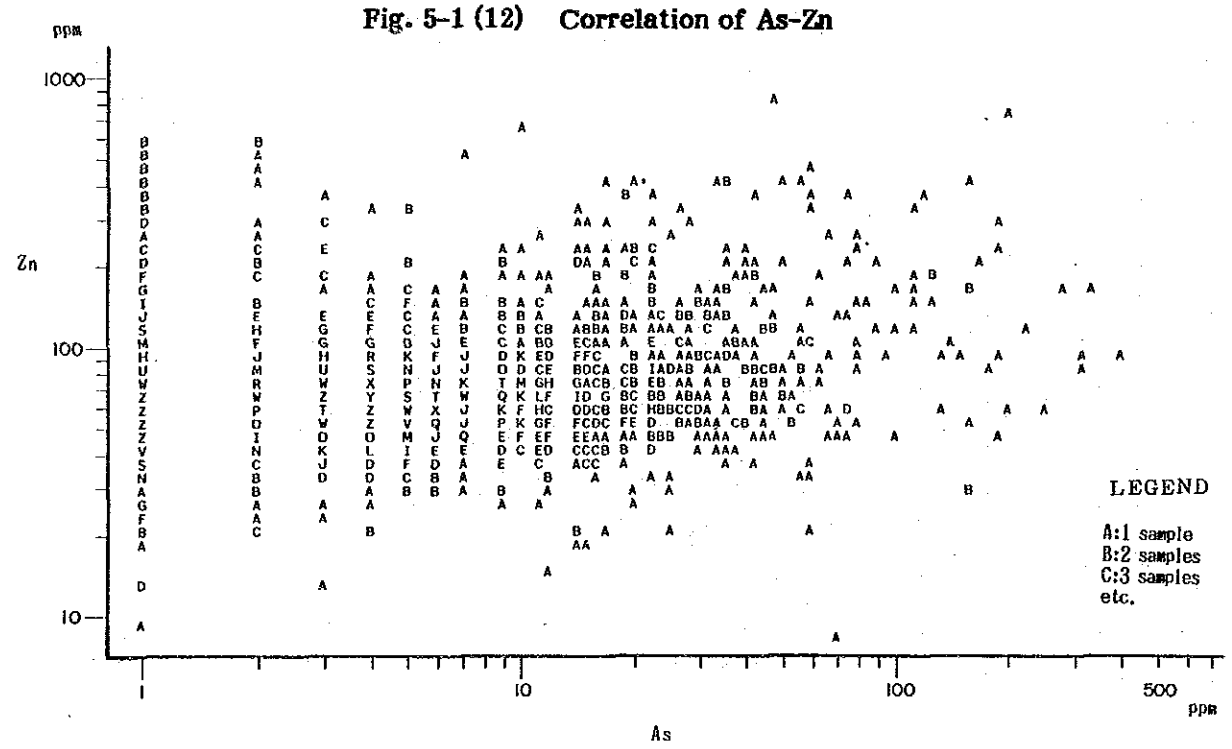

Fig. 5-1 (13) Correlation of Cu-Pb

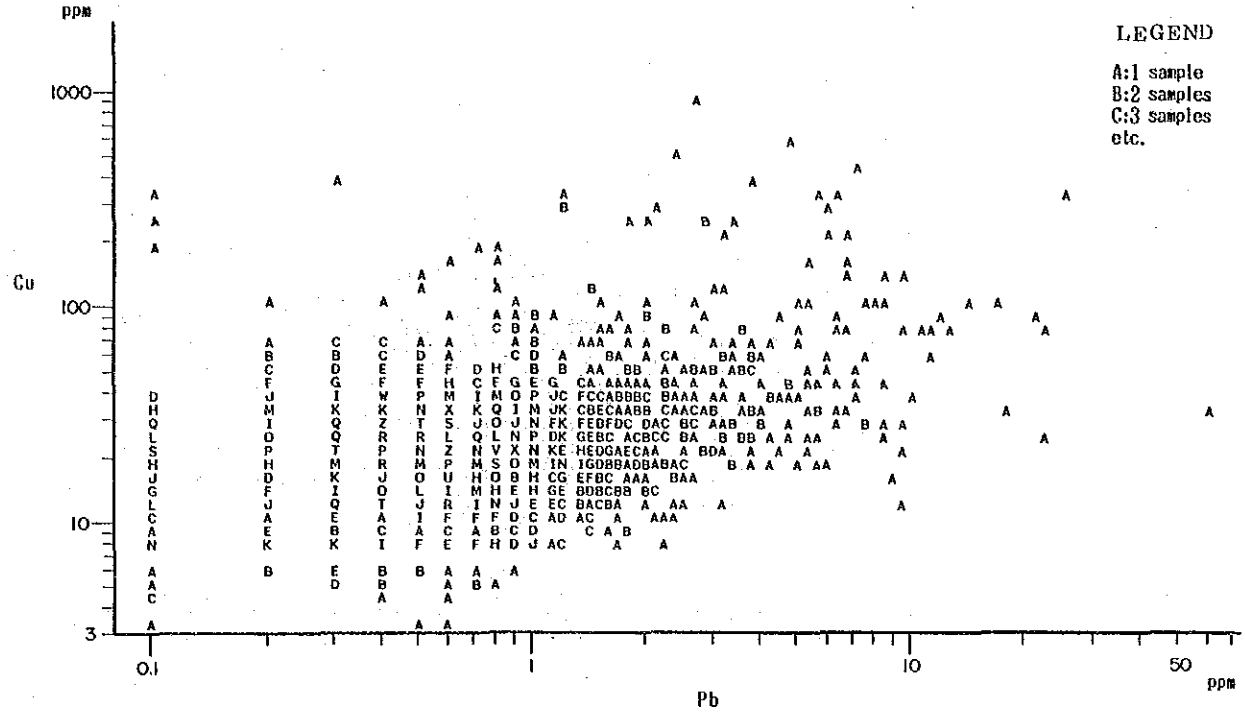

Fig. 5-1 (14) Correlation of Cu-Zn

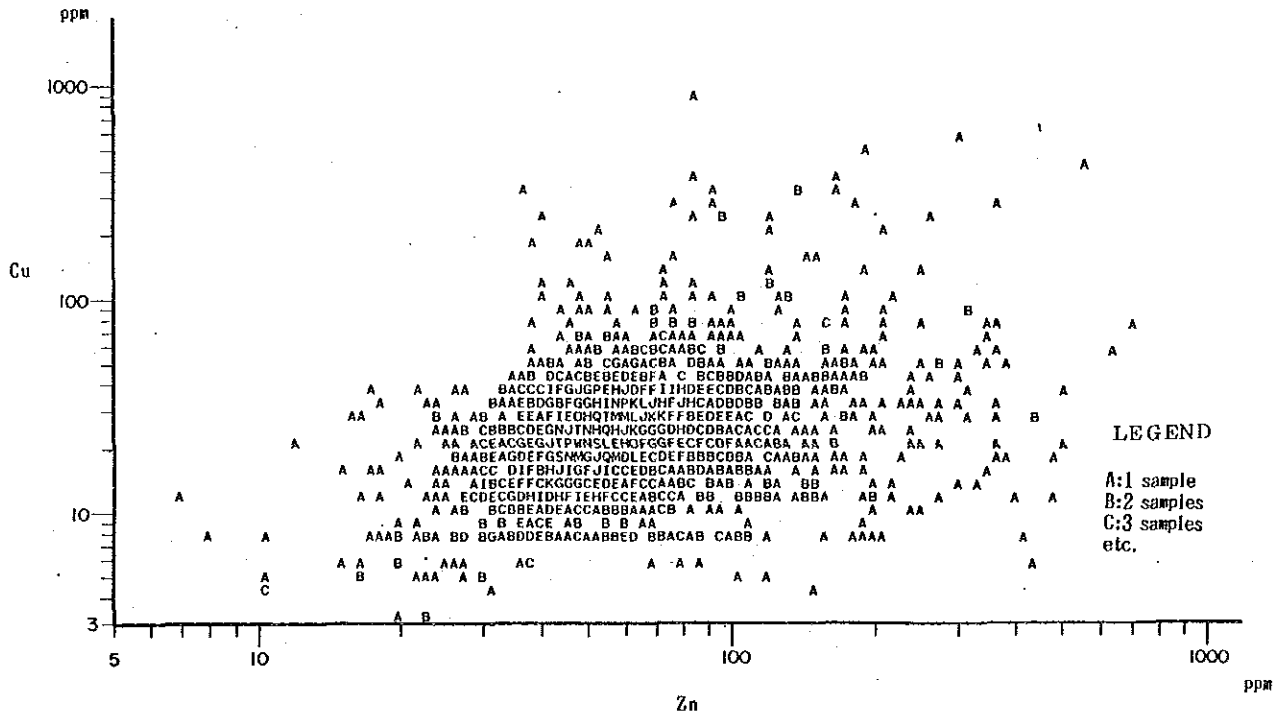

Fig. 5-1 (15) Correlation of Pb-Zn

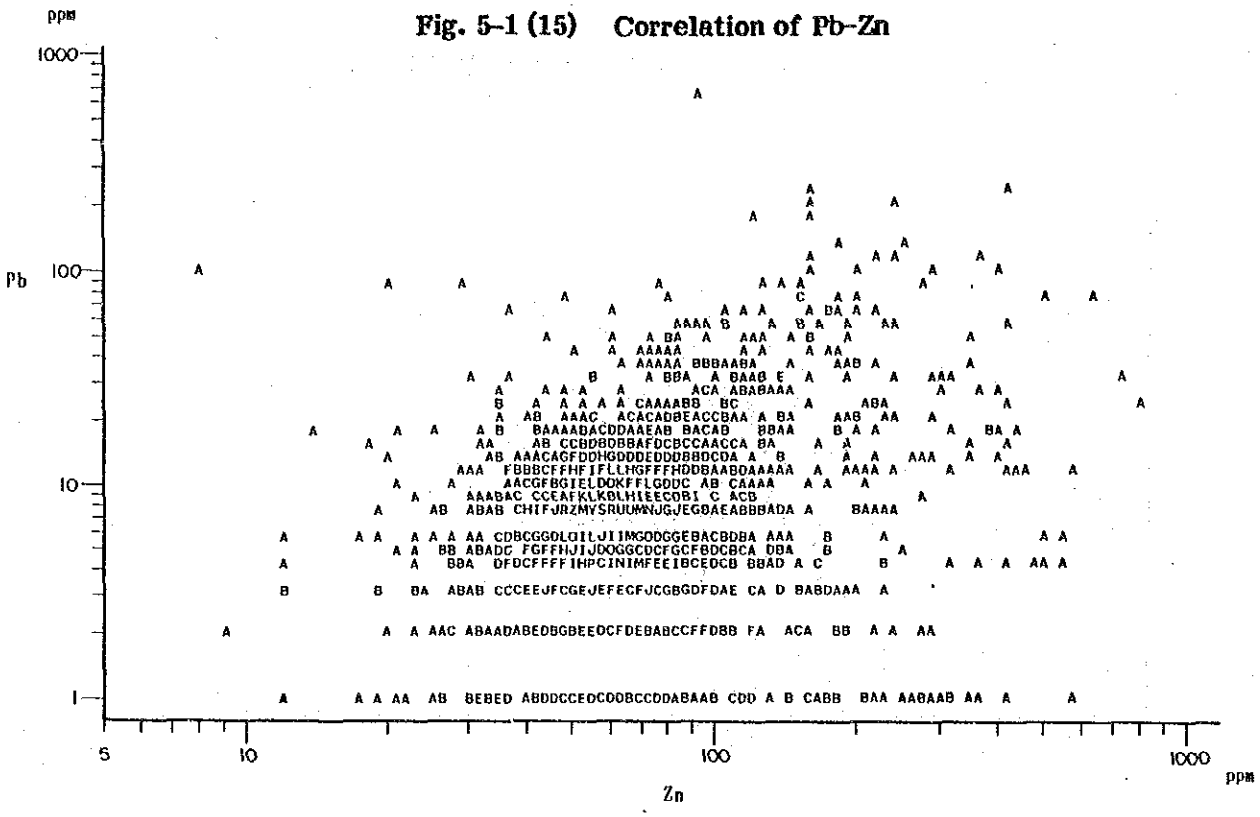

Fig. 5-2 (1) Histogram and Cumulative Frequency Diagram (Au)

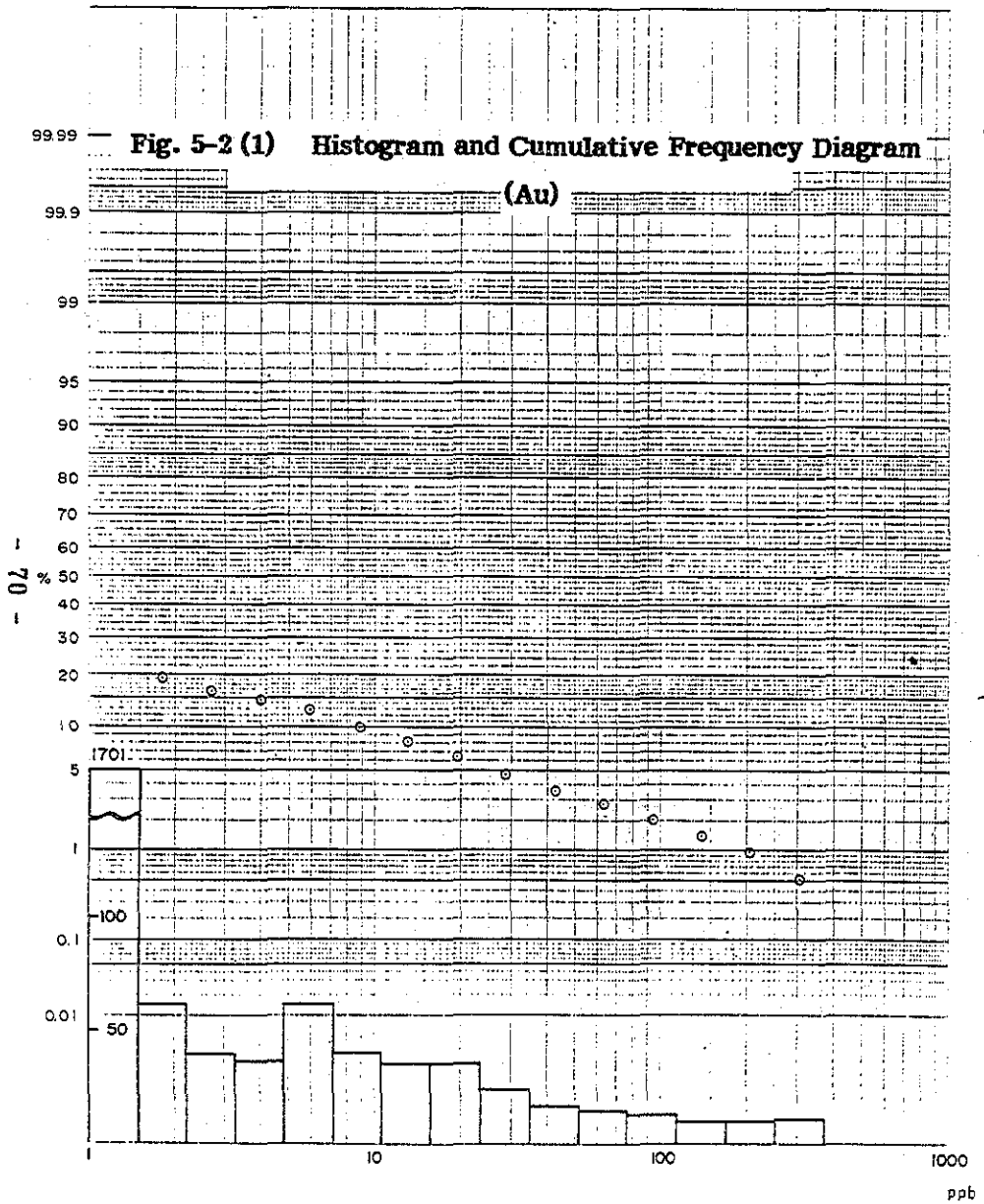

Fig. 5-2 (2) Histogram and Cumulative Frequency Diagram (Ag)

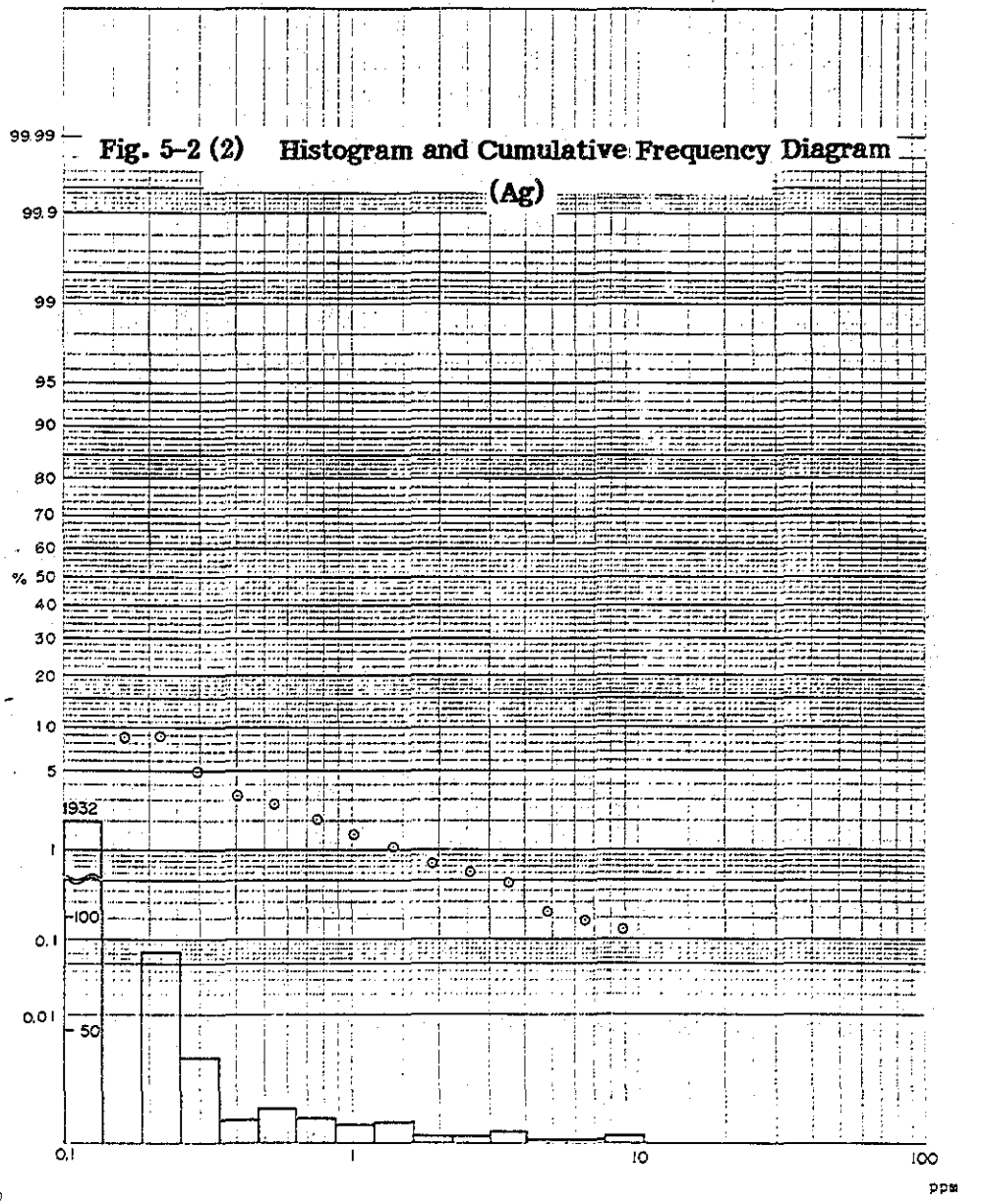

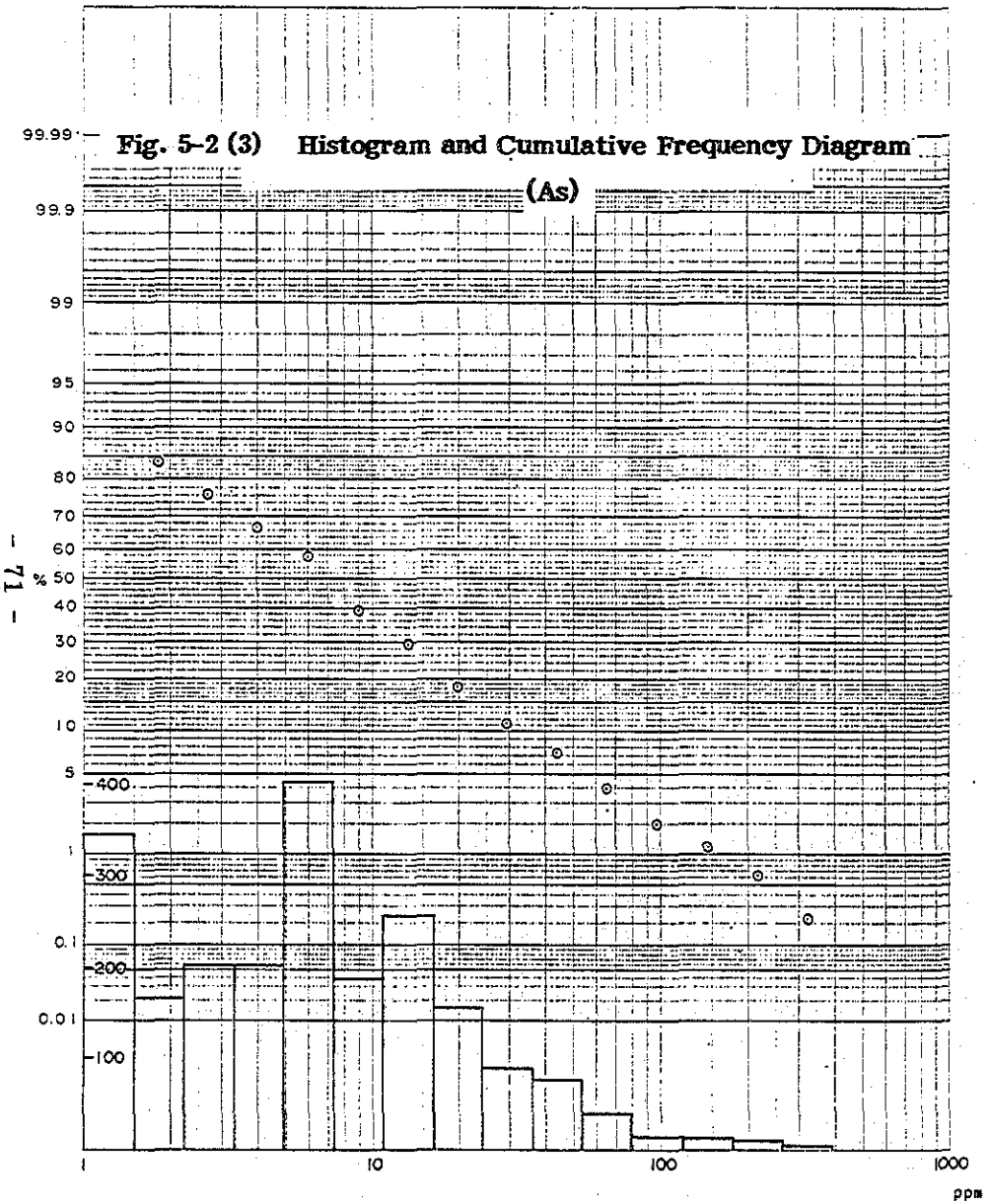

Fig. 5-2 (3) Histogram and Cumulative Frequency Diagram (As)

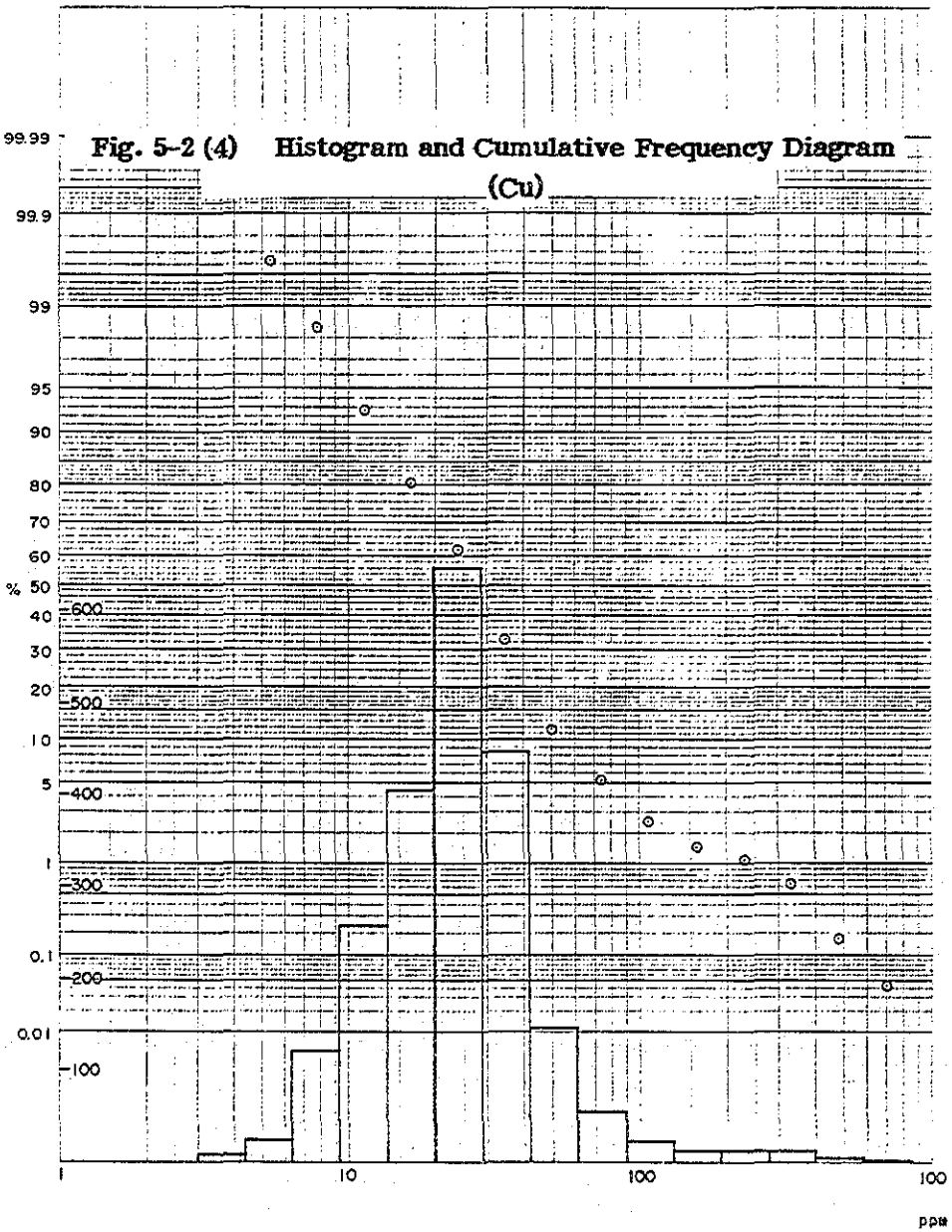

Fig. 5-2 (4) Histogram and Cumulative Frequency Diagram (Cu)

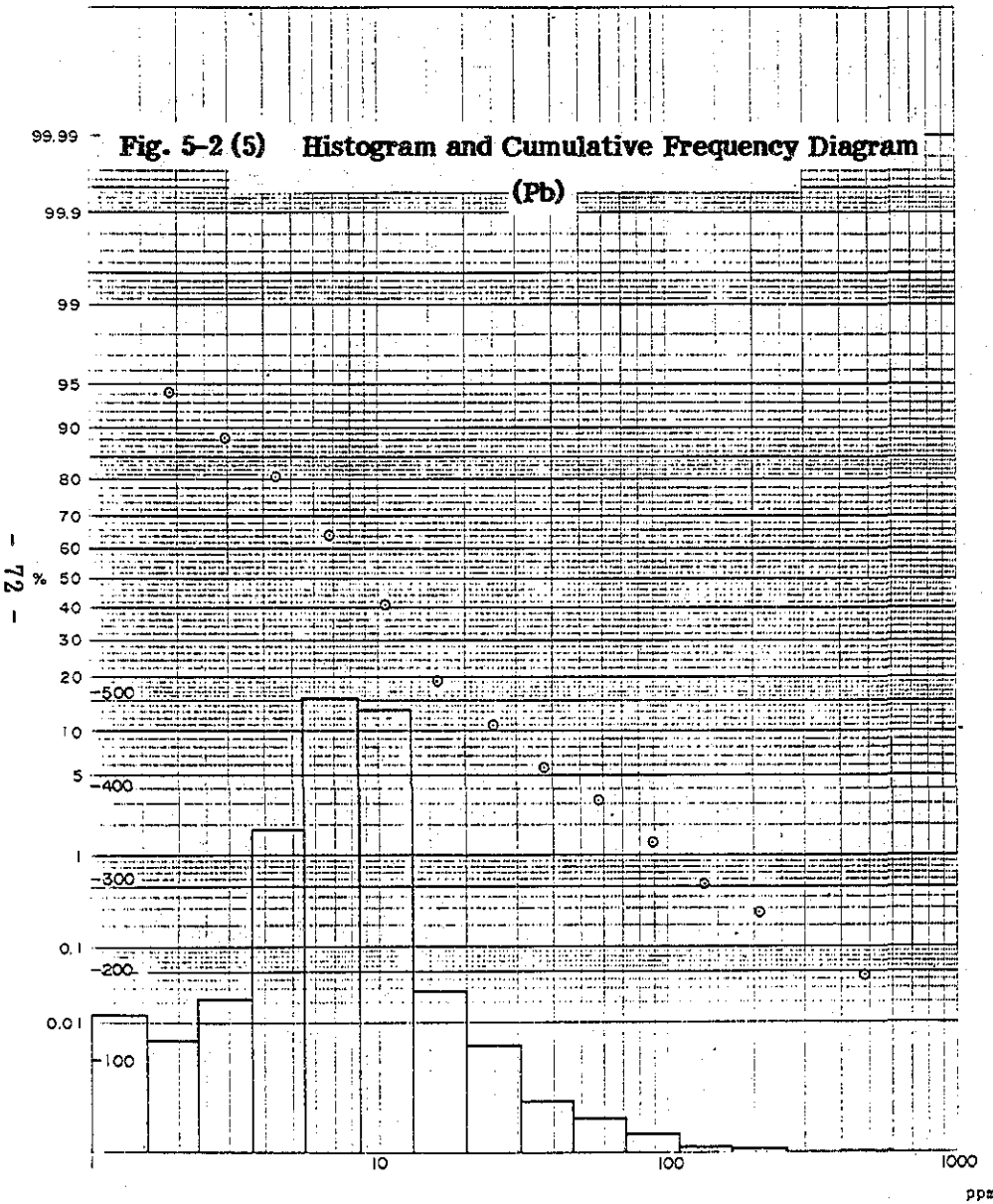

Fig. 5-2 (5) Histogram and Cumulative Frequency Diagram (Pb)

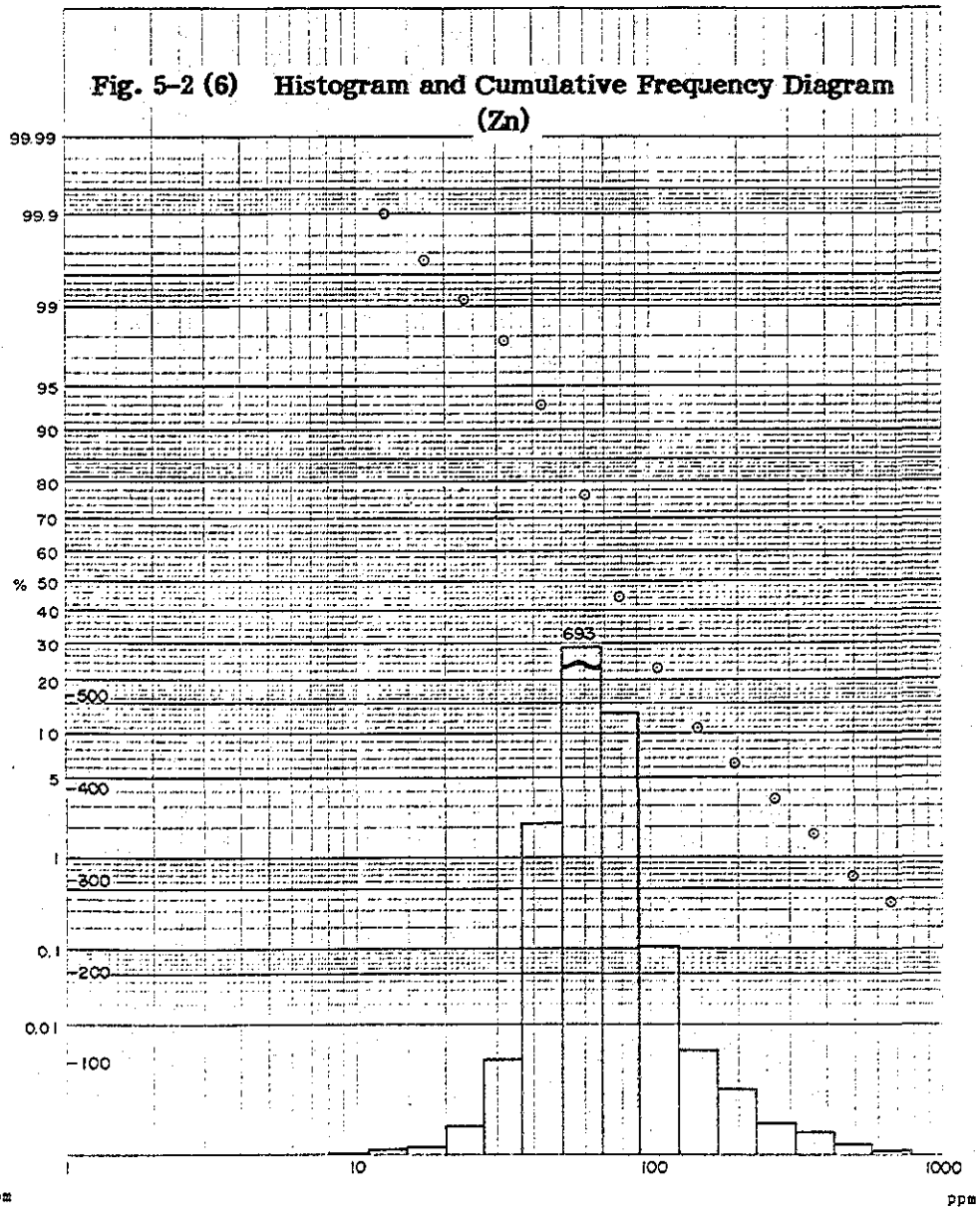

Fig. 5-2 (6) Histogram and Cumulative Frequency Diagram (Zn)

Au: In the Cotahuasi area, the number of samples of which the analytical value is 1 ppb or less amounts to 1,651, and the standard deviation (3.0) is close to twice as much as the mean value (1.57), indicating that the values above the mean value are quite varied. On the cumulative frequency distribution curve, bending is observed in the neighborhood of 6 ppb, indicating good linearity at higher values. The number of samples of which the analytical value is same as threshold value ($M + 2\sigma$, 14.1 ppm) or above amounts to 159 and this is equivalent to 7.5% of the total samples.

In the Orcopampa area, though the number of samples collected is only 50, the content varies in a wide range, from less than 1 ppb to 813 ppb. Among them the number of samples having a content up to the mean value of the Cotahuasi area is only 19, which is only about 38% of the whole samples. On the cumulative frequency distribution curve, bending toward the higher-content side is observed in the neighborhood of 10 ppb, and from this existence of an anomalous population can be assumed. The threshold value adopted for this area is pretty high ($M + 2\sigma = 609$ ppb), and the mean value is also high (8.1 ppb), indicating a characteristic having of high content background compared with the Cotahuasi area.

Ag: In the Cotahuasi area, the content ranges from 0.1 ppm to 21 ppm. Although the mean value of samples in this area, excluding two samples having a high content of 11 ppm or higher, is only 0.11 ppm, the standard deviation is large (1.61). This is caused by the variation of content recognized on the samples of high-content side. On the cumulative frequency distribution curve, bending toward the higher content side is seen in the neighborhood of 0.4 ppm, and existence of an anomalous population is assumed. The adopted threshold value is 0.29 ppm, and the number of samples having a value higher than the threshold value is 108, or 5.1% of the whole samples.

In the Orcopampa area, though the number of samples is only 50, the content ranges widely from 0.1 ppm to 33.0 ppm. The mean value is 0.47 ppm which is higher than that of the Cotahuasi area and the standard deviation is 6.41. The number of samples having the minimum value of 0.1 ppm is 25 and the number of samples having a high content of 1.0 ppm or more is 16, indicating a relatively high ratio of samples having a high content. On the cumulative frequency distribution curve, a bending is observed in the neighborhood of 14 ppm. The adopted threshold value is 19.0 ppm and only one sample has a

content that is higher than the threshold value. This is because the content of background is higher in the area than in the Cotahuasi area. If the threshold value of the Cotahuasi area is used, 46% of the samples in the area have anomalous contents.

As: The content range is as wide as from 1 ppm to 390 ppm, and the mean value and the standard deviation is 5.9 ppm and 3.3, respectively. On the cumulative frequency distribution curve, a bending is seen in the neighborhood of 9 ppm and further the distribution becomes denser toward the high-content side in the neighborhood of 100 ppm, suggesting the existence of an anomalous population in the high-content side. The adopted threshold value is 65 ppm and the number of samples having a higher content than the threshold value is 64 (among which one is from the Orcopampa area), occupying 2.9% of the whole samples.

Cu: The content ranges widely from 3 ppm to 845 ppm, the mean value is 22.6 ppm and the standard deviation is 1.9. On the cumulative frequency distribution curve, bending is seen in the neighborhood of 50 ppm, which goes to the higher content side in the neighborhood of 150 ppm, suggesting the existence of anomaly in the high-content side. The number of samples having a value higher than the adopted threshold value of 81 ppm is 68. All of them are the samples collected in the Cotahuasi area, and those occupy 3.1% of the whole sample.

Pb: The content ranges from 1 ppm to 610 ppm, the mean value is 7.1 ppm and the standard deviation is 2.5. The fact that the standard deviation is small compared with the mean value indicates the values are not scattered widely. On the cumulative frequency distribution curve, bending is seen in the neighborhood of 16 ppm, and the curve leans slightly toward the high-content side in the neighborhood of 150 ppm. This also hints existence of anomaly in the high-content side. The threshold value adopted is 45 ppm and the number of samples having a value higher than that is 85 (83 from the Cotahuasi area and 2 from the Orcopampa area), occupying 3.9% of the whole samples.

Zn: The content range is from 8 ppm to 780 ppm, the average value is 69.6 ppm and the standard deviation is 1.71. The standard deviation is small compared with the mean value, and this indicates that the content values are not

scattered widely, as seen on Cu and Pb. On the cumulative frequency distribution curve, some deviation is seen in the neighborhood of 35 ppm and bending is seen in the neighborhood of 140 ppm. The average point is located at about the center of these two. The threshold value is 202 ppm, and the number of samples having a value higher than that is 99 (78 from the Cotahuasi area and 21 from the Orcopampa area), occupying 4.6% of the whole samples. However, 21 samples among 50 samples have anomalous values in the Orcopampa area, occupying 42% of the whole samples. This shows that the Zn value is pretty high in the Orcopampa area, as same as in the cases of Au and Ag.

5-2-1-(4) Classification of Density and Threshold Value

Based on the statistical processing of data, the analytical values of each indicator element were classified into three groups, High-background value, B-grade anomalous value and A-grade anomalous value. Classification of anomalous values, number of samples belonging to each group and the percentages to the total number of samples are listed in Table 5-4.

The density distribution maps for each element are shown in PL12-(1) through (6) and Apx.14 through 19.

Table 5-4 Classification of Anomalous Value and Thresholds

Element	High-background value	B-grade anomalous value	A-grade anomalous value	Threshold value	Unit
	M+σ≦ <M+2σ	M+2σ≦ <M+3σ	M+3σ≦		
Au (C)	4.7≦(128, 6.0)<14.1	14.1≦(79, 3.7)<42.4	42.4≦(80, 3.8)	14.1	ppb
Au (O)	70.5≦(11, 22.0)<609.3	609.3≦(1, 2.0)<5269.9	5269.9≦(-, -)	609.3	ppb
Ag (C)	0.18≦(84, 4.0)<0.29	0.29≦(46, 2.2)<0.47	0.47≦(61, 2.9)	0.18	ppm
Ag (O)	2.98≦(11, 22.0)<19.13	19.13≦(1, 2.0)<122.63	122.63≦(-, -)	19.13	ppm
As	19.6≦(285, 13.1)<64.6	64.6≦(58, 2.7)<213.3	213.3≦(6, 0.3)	64.6	ppm
Cu	42.8≦(179, 8.2)<80.9	80.9≦(40, 1.8)<152.9	152.9≦(28, 1.3)	80.9	ppm
Pb	17.8≦(210, 9.7)<44.5	44.5≦(74, 3.4)<111.4	111.4≦(11, 0.5)	44.5	ppm
Zn	118.2≦(186, 8.6)<201.9	201.9≦(67, 3.1)<344.9	344.9≦(32, 1.5)	201.9	ppm

Note: (C) means the Cotahuasi area and (O) means the Orcopampa area.
Numerals in parentheses, i.e. (143, 6.7), mean the former number, i.e. (143) the number of samples and the latter number, i.e. (6.7) the ratio (%) to the total number of samples.

5-2-2 Principle Component Analysis

5-2-2-(1) Standard Statistic Values

Based on the standard statistic values obtained by univariate analysis, each indicator element was standardized and the statistic values of the principle component analysis were calculated based on the standardized values. The results are shown in Table 5-5.

The distribution state of contents of each standardized indicator element (hereinafter refered to as the characteristic values) in the 6th dimensional space can also be expressed as the distribution state in the 6th dimensional space having an axis of the first through sixth principle components which are equivalent to the converted orthogonal coordinates system in the space. As can be understood from the eigenvalues and cumulative contributions shown in Table 5-5, the ratio of scattering to the whole scattering in the characteristic space that can be explained by using the first through third principle components in the principle component space reaches 77.0%. At the same time, the cumulative contribution of each characteristic value to the principle component reaches more than 50% in all cases by calculating the first through third main components. If the eigenvalue only is taken up, a value of 0.9 or higher (2.6 or higher in the case of the first principle component only) is obtained when the first through third principle components are calculated. In this analysis, the principle components up to the third are investigated as a general treatment.

5-2-2-(2) Meaning of Principle Components

When the contributions of the first principle component to the main components are reviewed on the eigenvalue, factor loading and characteristic value, the six indicator elements of Au, Ag, As, Cu, Pb and Zn have large positive values on the eigenvalue and factor loading. The four indicator elements of Pb, As, Au and Ag have especially large values in descending order. The ratio of these four elements to the first principle component reaches 78.0% and the ratio of the whole scattering is 44.1%. When the trend of correlation between elements and the comparison of each element on the crustal abundance (abundance in Earth's Crust) are taken into consideration, the first principle component can be determined as a component mainly indicating mineralization of gold and silver and related alternation and partly indicating mineralization of lead with subordinate copper, and zinc.

The second principle component has positive and high eigenvector and factor

loading values on Cu and Zn. These two elements occupy 54.5% in the scattering of the second principle component, or occupy 9.6% in the scattering of the whole principle components. On the other hand, Au, Ag and Pb have negative eigenvector and factor loading values, with only as showing a positive value but it occupies only 0.6% in the scattering of the second principle component. The second principle component can be explained by Cu and Zn, but the ratio of Cu and Zn is about 2:1, indicating that the component can be explained mainly by Cu. When the fact that Cu and Zn have similar values on the crustal abundance is taken into consideration, the second principle component in this area is estimated to be the component that shows local mineralization of copper.

On the third principle component, when the eigenvector and factor loading values are regarded, Zn has a high positive value. The ratio of Zn in the scattering of the third principle component is 44.9%, and its ratio to scattering of the whole principle components is only 6.9%. Ag, which shows positive correlation with Zn, has a ratio of only 12.8% of the scat-tering of the third principle component. The values of Au and Cu are even lower, and both of As and Pb have a negative factor loading values. Assuming from the crustal abundance of Zn, the third principle component is interpreted to represent volcanic rocks widely distributed in this area.

Table 5-5 Results of Principle Component Analysis

Principle component	Eigen value	Principle contribution ratio	Cumulative contribution ratio	Eigenvector						Factor loading (up) and contribution ratio of characteristic value (low)					
				Au	Ag	As	Cu	Pb	Zn	Au	Ag	As	Cu	Pb	Zn
1	2.6468	0.4411	0.4411	0.27453	0.23955	0.28033	0.22233	0.28872	0.18357	0.727 0.5285	0.634 0.4020	0.742 0.5506	0.588 0.3457	0.764 0.5837	0.486 0.2362
2	1.0515	0.1753	0.6164	-0.40510	-0.50644	0.10892	0.57885	-0.01812	0.42796	-0.426 0.1815	-0.533 0.2841	0.115 0.0132	0.609 0.3709	-0.019 0.004	0.450 0.2025
3	0.9210	0.1535	0.7699	0.15706	0.37189	-0.53126	0.00685	-0.39126	0.69817	0.145 0.0210	0.343 0.1176	-0.489 0.2391	0.006 0.0000	-0.360 0.1296	0.643 0.4134
4	0.5275	0.0963	0.8661	0.33657	0.19222	-0.11690	0.87332	-0.63647	-0.63231	0.194 0.0376	0.111 0.0123	-0.068 0.0046	0.504 0.2540	-0.368 0.1354	-0.365 0.1332
5	0.4304	0.0717	0.9379	1,11060	-0.99619	-0.25752	-0.12742	0.04713	0.11251	0.478 0.2285	-0.429 0.1840	-0.111 0.0123	-0.055 0.0030	0.020 0.0004	0.048 0.0023
6	0.3728	0.0621	1.0000	0.15405	-0.08298	1.13837	-0.43130	-1.03981	0.29728	0.057 0.0032	-0.031 0.0010	0.424 0.1798	-0.161 0.0259	-0.388 0.1505	0.111 0.0123
Cumulative contribution ratio of characteristic values of principle components up to the third										0.7310	0.8037	0.8029	0.7166	0.7137	0.8521

Fig. 5-3 Unrotated Factor Loadings

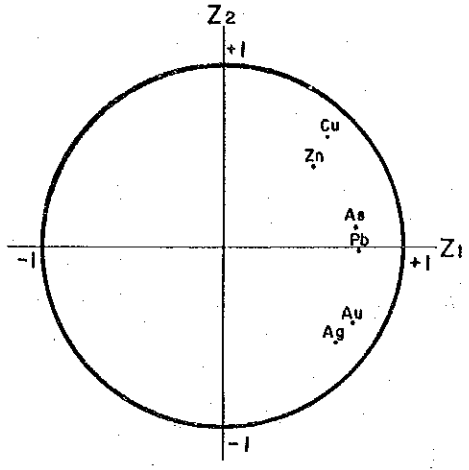

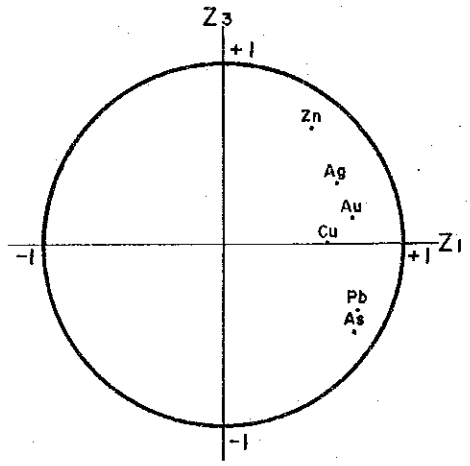

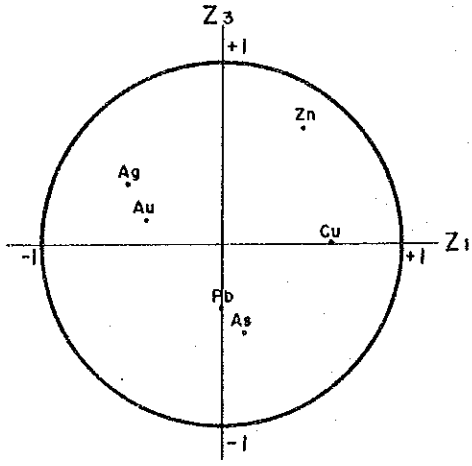

Fig. 5-4 (1) Histogram and Cumulative Frequency Diagram (First Principal component)

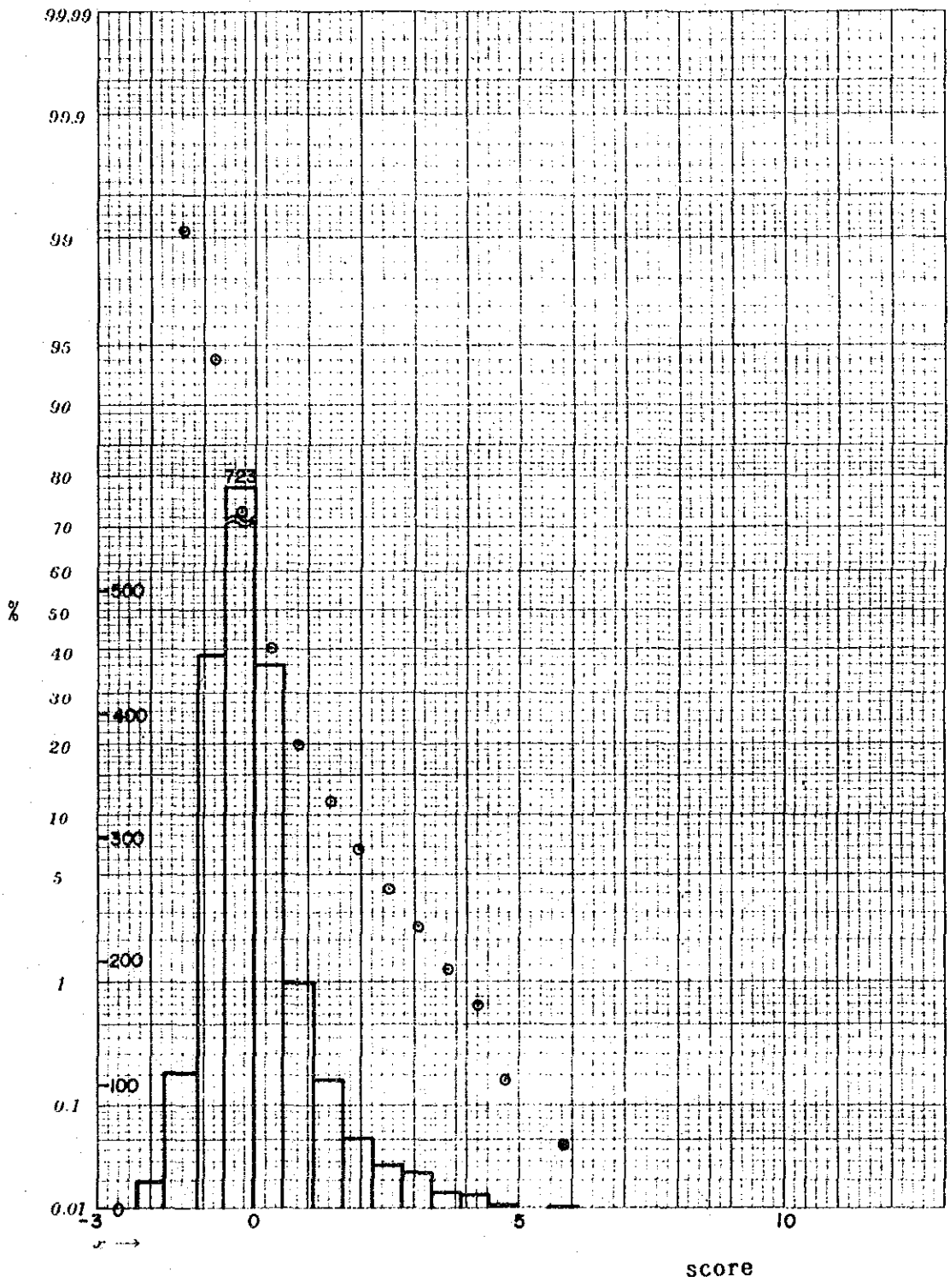

Fig. 5-4 (2) Histogram and Cumulative Frequency Diagram (Second Principal Component)

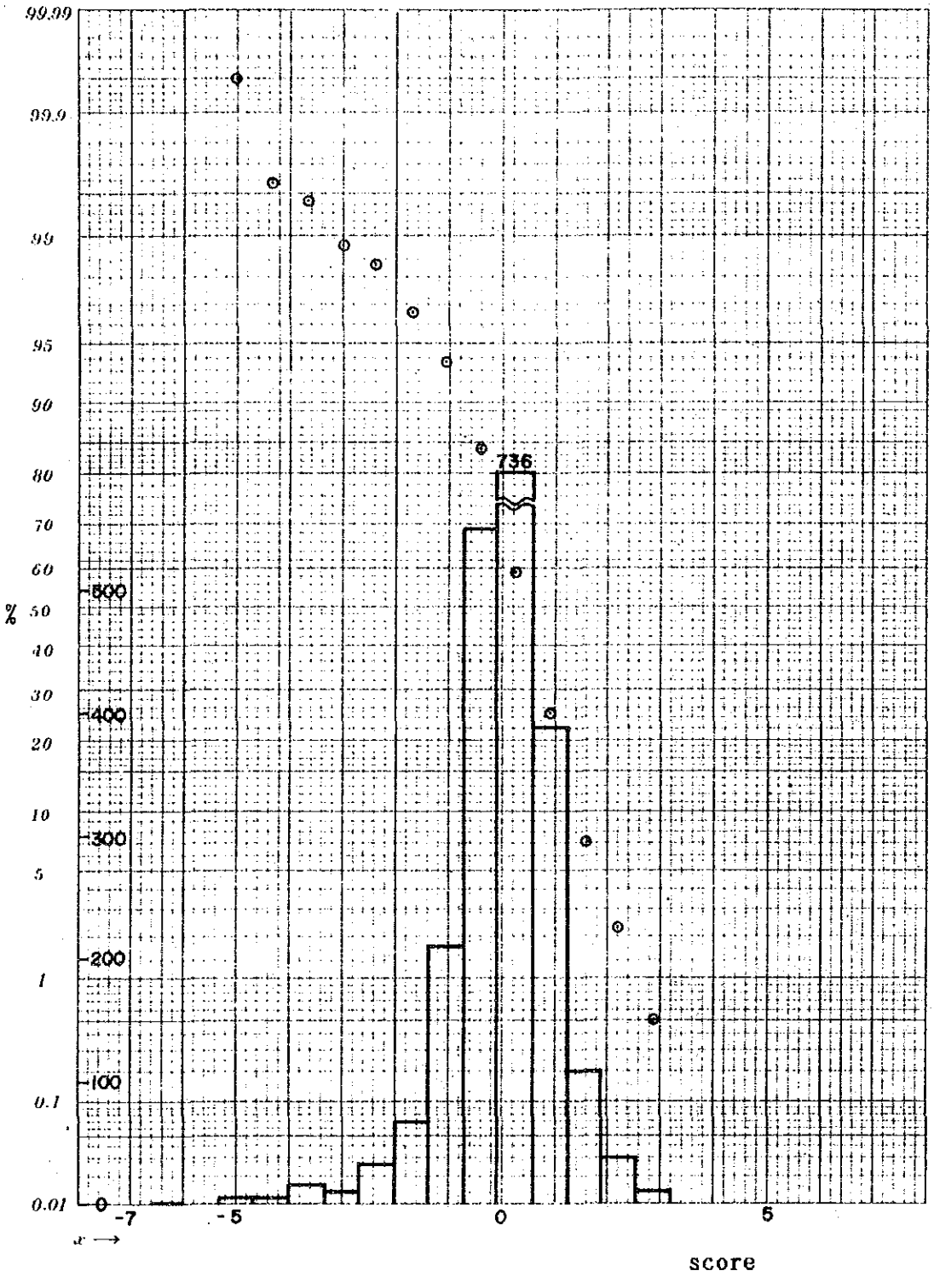

Fig. 5-4 (3) Histogram and Cumulative Frequency Diagram (Third Principal Component)

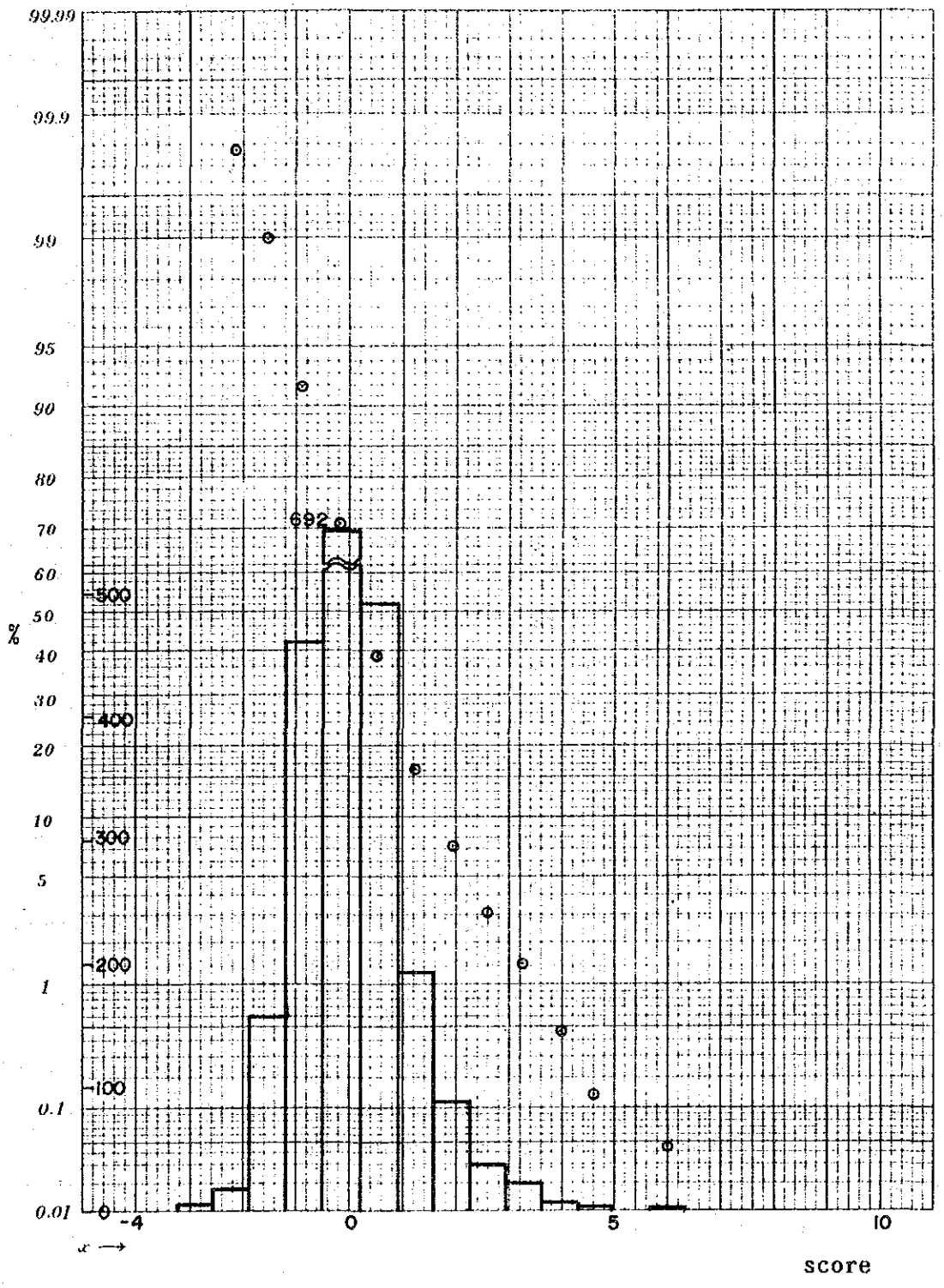

5-2-2-(3) Cumulative Frequency Distribution and Threshold Values

The scores for each principle component on all samples from the eigenvectors obtained on the first through third principle components and from the characteristic values of all samples were calculated, and the obtained scores of each principle component were plotted on cumulative probability papers and the characteristics were investigated. The cumulative frequency distribution plots and frequency distribution diagrams for each principle component score are shown on Fig. 5-4-1 through 3. Based on the results, score 2 is adopted for threshold value for each component.

First principle component (Z_1):

On the cumulative frequency distribution curve, the Z_1 score bends in the neighborhood of 0.8 and further biases toward the high score side around 2.0, indicating excess in the high-score side. The high anomalous populations having a value above 2, threshold value, occupy 5.2% of the whole and 114 samples fall in this category.

Second principle component (Z_2):

On the cumulative frequency distribution, the curve bends in the neighborhood of Z_2 score 4.4, and excesses are included in the low score side. The distribution in the high-score side, on the other hand, is almost linear and anomalous high populations are not clearly recognizable. The number of samples having a value above the threshold value of Z_2 score, 2, is 39, occupying 1.8% of the whole.

Third principle component (Z_3):

On the cumulative frequency distribution, the curve is almost linear in the low-score side, but in the high-score side, it bends in the neighborhood of 1.2, suggesting the existence of high anomalous populations. The threshold value of Z_3 is 2 and the number of samples having a value higher than the threshold value is 94, corresponding to 4.3% of the whole samples.

The principle component scores are classified into three groups using 1, 2 and 4 corresponding to M, M + 2σ and M + 4σ, respectively. Table 5.6 shows the classification of scores of each principle component and the threshold values. Densitity distribution of principle components based on Table 5-6 are shown in PL.14 (1) through (3).

Table 5-6 Classification of Each Principle Component

Score	1≦	<2	2≦	<4	4≦		Thresh-old value
Principle component	No. of samples	%	No. of samples	%	No. of samples	%	
Z_1	161	7.4	92	4.2	12	0.5	2
Z_2	194	8.9	39	1.8	-	-	2
Z_3	195	9.0	90	4.1	4	0.2	2

Remarks) Percentage shows the ratio of the number of samples to whole samples.

5-2-3 Extraction of Geochemically Anomalous Zones

5-2-3-(1) Extraction of Geochemically Anomalous Zones

Geochemical anomaly by univariate analysis:

Geochemically anomalous zones by the univariate analysis method were extracted under the following standards using the geochemical anomalies determined by the univariate analysis and the positive correlation of indicator elements that reached the 5% significant level. In other words, when two or more indicator elements that are significantly correlated each other show anomaly in the same place or in two or more places of nearby, or when a single indicator element shows an anomalous value in two neighboring places, these places are collectively called an anomalous zone. Geochemical anomalies that do not fall in the above standards are called as anomaly simply. The range that is determined to be an anomalous zone or anomaly includes the site where the samples of anomalous values were collected and upward from it for about 1 km in the river, stream, mountain slope, etc. PL.13 shows the distribution of geochemically anomalous zones and anomalies that are extracted under these standards.

In the Cotahuasi area, there are numeral anomalous zones of various sizes, and comparatively large scale ones are mainly distributed in the western and northern parts from the center of the survey area. In the Orcopampa area, on the other hand, there are four large and small anomalous zones and significantly anomalous zones among them are distributed in the central and northeastern parts. Table 5-7 shows the names, locations, distribution ranges and indicator elements that show anomaly, as well as their significances, on major anomalous zones in the two areas.

Geochemical anomalies by principle component analysis:

PL.15 summarizes the geochemically anomalous zones and the anomalies obtained through principle component analysis of the first through third principle components. On the main anomalous zones, Table 5-7 shows the roles of each principle component together with the results of univariate analysis.

Overall geochemical anomalous zones:

The anomalies obtained from both results of the univariate analysis and principle component analysis were combined and summarized on PL.16. As the map clearly shows, the geochemical anomalies extracted through the univariate analysis and that extracted through the principle component analysis coincide very well. All anomalies, mainly consisting of the combinations of Au and Ag, or Pb and As and other minor combinations, as found through the univariate analysis are also shown as anomalies of the first principle component anomalies. In the Cotahuasi area, as Table 5-7 shows, the first 7 anomalies, mainly consisting of anomalies of Au and Ag, Au and As or Au and Pb match fairly well, though the scales are different.

As to the second principle component anomalies, having much of information on Cu, there are such anomalous zones as the anomalous zone centering in Abandonada which is in the south of Quechnalla anomalous zone, Huayjo anomalous zone, Maran anomalous zone and Velinga anomalous zone. On the three anomalous zones of Abandonada, Huayjo and Maran among them, anomaly of Cu is also shown comparatively strongly on the results of univariate analysis.

In the Orcopampa area, the anomalies extracted through the univariate analysis coincide with the results of first principle component on both anomalous zones of Orcopampa and Orcopampa north.

5-2-4 Relation between Geochemically Anomalous Zones and Geology

Major geochemical anomalous zones in the Cotahuasi area are distributed in the west and north areas of Cotahuasi River that flows from northeast to south through the central part of area and only small-scale anomalous zones are distributed in the eastern part of the river. This seems to reflect the geological structure, mineralization and alteration environment of this survey area.

The Mina Pararapa anomalous zone is distributed in the Tacaza Formation and Alpabamba Formation and has its center of anomaly in the neighborhood of the Pararapa mine. The major anomaly of this anomalous zone is Au. Au anomaly is also detected in the gullies at the east and west sides of the mine, and it is widely distributed, coinciding well with the anomaly of the first principle com-

Table 5-7 List of Anomalous Zones

Anomalous zone	Location	Scale	Indicator element						Principle component			Remarks
			Au	Ag	As	Cu	Pb	Zn	Z_1	Z_2	Z_3	
		(km × km)										
- Cotahuasi Area -												
1 Mina Pararapa	Approx. 20 km north-northwest of Cotahuasi	8 × 9	++	++	+		-		++		+	Au>Ag
2 Quechualla	Along Cotahuasi River in the center of the Survey Area	11 × 14							+		+	
Picha	Northern part of Anomalous zone		++	++	+	-	+	-	++			Ag>Au
Quechualla	Along Cotahuasi River		++	++	-		+	-				Au>Ag
Abandonada	South of Quechualla		+	+	-	+	-	++	+	+	-	
Tanisca	Western part of Anomalous zone		++	+			+		+			
3 Huayjo	Approx. 10 km south of Quechualla	2 × 10	++	+	-	++	+	-	++	+		
4 Maran	Approx. 10 km southeast of Pausa	6 × 7	++	-	+	++	+	-	+	+		Cu>Au
5 Mina Luicho	Approx. 4 km northeast of Pausa	4 × 4	++	++		++	+	-	++		+	Au>Ag,Cu
6 Marcabamba	Marcabamba in the northeast of the survey area	3 × 6	+	++		-	-	+	+			
7 Velinga	Approx. 15 km west-southwest of Cotahuasi	4 × 7	+		+	-		-	-	-	-	Au>As
8 Alca	Approx. 15 km northeast of Cotahuasi	4 × 10	+	+				-			+	
9 Huaynacotas	Approx. 6 km northwest of Alca	3 × 5	+					++			++	
10 Colta	Approx. 15 km north-northeast of Colta	3 × 6	+	+			-		-			Ag>Au
11 Pirca	Approx. 13 km south of Pausa	4 × 4		-				+				
12 Taurisma	Approx. 3 km north of Cotahuasi	1.5 × 2	-	-			-		-			
13 Cerro Kiura	Northeastern margine of the Survey Area	1.5 × 4	+									
14 Pucaccocha	Approx. 10 km west of Quechualla	2.5 × 2.5	+									
15 Oyolo	Approx. 20 km northeast of Pausa	1.5 × 2	+									
16 San Sebastián Sacraca	Approx. 7 km north of Pausa	1.5 × 2	+									
17 Salamanca	Approx. 10 km southeast of Nevada Sollman	1.5 × 2	+									
- Orcopampa Area -												
18 Orcopampa	Central part of the Orcopampa Area	10 × 6	(++)	(+)			-	+	+		+	
19 Orcopampa North	Approx. 5 km northeast of Orcopampa	4 × 6	(++)	(++)					+		-	

(Note) ++ : Existing three of more samples having a value of $\geq M+3\sigma$ or $\geq$ score 4
+ : Existing one of more samples having a value of $\geq M+3\sigma$ or $\geq$ score 4
- : Existing two of more samples having a value of $\geq M+2\sigma$ or $\geq$ score 2
( ) : Classification standard in the Cotahuashi Area

ponent. An andesite dyke runs almost in the south-north direction in an area about 3 km west of the mine. Since this dyke is distributed in the same way as the host rock of the ore deposit and since a strong anomaly of Au is extracted downward of the dyke, existence of some mineralization and alteration is assumed.

The Quechualla anomalous zone consists of anomalies of multiple elements and the anomaly is distributed in a wide range. It shows good matching with the anomalous zone of the first principle component found through the principle component analysis. This anomalous zone has four strong centers of anomaly. The zone in the neighborhood of Mina Picha in the northern part mainly consists of strong anomalies of Au, Ag, Pb and As, and it is situated in the Skarn zone which is a contact zone of the limestones of the Arcurguina Formation and quartz diorite. In the neighborhood of Tanisca in the western part, Hayllura mineralized and alternation zone having quartz veins containing Au and Ag is distributed, and several small-scale old adits are scattered. Several old adits exist also in the area from Quechnalla to Abandonada of southern part. Thus, the Quechualla anomalous zone has mineralized and alteration zones in its centres, strongly reflecting the mineralization and alteration.

The Huayjo anomalous zone is distributed in the downstream of the Cotahuasi River and consists of strong anomalies of Au, Cu and Ag. This coincides well with the anomaly found through the principle component analysis. The anomalous zone is located in the area where the Basement rocks and Coast batholith are distributed. Although existence of a mineralized zone or alteration zone has not been confirmed, because of the strength of anomaly of each element, it is assumed that some mineralized and alteration zone would exist in the neighborhood of the anomalous zone.

The Maran anomalous zone has prominent anomaly of Au and Cu and is distributed widely. This coincides with the anomaly found through the principle component analysis. In the anomalous zone, the Maran south mineralized zone which mainly consists of gold silver beraing quartz veins exists in the contact area between the Chocolate Formation and the Coast batholith and the zone forms the center of the anomalous zone. Strong anomaly is also recognized in the northern part of the anomalous zone. Although existence of either mineralized zone or alteration zone has not been confirmed, because of the strong anomaly, existence of mineralization or alteration is assumed also in the northern part.

The Mina Luicho anomalous zone consists of strong anomalies of Au and Ag and this coincides strongly with the first principle component anomaly. The Mina Luicho mineralized and alteration zone with quartz veinlets and contamination by

ferrous oxides exists near the anomalous zone, greatly reflecting mineralization and alteration.

The Marcabamba anomalous zone is distributed along Huanca Huanca River and it embraces the Sequella alteration zone at the north part. The Sequella alteration zone shows geochemical anomaly of mainly Ag. In the neighborhood of Cotalan in the south, anomalies of Cu, Pb and Zn are also distributed, in addition to Au and Ag. The first principle component anomaly is distributed in the Sequella alteration zone and Cotalan, proving that it is a strong anomaly of mainly Au and Ag. In the neighborhood of Cotolan, mineralization or alteration has not been confirmed, but since the eneter of anomaly is in the contact area between the Tacaza Group and quartz diorites, existence of a mineralization or alteration is assumed.

The Velinga anomalous zone is situated in northeast of the Quechnalla anomalous zone and the anomaly is mainly of Au. The anomaly of Cu is comparatively clear, although the distribution range is small. The anomaly zone is mainly distributed in the Yura Group and partly in diorite.

The Alca anomaly zone is mainly of Au and Ag and the zone is distributed in the Tacaza Group and quartz diorites. No anomaly by principle component analysis has been found in the zone. Also, no distinct mineralized zone has been found in the zone though pyritization is observable in the part of quartz diorites.

The Huaynacotas anomalous zone has much of Zn and is accompanied by Au, and it is mainly distributed in the Alpabamba Formation and the Huanca Formation. The third principle component anomaly is very prominent in the zone.

The Colta anomalous zone has Au anomaly in the northern part and Ag anomaly in the southern part, and it is distributed in the Tacaza Group, Arcurquina Formation and diorites. The Colta East alteration zone accompanied by silicification and argillization exists in the neighborhood of this anomalous zone, thus the Colta anomalous zone is considered to reflect this alteration zone.

The Pirca anormalous zone consists mainly of Zn and Ag anomaly and is distributed in the Pirca alteration zone accompanied by silicification and argillization. The south of Maran mineralized zone of gold is situated to the east of the Pirca anomalous zone, suggesting the possibility of gold mineralization in the anomalous zone.

The Taurisma anomalous zone consists of anomalies of Au, Pb and As, and is distributed in the Arcurquina Formation. The anomaly of the first principle component coincides with this anomalous zone.

The Cerro Kiura anomalous zone is situated in the northeastern edge of the

survey area. It has strong Au anomaly and is distributed in the Alpabamba Formation. This anomaly is detected in two places that are about 2 km apart and the value was 67 ppb or higher in both places. Weak solfataric alteration is recognized in the neighborhood and the Cerro Kiura anomalous zone seems to reflect this alteration.

The Pucaccocha anomalous zone is situated to the southwest of the Quechualla anomalous zone and consist mainly of Au anomaly. This anomalous zone is distributed in the Tanisca West alteration zone being accompanied with silicification and argillization.

The Oyolo anomalous zone is of Au anomaly and is distributed in the southern edge of Oyolo alteration zone which is a result of argillization caused by hydrothermal process. The Oyolo anomalous zone is considered to be an anomalous zone reflecting a part of this alteration zone.

The San Sebastien Sacraca anomalous zone consists of only Au anomaly and is distributed in the Tacaza Group. Although the analytical value of Au is as high as 162 ppb, the anomaly comprises only one sample.

The Salamanca anomalous zone consists of Au anomaly composed of anomalous samples from two places, and is situated in the Alpabamba Formation. Granodiorites of Coast batholith are distributed in the neighborhood and contact to the Alpabamba Formation. No distribution of mineralized or alteration zone has found in this anomalous zone until now.

Among the major anomalous zones distributed in the western side of the Cotahuasi River, the Quechualla, Huayjo, Maran, Mina Luicho and Marcabamba anomalous zones consist of anomalies of four to six elements according to the results of univariate analysis. Au and Ag indicate strong anomaly, and the element showing the next strong anomaly is Cu. Coast batholith and diotites of Accha stock are distributed in four of these anomalous zones, excluding the Mina Luicho anomalous zone, and mineralized zones or alteration zones have been formed in the contact area between these intrusive rocks and other formations in the Quechualla and Maran anomalous zones. Because of this, these intrusive rocks are considered to be closely related with the geochemically anomalous zones in this survey area.

Anomaly of Zn, which is one of the indicator elements of univariate analysis in this area, is distributed in the whole survey area, and it frequently appears in the Alpabamba Formation of the upper Tertiary and in young formations of the Quarternary. It has been said that the alteration in the survey area ranges from the Basement complex to the Alpabamba Formation of the Miocene, and there is

little reason to consider that the majority of weak Zn anomalies that appears in young formations reflects mineralization.

There are two anomalous zones of Orcopampa and Orcopampa North in the Orcopampa area. The central part of the Orcopampa anomalous zone is located in the Alluvium, on the other hand, the Tacaza Formation, which is the host rock of ore deposits of the Orcopampa mine is distributed in the eastern part. The anomaly is considered to strongly reflect the silver, copper, lead, zinc and gold bearing vein-type deposits.

Au anomaly is strong in the Orcopampa North anomalous zone and the zone is mainly distributed in the Tacaza Formation. No mineralized/alteration zone has been found in the zone.

Compared with the Cotahuasi area, the Orcopampa area has high Au and Ag values.

Potential geochemically anomalous zones:

The potential geochemically anomalous zones extracted from this geochemical prospecting are zones of Mina Pararapa, Quechualla, Maran, Huayjo, Mina Luicho and Marcabamba. Prominent anomalies appear in these zones on both cases of the univariate analysis and principle component analysis.

Promising anomalous zones in the aspect of single element anomaly or anomalies of a few elements are four anomalous zones of Cerro Kiura, Pucaccocha, (a part of West of Tanisca alteration zone) Alca and Colta.

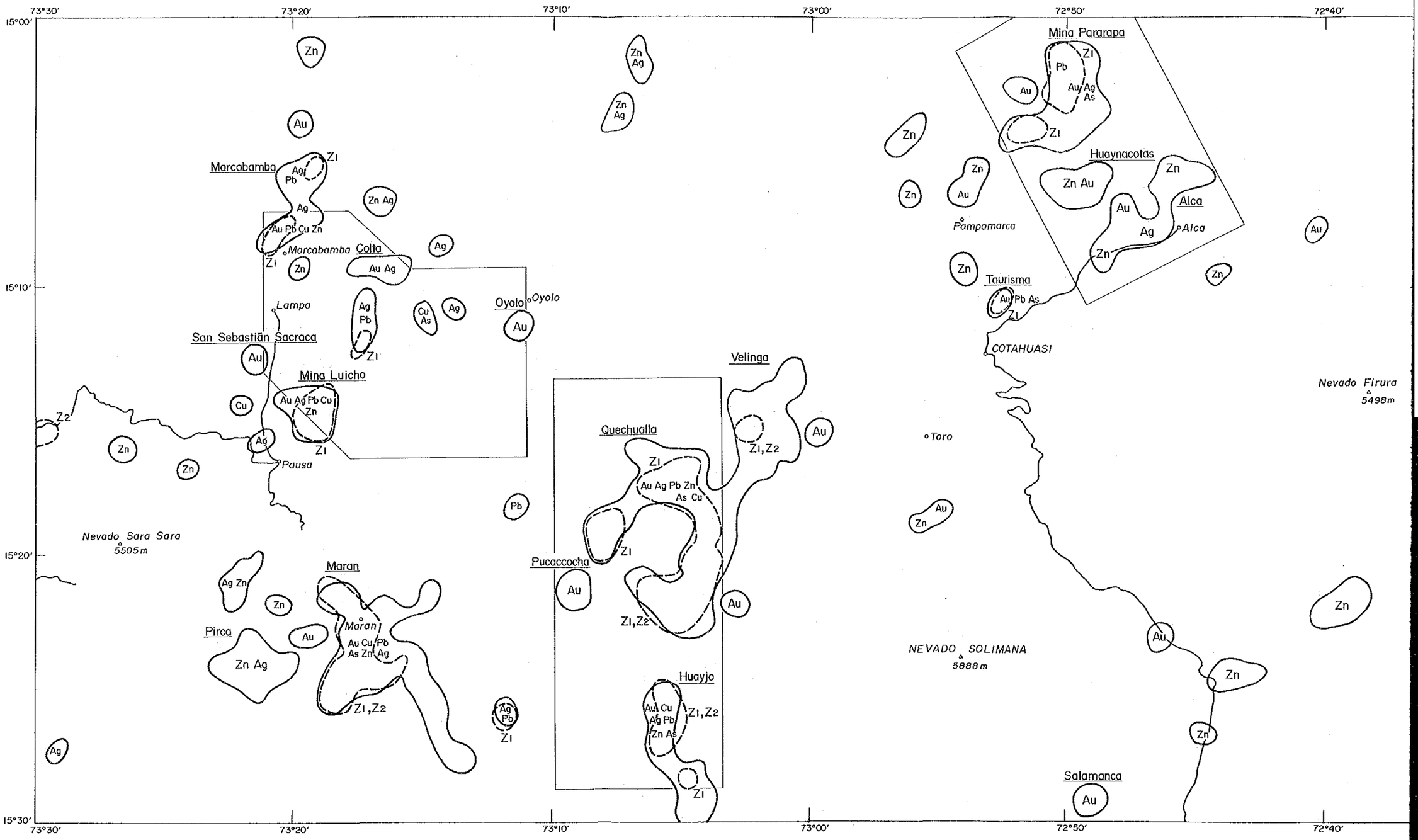
73°30'
73°20'
73°10'
73°00'
72°50'
72°40'
15°00'
15°10'
15°20'
15°30'
Marcabamba
Ag Pb
Z1
Ag
Au Pb Cu Zn
Z1
Marcabamba
Colta
Au Ag
Zn Ag
Ag
Zn
Lampa
Ag Pb
Z1
Cu As
Ag
Oyolo
Oyolo
Au
San Sebastián Sacraca
Au
Mina Luicho
Au Ag Pb Cu Zn
Z1
Cu
Ag
Pausa
Z2
Zn
Zn
Nevado Sara Sara
5505 m
Pb
Ag Zn
Zn
Pirca
Zn Ag
Au
Maran
Maran
Au Cu Pb As Zn Ag
Z1, Z2
Ag
Pb
Z1
Ag
Velinga
Quechualla
Z1
Au Ag Pb Zn As Cu
Z1, Z2
Z1
Pucaccocha
Au
Z1, Z2
Au
Huayjo
Au Cu Ag Pb Zn As
Z1, Z2
Z1
Mina Pararapa
Zn Ag
Pb
Au
Au Ag As
Z1
Z1
Zn
Zn
Au
Pampamarca
Huaynacotas
Zn Au
Zn
Au
Ag
Alca
Alca
Zn
Zn
Zn
Taurisma
Au Pb As
Z1
COTAHUASI
Toro
Au
Zn
Nevado Firura
5498m
Au
NEVADO SOLIMANA
5888m
Au
Zn
Zn
Zn
Salamanca
Au

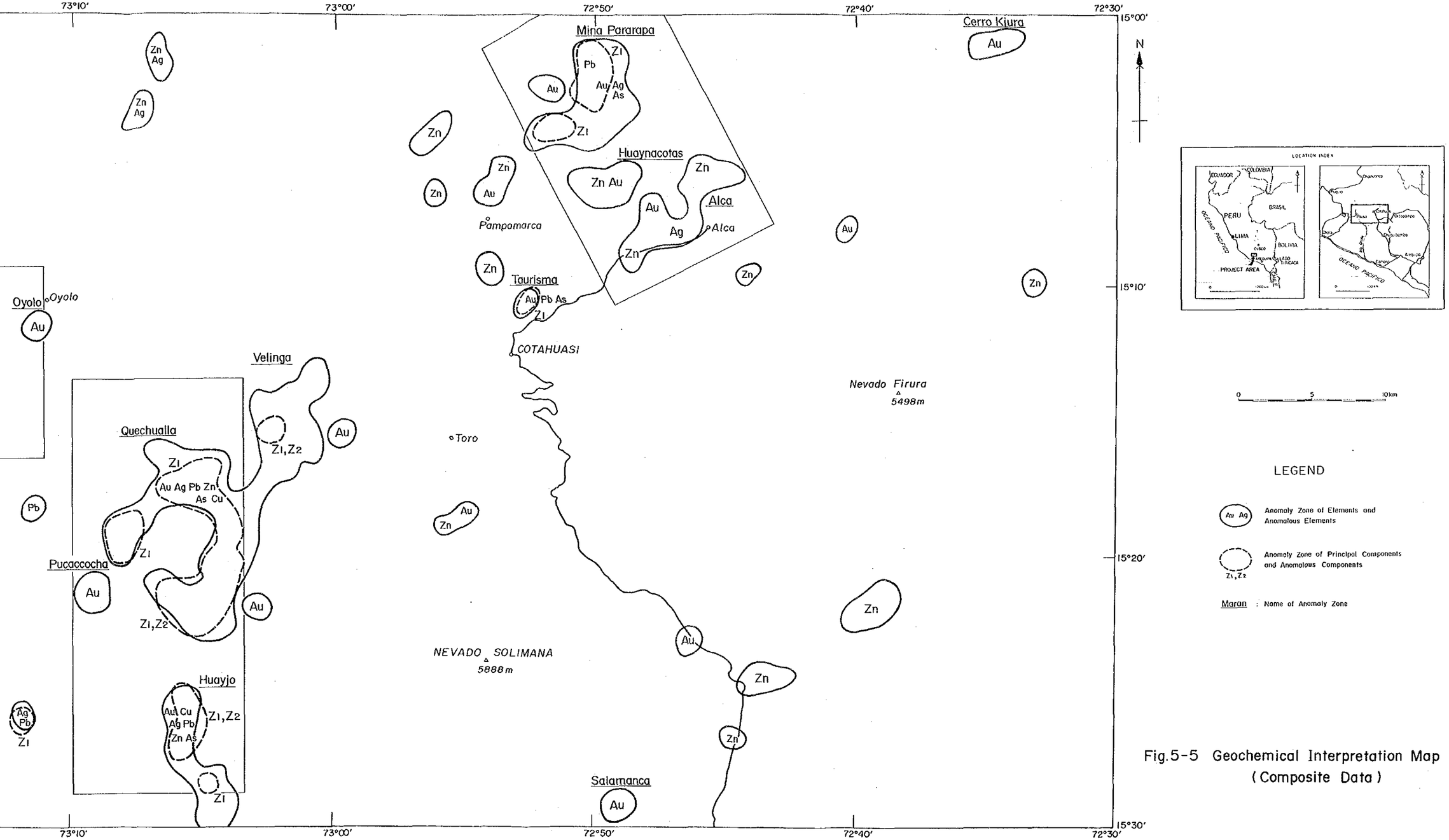

LEGEND

Au Ag — Anomaly Zone of Elements and Anomalous Elements

Zl,Z2 — Anomaly Zone of Principal Components and Anomalous Components

Maran : Name of Anomaly Zone

Fig.5-5 Geochemical Interpretation Map
(Composite Data)

CHAPTER 6 RECAPITULATION AND SUGGESTION

CHAPTER 6 RECAPITULATION AND SUGGESTION

6-1 Recapitulation

The first-year programme of the Mineral Exploration Project in the Cotahuasi Area consists of LANDSAT image analysis, geological survey and geochemical prospecting carried out in the field. A geochemical prospecting was also carried out in the vicinity of the Orcopampa deposits to the east of the survey area for the purpose of a model survey for ore deposits. These surveys were aimed at determining the possibility of occurrence of mineral deposits in the survey area by shedding light on its geological conditions. The priority task of the survey was to extract target areas having potential mineral resources through synthetic analysis of the relationship between the geological structure and mineralization, and the geochemical characteristics of the survey area.

The surveys have provided important data relevant to the geology, geological structure, igneous activity, mineralization, alternation, geochemically anomalous zones and the relationship among these factors, shedding light on many hitherto unknown factors. However, there are still some items to be clarified by more detailed surveys which will follow in succeeding fiscal years.

The survey results are sumarized below.

(1) Geological Survey

Basement

The basement of the survey area is composed of greenish grey granites and diorites having strong gneissosed structure which are considered to be of Precambian age (600 to 2,000 Ma).

Jurassic and Cretaceous Systems

These Systems are distributed in the steep slopes along the Cotahuasi River and Maran River.

The lowermost part of the Jurassic System comprises altered andesitic volcanic rocks, Chocolate Volcanic Rocks (Cho), which cover the Basement rocks discordantly. The Chocolate Volcanic Rocks are also discordantly overlain by the Socosani Formation in which calcareous shales and limestones predominate in the upper and lower part, respectively.

The Yura Group (Yu) in which predominate sandstones and quartzites accumulated during Jurassic to Cretaceous age covers the Socosani Formation conformably, and is overlain conformably by the Murco Formation (Mo) of Cretaceous age composed of alternating beds of red brown sandstone and shale. The Murco

Formation is in turn overlain conformably by the Arcurquina Formation (Ar) comprising thickly stratified limestones.

The strikes and dips of these Jurassic and Cretaceous rocks are disrupted by faults and folds and judging from the distribution of the rocks, it seems that they generally dip gently to northwest with a northeasterly strike.

Tertiary System

The Tertiary System which covers the underlying Jurassic and Cretaceous formations discordantly has a wide distribution in the upper reaches of the Cotahuasi and Maran drainage systems. In the base of the Tertiary System, the Huanca Formation (Hc) composed of alternating beds of conglomerate and sandstone is locally distributed near the village of Cotahuasi. However, the main constituents of the system consist of volcanic rocks.

The Tacaza Group (Tc) composed of andesitic volcanic rocks extruded during the Early Miocene is widespread and is covered discordantly by the Alpabamba Formation (Al), Huaylillas Formation (Hy) and Senecca Formation (Vse) consisting of dacitic and rhyolitic volcanic rocks extruded during the middle to late Miocene epoch.

The K-Ar dating of a sample of the Alpabamba Formation collected during the present survey period shows that it is 4.8 $\pm$ 0.2 Ma and corresponds to the Pliocene. However, the existing data indicate that the period of the eruption of the formation ranges from the Middle to Late Miocene. In the survey area, mineral deposits occur in the Tacaza Group constituting the lower part of the Tertiary System and weak mineralization is also observable in the Alpabamba Formation. For this reason, the real period of activity of this formation has an important meaning. It is necessary, therefore, to investigate further into the age of the Alpabamba Formation during succeeding fied surveys.

Quaternary System

The Quaternary System is distributed widely around the Quaternary volcanos of Firura, Solimana and Sara Sara rising over the Altiplano district and is also observed in the north of the survey area.

In the base of the Quaternary System, the Lower Formation (Vbl) of the Barroso group composed of two-pyroxene andesitic volcanic rocks covers the Tertiary System discordantly and is distributed widely. The result of K-Ar dating of these volcanic rocks shows 1.30 $\pm$ 0.11 Ma which corresponds to the Pleistocene. The two-pyroxene andesitic volcanic rocks are covered by the Upper Formation (Vbu) of the Barroso Group consisting of dactic volcanic rocks which erupted locally during the Late Pleistocene, and the Moraines (Mo) formed by

glaciers are distributed in the vicinity of Mt. Firura and Mt. Solimana.

During the Holocene, andesitic to basaltic lavas and pyroclastic materials, such as volcanic deposits of Pausa (Vsp) and volcanic rocks of Mollebamba (Vm) erupted locally and alluvial deposits (al) have been formed in the river beds and in the lowlands of the Altiplano district.

Intrusive Rocks

Intrusive rocks, of the survey area comprise Coast Batholith (CB) consisting of quartz diorites and granodiorites, Accha stock (Di) of diorites and quartz diorites, and stocks and dikes composed mainly of hornblende andesites. The Coast Batholiths are distributed widely in the south of the survey area, while the Accha Stocks and stocks and dikes of hornblende andesite are arranged in NW-SE direction along the Cotahuasi River and also occur in NW-SE direction in the neighborhood of Marcabamba in the northeast of the survey area.

The results of K-Ar dating of samples obtained from the Coast Batholith show 80.3 $\pm$ 4.0 Ma and 57.1 $\pm$ 2.9 Ma which correspond to the Late Cretaceous and the Paleocene epoch of the Tertiary, respectively. The results of K-Ar dating of samples from the Accha Stock occurring near Alca in the northeast of the survey area shows 53.7 $\pm$ 2.7 Ma which corresponds to the early Eocene epoch of the Tertiary. Some of the Accha Stock have penetrated the Tacaza Group (Tc) and the period of intrusion is considered to range to the Miocene epoch of the Tertiary.

The stage of intrusion of the hornblende andesites is uncertain but it is considered to range from the Middle to the Late Miocene since they have intruded into the Alpabamba Formation.

Geological Structure

The geological structure of the survey area is highly characterized by folds and faults in the Jurassic and Cretaceous systems caused by the orogenic movements of the Andes. In some parts of the Tertiary System the strata dip gently and small faults are observable and there are observed almost no traces of strong tectonic movements.

Folds in the Jurassic and Cretaceous systems are generally synclines and anticlines having NW-SE fold axis and small folds with N-S or NE-SW fold axis are also observable in some parts of the systems. Faults running NW-SE, nearly the same direction as the folding axis, are most conspicuous and generally have a big throw.

In the Tertiary System, faults extending NW-SE and NE-SW directions are found in the Tacaza Group of the Early Miocene and small folds are also obser-

vable in some parts.

Taking the whole survey area, the major faults and folding axes have nearly the same directions of the lineaments and the direction of arrangement of circular structures defined by the LANDSAT image analysis.

Alteration and Mineralization

A total of 15 alteration zones and mineralized zones, large and small, are found in the survey area. Of these zones, the major ones are as listed below.

No.	Name of Mineralized or Alteration Zone	Size of Mineralized or Alteration Zone	Host Rock	Alteration	Mineralization
(1)	Minas Pararapa	1 km x 2.5 km	Andesite (An) dikes and andesitic volcanic rocks (Tc)	Hydrothermal alteration, primarily silicification; browning of ferrous oxide	Gold-silver bearing quartz veins, 0.5 - 1.5 m wide, 1.3 km long
(2)	Mina de Huayllura (East of Tonisca)	1 - 2 km x 10 km	Sandstone (Yu)	Browning by ferrous oxide; hydrothermal alteration with fine quartz vein	Oxidized zones along fracture zones and joints; fine quartz vein with gold and silver
(3)	West of Tonisca	1.5 km x 4 km	Andesitic volcanic rock (Tc)	Hydrothermal alteration accompanied by argillization and silicification	Noticeable mineralization not observed
(4)	Mina Luicho	1 km x 2 km	Sandstone (Yu)	Silicification around fine quartz veins; browning by ferrous oxide	Gold-silver bearing fine quartz veins and browning of ferrous oxide
(5)	Mina Picha	1 km x 2 km	Limestone (Ar)	Skarn zones formed by intrusion of diorite; mainly garnet skarns	Composed of small-scale lense and massive ores, galena black jack and chalcopyrite and bearing gold and silver
(6)	South of Maran	1.5 km x 3.5 km	Andesitic tuff breecia and tuff (Cho)	Silicification around fine quartz veins and browning by ferrous oxide	Gold-silver bearing fine quartz veins and gold-bearing brown contaminated zone by ferrous oxide along fracture zones
(7)	Oyolo	2 km x 8 km	Andesitic to dacitic pyroclastic rock (Tc - Al)	Hydrothermal alteration, primarily argillization; browning by ferrous oxide	Noticeable mineralization not observed
(8)	Pirca	2 km x 5 km	Andesitic volcanic rock (Tc)	Hydrothermal alteration with silicification	Contaminated zone by ferrous oxide

Among the mineralized zones and alteration zones tabulated here, the largest unit deposit is the gold-silver bearing quartz vein occurring in the mineralized zone of Mina Pararapa. This vein is 0.5 to 1.5 m wide and 1.3 km long. According to the unpublished data of the mine, the highest grade of gold is 40 g/ton and the average grade 4.6 g/ton. According to the results of the present survey, the average grade for 0.8 m of vein width is 4.6 g/ton for gold and 288.0 g/ton for silver.

Analysis of local samples collected from contaminated part by brown ferrous oxides occurring along fissures in the mineralized zones of Mina Luicho, though on a small scale, shows a grade of 26.0 g/ton for gold and 114.1 g/ton for silver.

Massive ores collected from the stockpile of the Mina Richa show a grade of 7.7 g/ton for gold, 777 g/ton for silver, 23.4% for lead, 21.6% for zinc and 1.38% for copper. Such high-grade ores cannot be found in the other mineralized zones surveyed.

(2) Geochemical Prospecting

Geochemical analyses of the elements--Au, Ag, As, Cu, Pb and Zn--were made with respect to 2,174 samples of stream sediments collected in the survey area, and geochemically anomalous zones were identified on the basis of the statistical analysis.

The major geochemically anomalous zones are as listed below.

No.	Name of Geochemically Anomalous Zone	Anomaly in Univariate Statistical Analysis (Plural Elements)	Existance of Anomaly in Principal Component Analysis		Size of Anomalous Zone	Area
			1st Principal Component	2nd Principal Component		
1	Mina Pararapa	Au, Ag, (As), (Pb)	Yes	No	7 km x 4 km	28 km^2
2	Quechualla (Tanisca)	Au, Ag, Pb (Zn)(As) (Cu)	Yes	No	13 km x 10 km	130 km^2
3	Huayjo	Au, Cu, Ag (Pb), (Zn)(As)	Yes	Yes	10 km x 2 km	20 km^2
4	Marcabamba	Au, Ag, Pb (Cu)(Zn)	Yes	No	7 km x 3 km	21 km^2
5	Mina Luicho	Au, Ag, Pb (Cu)(Zn)	Yes	No	4 km x 3 km	12 km^2
6	Maran	Au, Cu, Pb, (As), (Zn)(Ag)	Yes	Yes	9 km x 4 km	36 km^2
*	Orcopampa	Zn, Pb, (Au)(Ag)	Yes	No	6 km x 5 km	30 km^2
*	North of Orcopampa	Au, Ag	Yes	No	5 km x 4 km	20 km^2

Note 1. The elements for which the amount of information provided by the first principal component are Pb, As, Au and Ag in decreasing order. For Cn and Zn, the amount of information is smaller than the other four elements.

Note 2. The asterisked locations are those where a geochemical exploration was carried out by way of a model for a survey deposit.

(3) Relationship between Mineralized/Alteration Zones and Geochemically Anomalous Zones

Mineralized/Alteration zones, such as Mina Pararapa composed mainly of gold bearing quartz veins, Minas de Huayllura (east of Tanisca) composed of gold bearing fine quartz veins and oxidized zones, Mina Luicho and southern Maran, substantially overlap geochemically anomalous zones consisting mainly of Au and Ag. Mina Picha displaying contact metasomatic mineralization overlap geochemically anomalous zones of Au, Ag, Pb, (Zn) and (As) in a conspicuous manner.

Interesting alteration zones which are close to known mineralized zones and which overlap weak geochemically anomalous zones include the alteration zone in the west Tanisca overlapping an anomalous zone of Au and the alteration zone of Pirca overlapping anomalous zones of Zn and Ag.

Of the geochemically anomalous zones, those of Vellinga along the Cotahuasi River and of northern Huayjo reflect brown altered zones of ferrous oxide bearing small-scale gold deposits. The anomalous zones, including those of Alca in the northeast of the survey area, Quepacc and southern Huayjo in the south, and Marcabamba in the northwest, overlap intrusive bodies of diorite and reflect a weak pyritization caused by the intrusion.

6-2 Suggestion

The following tabulation gives the suggested survey areas and methods of survey for the second and succeeding survey years which are based on the results of the first-year survey.

Area	Method of Survey
1. Mina Pararapa	Detailed geological survey Geochemical exploration Geophysical prospecting Diamong Dorilling
2. West of Tanisca Alteration Zone	Detailed geological survey Geochemical exploration Geophysical prospecting
3. Mina Luicho	Detailed geological survey Geochemical exploration
4. Pirca Alteration Zone	Detailed geological survey Geochemical exploration Geophysical prospecting

However, it is necessary to examine the circumstances of the establishment of mining concessions in the selection of survey areas for the second and succeeding years.

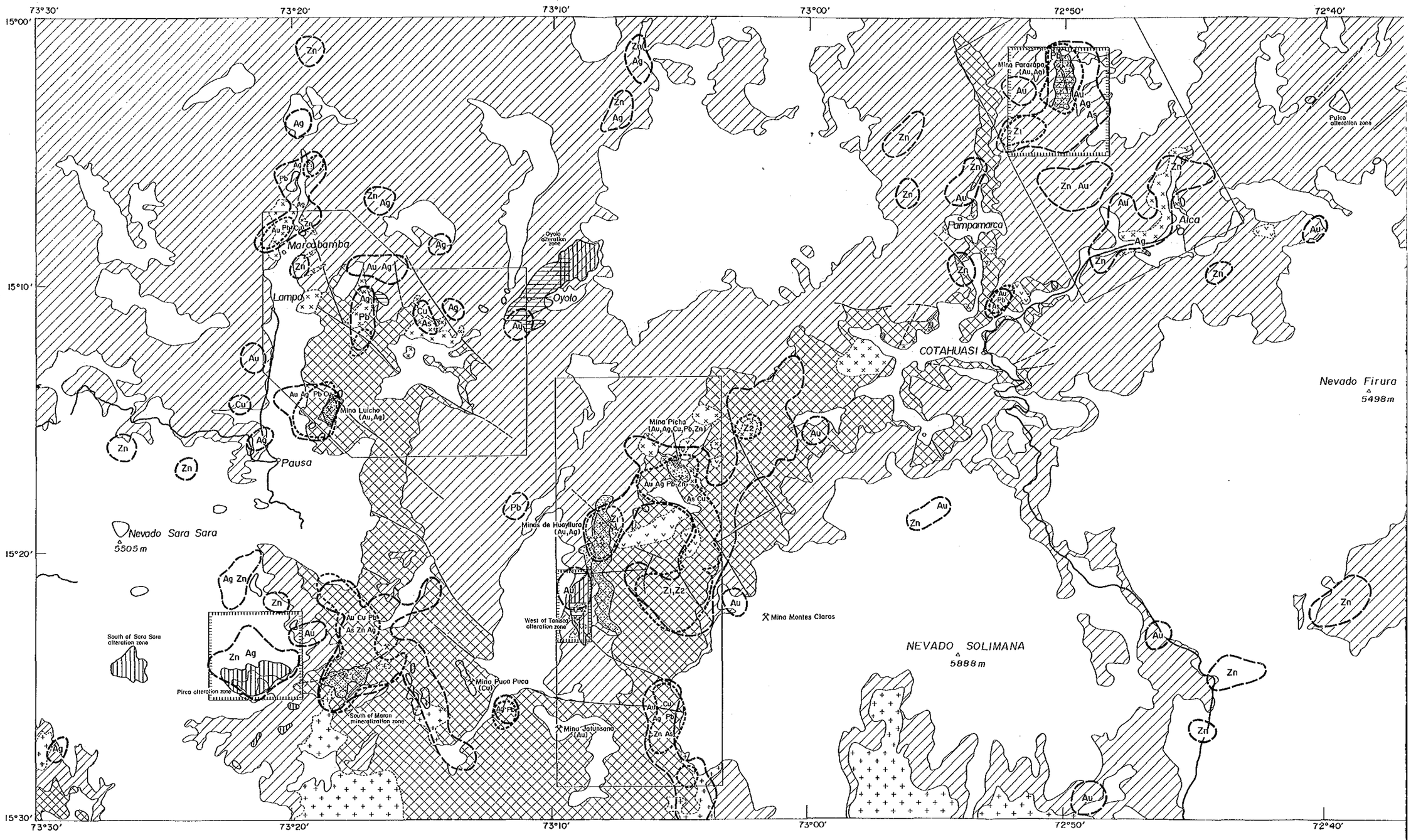
73°30'
73°20'
73°10'
73°00'
72°50'
72°40'
15°00'
15°10'
15°20'
15°30'
Marcabamba
Lampa
Oyolo alteration zone
Oyolo
Mina Luicho (Au,Ag)
Pausa
Nevado Sara Sara
5505 m
South of Sara Sara alteration zone
Pirca alteration zone
South of Maron mineralization zone
Mina Puca Puca (Cu)
Minas de Huayllura (Au,Ag)
Mina Picho (Au,Ag,Cu,Pb,Zn)
West of Tanisca alteration zone
Mina Jatunsana (Au)
Mina Montes Claros
Mina Pararápa (Au,Ag)
Pampamarca
Alca
Pulca alteration zone
COTAHUASI
Nevado Firura
5498m
NEVADO SOLIMANA
5888 m

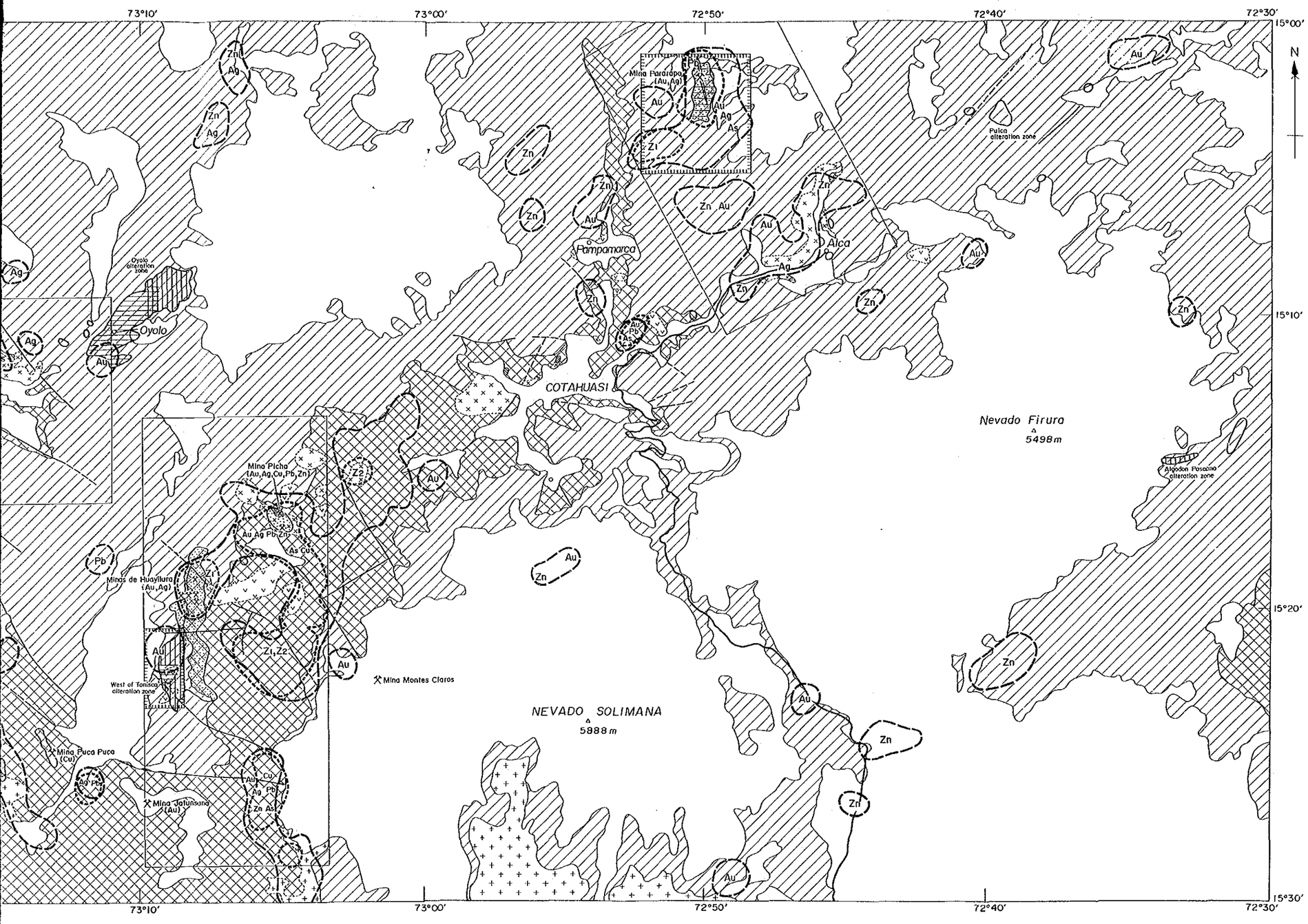

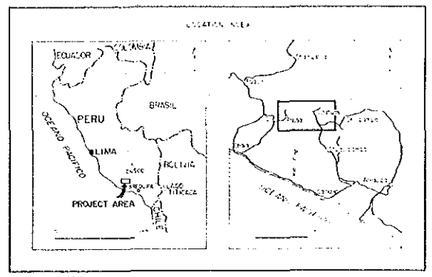

0 5 10km

LEGEND

Geochemical Anomaly

- (Au,Ag) Anomaly Zone and anomalous elements
- Principal Compornents anomaly

Alteration zone

- Mainly silicification
- Silicification+orgillization
- Others (iron oxides stained zone)
- Skarn
- Mineralization zone
- Mine

Geological System

- Quaternary System
- Tertiary System
- Pre-Tertiary System

Intrusive Rocks

- Stock and Dyke (Andesite)
- Stock (Dioritic Rocks)
- Batholith (Granitic Rocks)
- Recomended Area

Fig. 6-1 Interpretation Map of the Cotahuasi Area

REFERENCES

(1) Bernd, L., (1980): Distribucion de Plata en Rocas Volcanicas del Sur del Peru, Bol. Sociedad Geological del Peru No.66

(2) Carlos, G.R., David D.M., (1983): Estratigrafia y Tectonica Terciaria del Area Coracora Pacapausa, INGEMMET Bol. Sociedad Geologica del Peru No.71, 1983

(3) Donald, C.N., Edwin H.M., (1982): Nevado Portugueza Volcanic Center, Central Peru: A Pliocene Central Volcanic-Collapse Caldera Complex with Associated Silver Mineralization, Economic Geology Vol.77

(4) Edgardo, P.S., (1980): Metalogenia del Peru, INGEMMET

(5) Eleodoro, B.B., (1969): Sicopsis de la Geologia del Peru, INGEMMET Bol. No.22

(6) Fletcher, W.K., (1981): Handbook of Exploration Geochemistry Volume 1, Elsevier Science Publishers B.V., Amsterdam-Oxford-New York

(7) Howarth, R.J., (1983): Handbook of Exploration Geochemistry Volume 2, Elsevier Sceince Publishing Company Amsterdam-Oxford-New York

(8) Julio, C.V., (1975): Geologia de los Cuadranglos de Huambo y Orcopampa, Ministerio de Energia y Minas Direccion General de Mineria Servicio de Geologia y Mineria

(9) Kushiro, I., Aramaki, S., (1978): Iwanami-Koza "Earth Science" 3, (in Japanese) Iwanami-Shoten

(10) Luis, V.V., (1970): Geologia del Cuadrangulo de Arequipa, Editado por el Servicio de Geologia y Mineria Bol. No.24

(11) Mario, J.A.F., (1975): Geologia de la Mina Orcopampa y Alrededores, Arequipa, Boletin de la Sociedad Geologica del Peru Tomo 46 P9-24

(12) Michel, F., Cesar V.N., (1979): Mineralization Argentifera Asociada al Volcanismo Cenozoico en la Faja Puquio-Cailloma, Boletin de la Sociedad Geologia del Peru Tomo 60 Lima

(13) Miyashiro, A. and Kushiro I., (1977): Petrology I, II, and III (in Japanese), Kyoritsu Press

(14) Onuma, N., (1985): Collected Paper on Geochemical Investigation of the Central Andes Volcanic Zone, Southern Peru, 1980-1981, Overseas Scientific Research (Nos.504112 and 56043012)

(15) Petersen, G., Vidal C., (1983): Tres Epocas Metalogeneticas Evidenciadas en el Cenozoico del Peru, Bol. Sociedad Geologia del Peru No.71

(16) Richard, M.T. Edward F. and Alan H.C., (1981): K-Ar Geochronology of the Late Cenozoic Volcanic Rocks of the Cordillera Occidental, Southernmost Peru, Journal Volcanology and Geothermal Research, Elsevier Scientific Publishing Company, Amsterdam-Printed in Belgum

(17) Victor, P.G., (1983): Geologia de Los Cuadranglos de Pausa y Caraveli, INGEMMET Bol. No.37 Serie A., Lima

APPENDICES

（巻　末　資　料）

Abbreviations for appendices

Stratigraphic unit

			Simbol
Cenozoic Group	Quaternary System	Alluvium	al
		Mollebamba Volcanic Rocks	Vm
		Pausa Volcanic Sediment	Vsp
		Lampa Volcanic Rocks	Vla
		Moraine	Mo
		Barroso Group Upper	Vbu
		Lower	Vbl
	Tertiary System	Sencca Formation	Vse
		Huaylillas Formation	Hy
		Alpabamba Formation	Al
		Tacaza Group	Tc
		Huanca Formation	Hc
Mesozoic Group	Cretaceous System	Arcurquina Formation	Ar
		Murco Formation	Mu
		Yura Group	Yu
	Jurasic System	Socosani Formation	So
		Chocolate Volcanic Rocks	Cho
Precambrian Group		Basement (gneiss)	Gn

Intrusive rocks

		Simbol
Tertiary	Stock and Dyke	An
	Accha stock	Di
Paleogene		
Cretaceous	La Costa Batholith	CB

Apx. 1 Microscopic Observations of Rock Thin Sections

Abbreviations

Minerals

ol:	olivine	ze:	zeolite
hy:	hyperthene	ca:	calcite
ag:	augite	ep:	epidote
hb:	hornblende	ac:	actinolite
bi:	biotite	hd:	hedenbergite
pl:	plagioclase	ga:	garnet
or:	orthoclase	ab:	albite
qz:	quartz	cc:	calcedony
cr:	cristobalite	py:	pyrite
gl:	glass	mg:	magnetite
ch:	chlorite	hm:	hematite
sr:	sericite	al:	alunite
cl:	clay minerals	cp:	chalcopyrite
mon:	montmorillonite	sp:	sphalerite
kn:	kaolinite	gn:	galena
Au:	native gold	gr:	graphite
il:	ilmenite	fe-min:	Fe-mineral
po:	pyrrhotite		

Apx 1 Microscopic Observations of Rock Thin Sections

No.	Sample No.	Coordinates		Rock name	Geol. unit	Texture	Phenocryst								Groundmass								Secon						
		X (Km)	Y (Km)				pl	ol	hy	ag	hb	qz	or	bi	pl	hy	ag	fe-min	cr	qz	gl	hb	ch	sr	cl	ze	ca	ep	ab
1	Ab-6	689.4	8319.8	qz-porphyry	Di	porphyritic crystalline	◎					◎		○	◎					◎				○			○		
2	Ad-1	677.5	8321.8	altered hb(?)-andesite	Tc	porphyritic hyalopilitic	◎				○				◎						◎			○				○	◎
3	Ad-6	679.1	8326.6	glassy andesite	Vla	aphyric hyalopilitic									◎				○		◎								
4	Ae-1	680.0	8326.3	qz-diorite	Di	holocrystalline	◎				○	◎											○					○	
5	Ae-15	683.5	8320.8	hb-diorite	Di	holocrystalline	◎				○	◎											○	◎			○		
6	Af-1	678.7	8321.7	hb-andesite	Vla	(porphyritic) hyalopilitic	○				◎				◎						◎	○							
7	Af-2	679.3	8320.9	altered rock (qz-ab-sr-ch)	Di	(porphyritic)	○							○?									○	○					◎
8	Bb-3	701.2	8306.2	altered andesite	Tc	porphyritic, hyalopilitic	◎			◎?					◎		○?						○	○			◎		◎
9	Bb-10	700.2	8306.1	Silicified rock (altered andesite)	Tc	porphyritic	◎			◎?					◎?		●?				◎?		○	◎					
10	Be-1	706.8	8303.9	altered diorite	An	holocrystalline (porphyritic)	◎				◎												○	○				○	○
11	Bi-54	706.9	8287.6	gneiss	Gn	blastoporphyritic	◎																○	○				○	●
12	Ca-4	740.3	8326.6	(hb-ag) qz-diorite	Di	holocrystalline	◎			○	◎	◎																	
13	Ca-12	734.8	8324.6	altered andesite	Hc	porphyritic hyalopilitic	◎			◎					◎		●?				◎		●	◎			◎		
14	Cb-18	732.9	8336.6	altered andesite	Tc	porphyritic hyalopilitic	◎			●					◎						◎		●	◎	◎				
15	Ga-16	719.6	8316.0	qz-porphyry	Di	porphyritic	◎			●	●	◎		○															◎
16	Gb-30	729.6	8321.4	hb-andesite	An	porphyritic hyalopilitic	◎				◎			○	◎			○			◎								
17	Gb-56	752.4	8301.0	rhyolite	Vse	porphyritic glassy	◎				○	○			○						◎								●
18	Gb-58	757.1	8298.9	hb-andesite	Vbl	porphyritic glassy	◎				○	●			●						◎								●
19	Gb-72	760.4	8293.6	two px-andesite	Vbl		◎		●	●					◎	●	●	●			◎								
20	Gb-74	748.6	8290.5	hb-two px-andesite	Vbl		◎		●	●	◎	●			◎	●	●	●		●	◎								
21	Gb-93	688.5	8324.9	rhyolite	Al	porphyritic glassy	◎				●	◎		◎	●						◎								
22	Gb-97	696.2	8332.4	hb-andesite	Vm	porphyritic hyalopilitic	○				◎				◎							●							
23	Gb-100B	698.3	8323.8	silicified rock (altered andesite)	Tc		◎?																						

servations of Rock Thin Sections

dinates Y (Km)	Rock name	Geol. unit	Texture	Phenocryst									Groundmass									Secondary mineral											Remarks
				pl	ol	hy	ag	hb	qz	or	bi		pl	hy	ag	fe-min	cr	qz	gl	hb		ch	sr	cl	ze	ca	ep	ab	cr	qz	cc	py		
8319.8	qz-porphyry	Di	porphyritic crystalline	◎					◎		○		◎					◎					○			○								
8321.8	altered hb(?)-andesite	Tc	porphyritic hyalopilitic	◎				○					◎						◎				○				○	◎				○		
8326.6	glassy andesite	Vla	aphyric hyalopilitic										◎				○		◎															devitrification
8326.3	qz-diorite	Di	holocrystalline	◎				○	◎													○					○							
8320.8	hb-diorite	Di	holocrystalline	◎				○	◎													○	◎			○								
8321.7	hb-andesite	Vla	(porphyritic) hyalopilitic	○				◎					◎						◎	○														opacite
8320.9	altered rock (qz-ab-sr-ch)	Di	(porphyritic)	○							○?											○	○					◎		◎				qz-porphyry or rhyolite ?
8306.2	altered andesite	Tc	porphyritic, hyalopilitic	◎			◎?						◎		○?							○	○			◎		◎				◎		
8306.1	Silicified rock (altered andesite)	Tc	porphyritic	◎			◎?						◎?		•?				◎?			○	◎							◎		◎		
8303.9	altered diorite	An	holocrystalline (porphyritic)	◎				◎														○	○				○	○				○		
8287.6	gneiss	Gn	blastoporphyritic	◎																		○	○				○	•		◎				
8326.6	(hb-ag) qz-diorite	Di	holocrystalline	◎			○	◎	◎																									
8324.6	altered andesite	Hc	porphyritic hyalopilitic	◎			◎						◎		•?				◎			•	◎			◎				◎		◎		
8336.6	altered andesite	Tc	porphyritic hyalopilitic	◎			•						◎						◎			•	◎	◎								◎		
8316.0	qz-porphyry	Di	porphyritic	◎			•	•	◎		○																	◎		◎				
8321.4	hb-andesite	An	porphyritic hyalopilitic	◎				◎			○		◎			○			◎															
8301.0	rhyolite	Vse	porphyritic glassy	◎				○	○				○						◎									•	•		◎			devitrification
8298.9	hb-andesite	Vbl	porphyritic glassy	◎				○	•				•						◎									•	•		◎			
8293.6	two px-andesite	Vbl		◎		•	•						◎	•	•	•			◎															
8290.5	hb-two px-andesite	Vbl		◎		•	•	◎	•				◎	•	•	•		•	◎															
8324.9	rhyolite	Al	porphyritic glassy	◎				•	◎		◎		•						◎										◎		◎			devitriation
8332.4	hb-andesite	Vm	porphyritic hyalopilitic	○				◎					◎							•														
8323.8	silicified rock (altered andesite)	Tc		◎?																									◎	◎	he ◎	◎		he: hematite

Apx 1 (continued)

No.	Sample No.	Coordinates		Rock name	Geol. unit	Texture	Phenocryst								Groundmass								Secon						
		X (Km)	Y (Km)				pl	ol	hy	ag	hb	qz	or	bi	pl	hy	ag	Fe-min	cr	qz	gl	hb	ch	sr	cl	ze	ca	ep	ab
24	Gb-108	691.9	8292.2	glassy andesite	Vm	aphyric									◎			◎			◎								
25	Gb-110	688.4	8292.9	(hb-bi) qz-diorite	CB	holocrystalline	◎				◎			○									•						
26	Gb-112	687.9	8294.1	sr-qz semischist	Cho	porphyroclastic nematoblastic	◎																	◎					
27	Gc-47	746.9	8325.3	perlite	Al	perlite texture layered															◎					◎			
28	Gc-304	675.8	8300.5	hb-glassy andesite	Vbl	porphyritic cryptocrystalline	◎				◎										◎								◎
29	Gc-307	666.4	8294.3	two px-andesite	Vbl	porphyritic hyalopilitic	◎		○	◎					◎	○	○				◎								
30	Gd-32	733.8	8285.5	hb-bt granodiorite	CB	holocrystalline	◎				◎	◎	○	•															
31	Gd-46	700.8	8333.4	two px-andesite	Vse	porphyritic hyalopilitic	◎		•	◎					◎		•				◎								
32	Ge-19	736.0	8305.2	rhyolite	Vse	porphyritic flow texture	◎			•		◎		◎	•					○	◎								
33	Ge-50	726.1	8327.1	bi-dacite	An	porphyritic	◎					○		◎	◎						○								
34	Ge-80	682.5	8301.2	altered andesite	Cho	porphyritic	◎								○						◎			◎	◎				◎
35	Gf-24	719.9	8318.4	altered andesite	Di	porphyritic pilotaxitic	◎			○	○				◎						◎			◎	○			○	◎
36	Gf-36	746.6	8309.2	hb-andesite	Vbl	porphyritic hyalopilitic-intersertal	○				○				◎						◎	○							
37	Gf-52	715.0	8297.3	bi-hb-andesite	Vbl	porphyritic cryptocrystalline	◎				○		◎		•						◎	○							
38	Gf-85	720.4	8323.0	rhyolite	Al	porphyritic	◎					•		◎							◎								◎
39	Gi-83	667.8	8332.6	rhyolite	Al	porphyritic	◎				•	◎		○							◎					mor ◎			

nates				Phenocryst									Groundmass									Secondary mineral												Remarks
Y (Km)	Rock name	Geol. unit	Texture	pl	ol	hy	ag	hb	qz	or	bi		pl	hy	ag	Fe-min	cr	qz	gl	hb		ch	sr	cl	ze	ca	ep	ab	cr	qz	cc	py		
8292.2	glassy andesite	Vm	aphyric										◎			◎			◎															
8292.9	(hb-bi) qz-diorite	CB	holocrystalline	◎				◎			○											•												
8294.1	sr-qz semischist	Cho	porphyroclastic nematoblastic	◎																			◎							◎				volcanic rock origin
8325.3	perlite	Al	perlite texture layered																◎						◎					◎				devitrification
8300.5	hb-glassy andesite	Vbl	porphyritic cryptocrystalline	◎				◎											◎									◎			◎			devitrification
8294.3	two px-andesite	Vbl	porphyritic hyalopilitic	◎		○	◎						◎	○	○				◎															
8285.5	hb-bt granodiorite	CB	holocrystalline	◎				◎	◎	○	•																							
8333.4	two px-andesite	Vse	porphyritic hyalopilitic	◎		•	◎						◎		•				◎															
8305.2	rhyolite	Vse	porphyritic flow texture	◎			•		◎		◎		•					○	◎										◎		◎			
8327.1	bi-dacite	An	porphyritic	◎					○		◎		◎						○															
8301.2	altered andesite	Cho	porphyritic	◎									○						◎			◎	◎					◎				○		
8318.4	altered andesite	Di	porphyritic pilotaxitic	◎			○	○					◎						◎			◎	○			○		◎				•		
8309.2	hb-andesite	Vbl	porphyritic hyalopilitic-intersertal	○				○					◎						◎	○														
8297.3	bi-hb-andesite	Vbl	porphyritic cryptocrystalline	◎				○			◎		•						◎	○												◎		devitrification
8323.0	rhyolite	Al	porphyritic	◎					•		◎								◎									◎		◎	◎			
8332.6	rhyolite	Al	porphyritic	◎				•	◎		○								◎						mor ◎				◎		◎			mor. mordenite

Apx 1 (continued)

No.	Sample No.	Coordinates		Rock name	Geol. unit	Texture	Grain				Matrix						Rock fragment			Secondary mineral											
		X (Km)	Y (Km)				pl	qz	ca	gl	qz	pl	fe-min	gl	ca	gr	An	Silt	Tf	ch	mon	kn	ze	ca	ep	ac	hd	ga	gz	cr
40	Be-2	706.4	8303.3	marl	Mu	lamination of fine sandstone and marl					◎	◎	•		◎	•															
41	Be-7	705.1	8300.3	graphite bearing crystalline limestone	So	slaty									◎	o															
42	Bg-8 (T, X)	705.5	8309.9	tactite (garnet skarn)	Ar	granoblastic																			•		◎	◎		
43	Ca-13	740.9	8323.8	welded tuff	Al	welded texture											◎	•					mor ◎							◎
44	Ce-4	736.0	8324.2	tuffaceous sandstone	Hc	grain and matrix	◎	o	◎		•	◎		◎	◎															
45	Gb-50	763.9	8334.8	rhyolitic tuff	Al	glass fragments grading	◎	o		◎	•	•		◎							◎									
46	Gb-106	690.4	8294.6	andesitic tuff	So	calcite lens-pool bearing														◎				◎						
47	Gd-12	723.4	8311.8	arkose sandstone	Yu	well sorting	◎	◎			•	•																		
48	Ge-83	683.0	8296.4	altered volcanic breccia	Cho	tuff matrix						◎		◎			◎		◎	◎										
49	Gf-25	719.9	8318.4	magnetite-skarn	Ar	inetasomatic																		◎	•		◎		•	
50	Gi-106	675.9	8294.5	alunitized rock	Tc?																	◎								

◎ : abundant o : common • : rare

dinates Y (Km)	Rock name	Geol. unit	Texture	Grain				Matrix						Rock fragment			Secondary mineral															Remarks
				pl	qz	ca	gl	qz	pl	fe-min	gl	ca	gr	An	Silt	Tf	ch	mon	kn	ze	ca	ep	ac	hd	ga	gz	cr	cc	mg	he	al	
8303.3	marl	Mu	lamination of fine sandstone and marl					◎	◎	•		◎	•																			
8300.3	graphite bearing crystalline limestone	So	slaty									◎	○																			
8309.9	tactite (garnet skarn)	Ar	granoblastic																				•		◎	◎				•		garnet skarn
8323.8	welded tuff	Al	welded texture											◎	•					mor ◎							◎	◎				mor: mordenite
8324.2	tuffaceous sandstone	Hc	grain and matrix	◎	○	◎		•	◎		◎	◎																				
8334.8	rhyolitic tuff	Al	glass fragments grading	◎	○		◎	•	•		◎							◎														
8294.6	andesitic tuff	So	calcite lens-pool bearing														◎				◎									◎		calcite-chloritized
8311.8	arkose sandstone	Yu	well sorting	◎	◎			•	•																							
8296.4	altered volcanic breccia	Cho	tuff matrix						◎		◎			◎		◎	◎															
8318.4	magnetite-skarn	Ar	inetasomatic																		◎	•		◎		•			◎			magnetite-skarn
8294.5	alunitized rock	Tc?																	◎												◎	

◎ : abundant ○ : common • : rare